



UNIVERSITÀ  
DEGLI STUDI  
DI PADOVA

## UNIVERSITÀ DEGLI STUDI DI PADOVA

**Dipartimento di Medicina Clinica e Sperimentale "G. Patrassi"**  
**Ematologia e Immunologia Clinica**

**SCUOLA DI DOTTORATO DI RICERCA IN  
ONCOLOGIA E ONCOLOGIA CHIRURGICA  
XXIV CICLO**

### **ROLE OF NOCODAZOLE ON THE SURVIVAL OF CHRONIC LYMPHOCYTIC LEUKEMIA B CELLS**

**Direttore della Scuola:** Ch.ma Prof.ssa Paola Zanovello

**Supervisore:** Dott.ssa Monica Facco

**Correlatore:** Dott. Livio Trentin

**Dottoranda:** Dott.ssa Valentina Trimarco



# INDEX

<b>ABBREVIATIONS</b> .....	pag.	3
<b>ABSTRACT</b> .....	pag.	5
<b>RIASSUNTO</b> .....	pag.	7
<b>INTRODUCTION</b> .....	pag.	9
1. B-cell Chronic Lymphocytic Leukemia (B-CLL).....	pag.	9
1.1 Epidemiology and etiology.....	pag.	9
1.2 Clinical features.....	pag.	9
1.3 Diagnosis.....	pag.	10
1.4 Prognosis.....	pag.	13
1.4.1 Clinical prognostic factors.....	pag.	13
1.4.2 Biological prognostic factors.....	pag.	14
1.5 Treatment.....	pag.	19
2. Neoplastic B lymphocytes.....	pag.	22
2.1 Control of apoptosis.....	pag.	24
2.2 BCR-mediated signal transduction.....	pag.	26
2.3 Proliferative activity and centrosome aberrations.....	pag.	32
2.4 Microenvironment.....	pag.	34
3. Microtubule inhibitors.....	pag.	36
3.1 Microtubules.....	pag.	36
3.2 Microtubule-interfering agents.....	pag.	39
3.3 Nocodazole.....	pag.	43
<b>AIM OF THE STUDY</b> .....	pag.	47
<b>MATERIALS AND METHODS</b> .....	pag.	49
1. Patients.....	pag.	49
2. Immunophenotypic analysis.....	pag.	49
3. Isolation of B lymphocytes from peripheral blood.....	pag.	51
3.1 Purification of B lymphocytes with sheep red blood cells.....	pag.	52
3.2 Purification of B lymphocytes using RosetteSep kit.....	pag.	53
4. Cell cultures.....	pag.	53
5. Co-cultures.....	pag.	54
6. Preparation of cell lysates.....	pag.	54
7. Polyacrylamide gel electrophoresis in SDS-PAGE.....	pag.	55
8. Western blotting.....	pag.	55
9. Apoptosis analysis by flow cytometry.....	pag.	57
10. Confocal microscopy analysis.....	pag.	58
11. RNA extracton.....	pag.	58
12. cDNA synthesis.....	pag.	59
13. Evaluation of Lyn gene expression through real-time RT-PCR.....	pag.	60
14. Statistical analysis.....	pag.	61
<b>RESULTS</b> .....	pag.	63
1. Nocodazole effect on cytoskeletal tubulin.....	pag.	63
2. Noodazole kills specifically B-CLL cells.....	pag.	63
3. Nocodazole kills B-CLL cells with preference for unmutated.....	pag.	64
4. Nocodazole kills leukemic B cells whereas it does not affect T cells from the same patients.....	pag.	68
5. Nocodazole effect on B-CLL cells is not counteracted by mesenchymal stromal cells.....	pag.	68
6. Nocodazole targets Lyn kinase activity.....	pag.	72
<b>DISCUSSION</b> .....	pag.	75
<b>BIBLIOGRAPHY</b> .....	pag.	81



# ABBREVIATIONS

<b>Ab</b>	Antibody
<b>Ag</b>	Antigen
<b>APC</b>	Allophycocyanin
<b>ATM</b>	Ataxia Teleangectasia Mutated
<b>BAD</b>	Bcl-2 Associated Death promoter
<b>B-CLL</b>	B-cell Chronic Lymphocytic Leukemia
<b>Bcl-2</b>	B-Cell lymphoma-2
<b>BCR</b>	B-Cell Receptor
<b>B-PLL</b>	B-cell Prolymphocytic Leukemia
<b>cDNA</b>	complementary DNA
<b>CDR</b>	Complementarity Determining Region
<b>CD40L</b>	CD40 Ligand
<b>CMV</b>	Cytomegalovirus
<b>GC</b>	Germinal Centre
<b>CR</b>	Complete Remission
<b>DAG</b>	Diacylglycerol
<b>ECL</b>	Enhanced ChemiLuminescence
<b>EDTA</b>	Ethylenediaminetetraacetic Acid
<b>ERK</b>	Extracellular signal Regulated Kinase
<b>Fab</b>	Antigen binding fragment
<b>FBS</b>	Fetal Bovin Serum
<b>Fc</b>	Crystallizable fragment
<b>F/H</b>	Ficoll/Hypaque
<b>FITC</b>	Fluorescein isothiocyanate
<b>GDP</b>	Guanosine diphosphate
<b>GSK3</b>	Glycogen Synthase Kinase 3
<b>GTP</b>	Guanosine triphosphate
<b>HBV</b>	Hepatitis B virus
<b>HCV</b>	Hepatitis C virus
<b>HLA</b>	Human Leukocyte Antigen
<b>HS1</b>	Hematopoietic lineage cell-Specific protein 1
<b>Hsp90</b>	Heat shock protein of 90kDa
<b>hTERT</b>	human Telomerase Reverse Transcriptase
<b>IFN-<math>\gamma</math></b>	Interferon- $\gamma$
<b>Ig</b>	Immunoglobulin
<b>IgV<sub>H</sub></b>	Immunoglobulin heavy chain variable regions
<b>IL</b>	Interleukin
<b>ITAM</b>	Immunoreceptor Tyrosine-based Activation Motif

<b>ITIM</b>	Immunoreceptor Tyrosine-based Inhibitory Motif
<b>mAb</b>	monoclonal Antibody
<b>MAP</b>	Microtubule-Associated Protein
<b>MAPK</b>	Mitogen Activated Protein Kinase
<b>Mcl-1</b>	Mantle cell lymphoma-1
<b>MHC</b>	Major Histocompatibility Complex
<b>MIIC</b>	MHC-class-II-peptide-loading-compartment
<b>MSC</b>	Mesenchymal Stromal Cell
<b>MTOC</b>	Microtubule Organizing Centre
<b>mTOR</b>	mammalian Target Of Rapamycin
<b>NF-<math>\kappa</math>B</b>	Nuclear Factor-kappa B
<b>NHL</b>	Non-Hodgkin Lymphoma
<b>NLC</b>	Nurse-like Cell
<b>NK</b>	Natural Killer
<b>OS</b>	Overall Survival
<b>PARP</b>	Poli-ADP-Ribose Polymerase
<b>PBMC</b>	Peripheral Blood Mononuclear Cell
<b>PBS</b>	Phosphate Buffered Saline
<b>PE</b>	Phycoerythrin
<b>PFS</b>	Progression Free Survival
<b>PI3K</b>	Phosphatidylinositol 3-Kinase
<b>Plc<math>\gamma</math>2</b>	Phospholipase C $\gamma$ 2
<b>PS</b>	Phosphatidylserine
<b>SD</b>	Standard Deviation
<b>SDF-1<math>\alpha</math></b>	Stromal Derived Factor-1 $\alpha$
<b>SDS-PAGE</b>	Sodium Dodecyl Sulphate/PolyAcrylamide Gel Electrophoresis
<b>SFKs</b>	Src Family Kinases
<b>SHM</b>	Somatic Hypermutation
<b>sIgM</b>	surface Immunoglobulin M
<b>Syk</b>	Spleen tyrosine kinase
<b>TC</b>	Tri-Color
<b>Th</b>	T helper lymphocyte
<b>WB</b>	Western blotting
<b>WBC</b>	White Blood Cell
<b>ZAP-70</b>	Zeta-Associated Protein of 70kDa

# ABSTRACT

B-cell Chronic Lymphocytic Leukemia (B-CLL) is the most common leukemia in adults and is characterized by the accumulation of clonal CD19+/CD5+/CD23+ B lymphocytes, due to uncontrolled growth and resistance to apoptosis. Leukemic cells from B-CLL show reduced crosslink with specific molecules and high susceptibility to microtubule disrupting drugs, which suggest cytoskeletal alterations.

Microtubules play a crucial role in the vital functions of neoplastic cells, including mitosis, motility and cell-cell contact, and for this reason they became an important target in cancer therapies. In particular, tubulin, a cytoskeletal member, is the target of specific drugs, named microtubule inhibitors. Among these inhibitors, nocodazole induces tubulin depolymerization, mitotic process blocking and shows an apoptotic effect in B leukemic cells.

The aim of this study was to define the effects of nocodazole on B-CLL cells.

First of all, we verified nocodazole capability to favour the depolymerization of tubulin cytoskeleton in different cell types. In addition, we tested nocodazole-induced apoptosis in normal and leukemic B cells, in cell lines (Jurkat, Raji, and K562), in mesenchymal stromal cells (MSCs), and in T lymphocytes of B-CLL patients. Our data pointed out the high specificity of nocodazole for B-CLL cell apoptosis (leukemic cells:  $57\pm 25\%$  vs normal B cells:  $98\pm 6\%$ ,  $p < 0.0001$ ; data are expressed as mean  $\pm$  standard deviation (SD) of percentage of viable cells after treatment with nocodazole) and the absence of toxicity to others cell types.

Growing evidence suggests that the marrow microenvironment, where MSCs are present, protects B-CLL cells from conventional anti-neoplastic drugs. The cultures of neoplastic B cells with MSCs and nocodazole demonstrated that nocodazole is able to overcome MSC protective effect, even after survival signal supplemental, such as CD40L or plasma from the same patients.

The action mechanism of nocodazole in B-CLL cells is still under investigation. However, we observed that nocodazole is able to turn off the

increased basal tyrosine phosphorylation of leukemic cells mediated by Src-kinase Lyn through the down-modulation of Lyn active site. Since the specific inhibition of Lyn induces B-CLL cells apoptosis, this linking will be further investigated.

The results obtained in this study suggest a future role of nocodazole as a possible agent for treatment of B-CLL, for its extreme selectivity, the absence of toxicity and its ability to counteract the protective effect provided by marrow microenvironment.

## RIASSUNTO

La Leucemia Linfatica Cronica di tipo B (LLC-B) è la forma più comune di leucemia nell'adulto ed è caratterizzata dall'accumulo clonale di piccoli linfociti B CD19+/CD5+/CD23+, dovuto sia ad una crescita incontrollata che ad una resistenza all'apoptosi. Le cellule leucemiche di LLC-B presentano inoltre alcune anomalie, come ridotta capacità di legare specifiche molecole e suscettibilità a farmaci che distruggono i microtubuli, che indicano la presenza di alterazioni a livello citoscheletrico.

Il ruolo cruciale che i microtubuli rivestono nelle funzioni vitali delle cellule neoplastiche, quali mitosi, motilità e contatti cellula-cellula, li ha resi un importante *target* nelle terapie anti-tumorali. In particolar modo la tubulina, componente dei microtubuli, è il bersaglio di una categoria specifica di farmaci anti-tumorali, gli inibitori dei microtubuli; di questa famiglia fa parte anche il nocodazolo, un agente sintetico che induce la depolimerizzazione della tubulina, arresta il processo mitotico ed ha una peculiare specificità nell'indurre l'apoptosi nelle cellule B di LLC-B.

Sulla base di queste considerazioni, abbiamo voluto approfondire gli effetti ed il meccanismo d'azione del nocodazolo sulle cellule di LLC-B.

Dopo aver verificato che il nocodazolo sia effettivamente responsabile della depolimerizzazione dei filamenti di tubulina citoscheletrica in numerosi tipi cellulari, abbiamo valutato l'effetto apoptotico indotto dal nocodazolo in cellule B normali e di LLC-B, in linee cellulari (Jurkat, Raji e K562), in cellule stromali mesenchimali (MSC) e nei linfociti T residui di pazienti affetti da LLC-B. I risultati ottenuti evidenziano l'estrema selettività del nocodazolo nell'indurre l'apoptosi nelle sole cellule B di LLC-B (linfociti B di LLC-B:  $57 \pm 25\%$  vs B normali:  $98 \pm 6\%$ ,  $p < 0,0001$ ; dati espressi come media  $\pm$  deviazione standard (DS) della percentuale di cellule vive dopo trattamento con nocodazolo) e l'assenza di tossicità nei confronti delle altre popolazioni cellulari prese in esame.

Studi recenti suggeriscono che il microambiente midollare, in cui si trovano anche le MSC, sia in grado di proteggere le cellule leucemiche dall'azione

dei farmaci chemioterapici convenzionali. La co-coltura di MSC e cellule B di LLC-B in presenza di nocodazolo ha dimostrato che tale inibitore è in grado di annullare l'effetto protettivo esercitato dalle MSC, nonostante la presenza di segnali di sopravvivenza quali CD40L o plasma ricavato dagli stessi pazienti.

I meccanismi d'azione del nocodazolo rimangono ancora da chiarire, tuttavia abbiamo osservato come nelle cellule leucemiche di LLC-B il nocodazolo sia in grado di ridurre l'aumentata fosforilazione tirosinica basale mediata dalla Src-chinasi Lyn, mediante *down*-regolazione del sito attivatorio di Lyn. Dal momento che abbiamo dimostrato che l'inibizione specifica di Lyn induce apoptosi nelle cellule di LLC-B, questi primi risultati diventano rilevanti e dovranno essere ulteriormente indagati.

In conclusione, i risultati ottenuti in questo studio hanno evidenziato l'estrema selettività del nocodazolo nell'indurre apoptosi nei linfociti B leucemici, l'assenza di tossicità *in vitro* e la capacità di contrastare l'effetto protettivo fornito dal microambiente midollare, suggerendo un futuro ruolo di questa sostanza quale possibile agente terapeutico per la cura della LLC-B.

# INTRODUCTION

## 1. B-cell Chronic Lymphocytic Leukemia (B-CLL)

### 1.1 Epidemiology and etiology

B-cell Chronic Lymphocytic Leukemia (B-CLL) is a lymphoproliferative disorder characterized by the accumulation of long-lived monoclonal B cells in the bone marrow, lymph node and blood. B-CLL lymphocytes show a CD19+/CD5+/CD23+ membrane phenotype and are blocked in G<sub>0</sub>/G<sub>1</sub> phase of the cell cycle<sup>1</sup>. B-CLL is the most common adult leukemia in the Western world and is more prevalent in men than in women with a male to female ratio of 1.5-2:1. The incidence rates between men and women are 5.6 (in men) and 4.3 (in women) cases per 100,000 inhabitants per year, respectively. In Europe, these incidence rates are 5.87 and 4.01 cases per 100,000 population per year, respectively. B-CLL is considered to be mainly a disease of the elderly, with a mean age at diagnosis of 70 years; however, it is not unusual to diagnose it in younger individuals from 30 years of age. The incidence increases rapidly with increasing age<sup>2</sup>.

The etiology is still unknown; the exposure to common carcinogens does not seem to be associated with the disease progression. More studies are in progress to assess a potential relation among B-CLL onset, inflammation, and autoimmune conditions<sup>3,4</sup>. A familiarity of this pathology is well documented in the 5-10% of cases. Moreover, it has been highlighted the phenomenon of the anticipation in which inherited disease is diagnosed at an earlier age and in a more aggressive form in the later generations of a family<sup>5</sup>.

### 1.2 Clinical features

Clinical course and survival of B-CLL patients are quite variable: some patients remain asymptomatic without any treatment, while others present an

aggressive outcome that is difficult to control with chemotherapy. B-CLL is often determined with routine laboratory tests; in other cases, the pathology occurs with asthenia, weight loss, fever, lymphadenopathy, splenomegaly, and hepatomegaly. Some patients could show autoimmune phenomena, such as hemolytic anemia (11% of cases) or autoimmune thrombocytopenia (2% cases) that are typically present in advanced and multi-treated disease. The typical B-CLL hypogammaglobulinemia could induce immunodeficiency and high mortality for infections<sup>6,7</sup>.

Although the causes of death are often attributed to the underlying disease, in some cases progressing syndromes with a poor prognosis could occur: one of these is the Richter's syndrome in which B-CLL changes into a fast-growing diffuse large B cell lymphoma. Another evolution could be the B-cell prolymphocytic leukemia (B-PLL) that is more aggressive and characterized by malignant B cells larger than average. The occurrence of acute lymphoblastic leukemia is very rare, while acute myeloid leukemia, such as non-hematological disease, could be correlated with B-CLL immunological deficit and chemotherapy<sup>8</sup>.

### **1.3 Diagnosis**

It is crucial to verify that the patient is really suffering from B-CLL and not by another lymphoproliferative disease that can masquerade as a B-CLL, such as hairy cell leukemia, or leukemic manifestations of mantle cell lymphoma, marginal zone lymphoma, splenic marginal zone lymphoma with circulating villous lymphocytes, or follicular lymphoma. To achieve this, it is essential to evaluate the blood count, blood smear, and the immune phenotype of the circulating lymphoid cells. The National Cancer Institute diagnostic criteria include<sup>9</sup>:

**1)** the presence of at least  $5 \times 10^9$  B lymphocytes/L (5,000/ $\mu$ L) in the peripheral blood. Leukemic cells found in the blood smear are characteristically small, mature lymphocytes with a narrow border of cytoplasm and a dense nucleus, lacking discernible nucleoli, with partially aggregated chromatin. These cells may be found mixed with larger or atypical cells, broken cells, or prolymphocytes,

which may comprise up to 55% of the blood lymphocytes. Finding a higher percentage of prolymphocytes would favour a diagnosis of B-PLL. Gumprecht shadows, found as cell debris, are other morphological features found in B-CLL (figure 1);

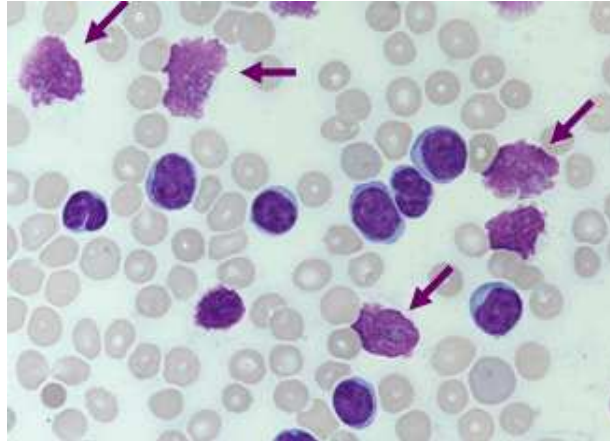


**Figure 1. Peripheral blood smear of a B-CLL patient.** Arrows indicate Gumprecht shadows typical of B- CLL.

2) bone marrow lymphocytic infiltration >30% (figure 2). This criterion is not essential in the case of a blood count <5,000/ $\mu$ L. However, the diagnosis should be confirmed by histopathologic evaluation of lymph node or bone marrow biopsy whenever possible. Marrow infiltration can occur in four configurations: diffuse, nodular, interstitial, and mixed. Nodular pattern suggests an early stage of the disease, while diffuse and interstitial patterns are typical of advanced stages;

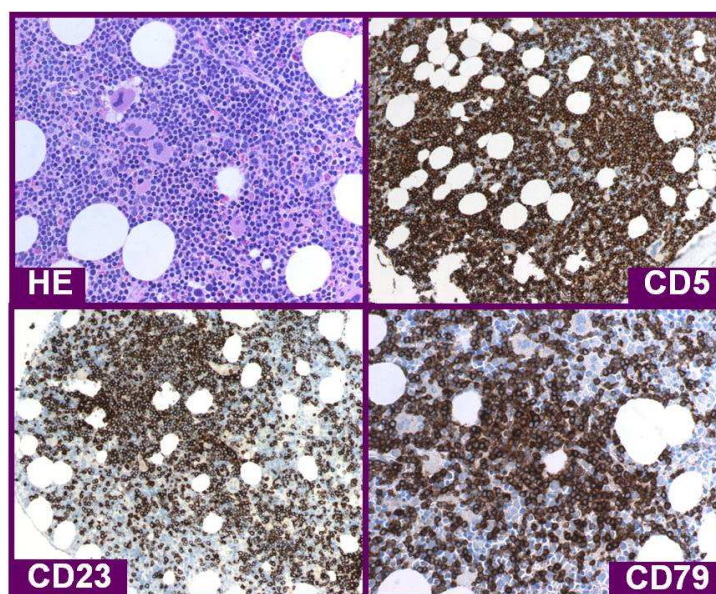


**Figure 2. Marrow biopsy of a B-CLL patient.** Preparation stained with hematoxylin-eosin (HE) and three immunohistological pictures that show some diagnostic markers.

3) immunophenotype analysis. B-CLL phenotype is characterized by three elements:

- a) the expression of a unique type of immunoglobulin light chains ( $\kappa$  or  $\lambda$ );
- b) the co-expression of the T-cell antigen CD5 and the B-cell surface antigens CD19, CD20, and CD23; CD23 is of particular importance in the differential diagnosis with mantle cell lymphoma (CD5+ but CD23-);
- c) low levels of CD79b and surface immunoglobulin (sIg) that in B-CLL appear to be mainly IgM followed by IgD, IgG, and IgA; it is not unusual to find an IgM and IgD co-expression (figure 3).

In B-CLL, T lymphocytes, in particular CD8+ T cells, are often increased, with a reduced CD4/CD8 ratio. They show activation markers such as CD25 and HLA-DR. Natural-Killer (NK) cells (CD16+/CD56+) are present in high levels. Several analyses are performed to confirm the diagnosis and to prevent complications: serum protein electrophoresis, Ig dosage, Coombs' test, and analysis of renal and liver function. Before starting an immunotherapy, it is important to assess the absence of viral infection (HBV, HCV, CMV)<sup>10</sup>.

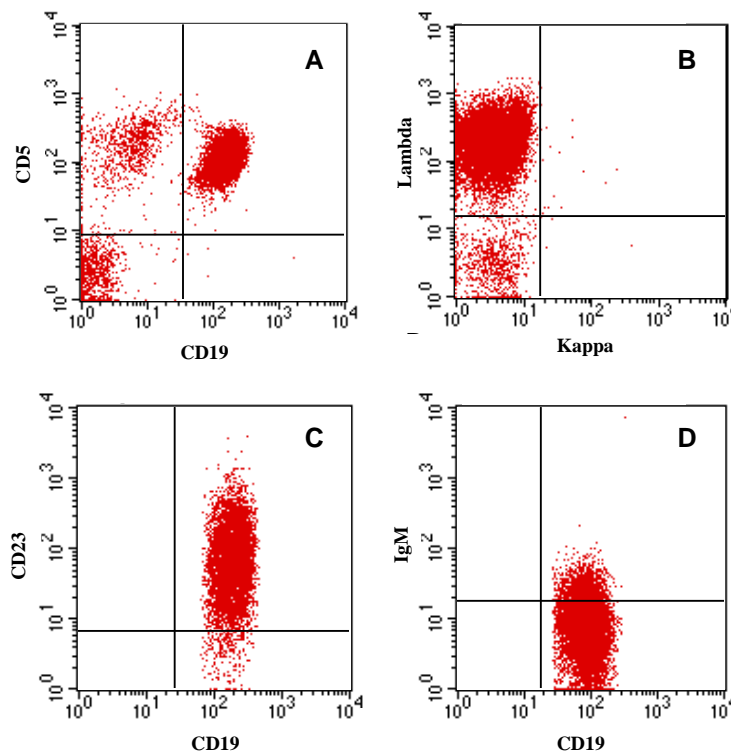


**Figure 3. Cytograms of a representative case of B-CLL.** B lymphocytes analyzed (CD19+) are positive to CD5 (panel A) and to CD23 (panel C), express one type of immunoglobuline light chain ( $\lambda$ , panel B), and surface IgM (sIgM), low density (panel D).

## 1.4 Prognosis

Since it is difficult to predict the course of the disease at the time of diagnosis and the value of an early treatment is uncertain, therapy is currently recommended only for patients with a disease progressive, symptomatic, or both<sup>11</sup>. During the years, different parameters or prognostic factors were proposed to define the clinical course of B-CLL patients.

### 1.4.1 Clinical prognostic factors

1) **Clinical staging:** There are two widely accepted staging methods in both patient care and clinical trials: the Rai and the Binet system. The original Rai classification was modified to reduce the number of prognostic groups from 5 to 3. Both systems now describe 3 major subgroups with different clinical outcomes. These 2 staging systems are simple, inexpensive, and can be applied by physicians worldwide. Both rely exclusively on physical examination and standard laboratory tests and do not require ultrasound, computed tomography (CT), or magnetic resonance imaging<sup>9</sup>.

The Rai system is so developed:

- **low-risk disease (stage 0):** absolute lymphocytosis  $>15,000/\mu\text{l}$  and marrow lymphocytosis  $>40\%$ ;
- **intermediate-risk disease (stage I or II):** lymphocytosis, enlarged nodes in any site, and splenomegaly and/or hepatomegaly (lymph nodes being palpable or not);
- **high-risk disease (stage III or IV):** disease-related anemia ( $\text{Hb} < 110\text{g/L}$ ) or thrombocytopenia (as defined by a platelet count  $< 100 \times 10^9/\text{L}$ );

The Binet system is based on the number of involved areas, as defined by the presence of lymph nodes with a diameter greater than 1 cm or organomegaly, and the presence of anemia or thrombocytopenia. It is subdivided into:

- **Stage A.**  $\text{Hb} \geq 100\text{g/L}$  ( $10\text{g/dL}$ ), platelets  $\geq 100 \times 10^9/\text{L}$ , and up to 2 lymph node areas involved.

- **Stage B.** Hb $\geq$ 100g/L, platelets $\geq$ 100x10<sup>9</sup>/L, and lymphadenopathy greater than that defined for stage A (i.e., 3 or more areas of nodal or organ enlargement).
- **Stage C.** All patients who have Hb<100g/L and/or a platelet count<100x10<sup>9</sup>/L, irrespective of lymphadenopathy.

**2) Lymphocyte doubling time:** it is less than 12 months and it is associated with a worse clinical course.

**3) Bone marrow infiltration:** a diffuse infiltration pattern correlates with a bad prognosis<sup>12</sup>.

#### 1.4.2 Biological prognostic factors

The less recent biological prognostic factors are correlated with the expansion of the leukemic clone; they thus become indicative only when the disease is worsening. Their utility is limited because it is not possible to program the therapeutic strategy basing on the progression risk of patients. The biological prognostic factors comprehend:

**1) Polymphocyte (PL) percentage:** if it is less than or equal to 10% (typical B-CLL) the probability of PL leukemia evolution is very low; if the percentage is between 11% and 55% there is an intermediate risk of B-CLL/PL leukemia, and if it is greater than 55% the transformation in PL leukemia may occur<sup>13</sup>.

**2)  $\beta$ 2 microglobulin:** this parameter is inversely correlated with the survival. It is related with the lymphocyte doubling time so that an increase in  $\beta$ 2 microglobulin indicates an high neoplastic cell proliferation<sup>13</sup>.

**3) Thymidine kinase (TK) level:** it has been shown that elevated serum thymidine kinase (s-TK) levels predict disease progression in B-CLL. Patients with s-TK values greater than 7.1U/L have a median progression free survival (PFS) of 8 months, whereas patients with s-TK values  $\leq$ 7.1U/L expect a much longer PFS<sup>14</sup>.

**4) Soluble CD23 value:** serum CD23 level provides significant additional prognostic information in terms of overall survival (OS) in B-CLL. Among early

stage patients, sCD23 determination, at diagnosis and during the course of the disease, may help to the early identification of patients who will rapidly progress to upper stages. Functions ascribed to sCD23 include prevention of germinal center (GC) B cells from their apoptosis, proliferation of myeloid precursor cells, and, more recently, costimulation of interferon- $\gamma$  (IFN- $\gamma$ ) production by T cells and triggering of monokine release by monocytes<sup>15</sup>.

The progressive discoveries on B-CLL pathogenesis have identified new prognostic markers that can better determine the clinical course. They describe biological characteristic of leukemic clone that are crucial to evaluate its proliferation and invasion capability. The study of these markers is performed by flow cytometry, cytogenetic and molecular biology techniques. The main markers are:

**1) Somatic Hypermutations (SHM) of the Ig heavy chain variable region (V<sub>H</sub>) genes.** Based on the numbers of somatic mutations detected in these genes, the cases were divided into 2 categories: "unmutated" (SHM-) or "mutated" (SHM+) (figure 4). Conventionally, patients with <2% differences from the most similar germline gene in both the expressed V<sub>H</sub> and V<sub>L</sub> genes were define unmutated; mutated cases were defined as those in which the B-CLL cells displayed  $\geq 2\%$  differences in either the expressed V<sub>H</sub> or V<sub>L</sub> gene<sup>16</sup>. In addition, the stereotyped V<sub>H</sub>3.21 gene is an unfavorable prognostic marker independent of the IgV<sub>H</sub> mutational status. However, this result has been highlighted especially in patients living in Northern Europe, while it was not confirmed in Mediterranean countries<sup>9</sup>.

**2) CD38 expression.** CD38 is a transmembrane glycoprotein expressed on the surface of cells in a significant percentage of patients with B-CLL. A previous study suggested that CD38 expression has prognostic value in B-CLL. Cases with CD38+ B cells >30% show a bad prognosis. Indeed, the cut-off to discriminate CD38+ to CD38- is not unanimously defined: some authors place it at 20%<sup>17</sup> or to 7%<sup>18</sup> of CD38+ B cells. CD38 has an independent prognostic value. Moreover, variability is the limit of this marker, in particular after treatment: chemotherapy

affects mainly CD38<sup>-</sup> cells, determining an increase of CD38<sup>+</sup> cells in a second time<sup>16</sup>.

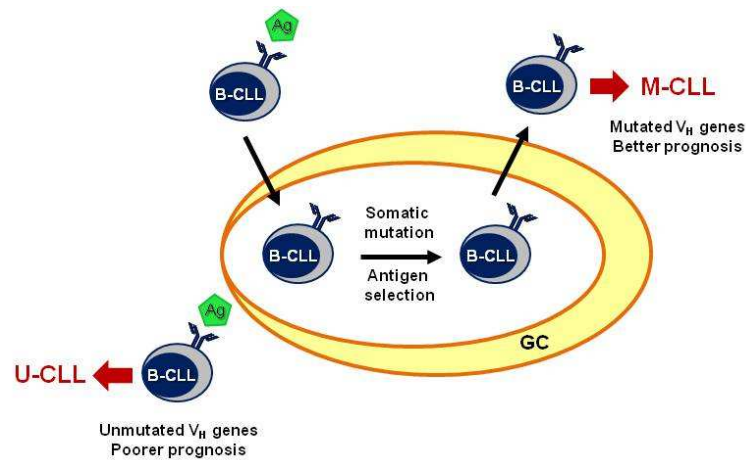


**Figure 4. Hypothesis on origins and features of the 2 subsets of chronic lymphocytic leukemia.** The development of unmutated B-CLL (U-CLL) is likely to be from a naive B cell that has encountered antigen but with insufficient stimulus to form a germinal center (GC). This subset has a poorer prognosis. In contrast, mutated B-CLL (M-CLL) develops from a cell that, following antigen encounter, has undergone somatic mutation and presumably antigen selection in the GC. The final neoplastic event is likely to have occurred after exit from the GC. This subset has a better prognosis. (Modified from Stevenson *et al.*<sup>19</sup>)

**3) Intracytoplasmatic expression of protein kinase associated to TCR  $\zeta$  chain of 70kDa (ZAP-70).** Zeta-associated protein of 70kDa (ZAP-70) is a cytoplasmic tyrosine kinase which is a key signaling molecule for T lymphocytes and NK cells. ZAP-70 expression may reflect an activation state of the malignant clone associated with progressive disease or may be involved in B-CLL progression because of its function as a tyrosine kinase that can signal downstream of many surface receptors. The expression of ZAP-70 may change over time in B-CLL, in particular during clinical progression, suggesting the interest in the evaluation of ZAP-70 during the evolution of the disease<sup>20</sup>. ZAP-70 expression analysis can be performed with different methods: flow cytometry, immunohistochemistry, western blotting, and Real-Time PCR. Among these, flow cytometry is the most advantageous for its diffusion and easiness of application. Anyhow interlaboratory variation is large and there is neither a consensus nor a regulatory approved methodology<sup>21</sup>.

**4) Chromosomal alterations.** Deletions (11q22-23, 17p13, 13q14, 6q21) and chromosome 12 trisomy are the most frequent chromosomal alterations in B-CLL (figure 5). Clonal genomic aberrations can be identified in approximately 80% of B-CLL patients by fluorescence *in situ* hybridization (FISH). The prevalence of

the most common alterations was estimated in a German multicentre study<sup>22</sup>: 13q- 55%, 11q- 18%, +12 16%, 17p- 7%, 6q- 7%. 17p- and 11q- are independent prognostic factors identifying subgroups of patients with rapid disease progression and short survival times in multivariate analysis, whereas 13q- as a single aberration is associated with favorable outcome. In addition, 17p- abnormalities and TP53 mutations have been associated with treatment failure. The presence of chromosome alterations with high risk justifies the use of more aggressive treatment<sup>23</sup>. Chromosome alterations are independent from IgV<sub>H</sub> mutational status though is evident a more frequency of 11q- and 17p- in unmutated and 13q- in mutated cases. These data show that analysis conducted by cytogenetics could be used as further risk stratification instrument together with the other prognostic factors<sup>24</sup>.

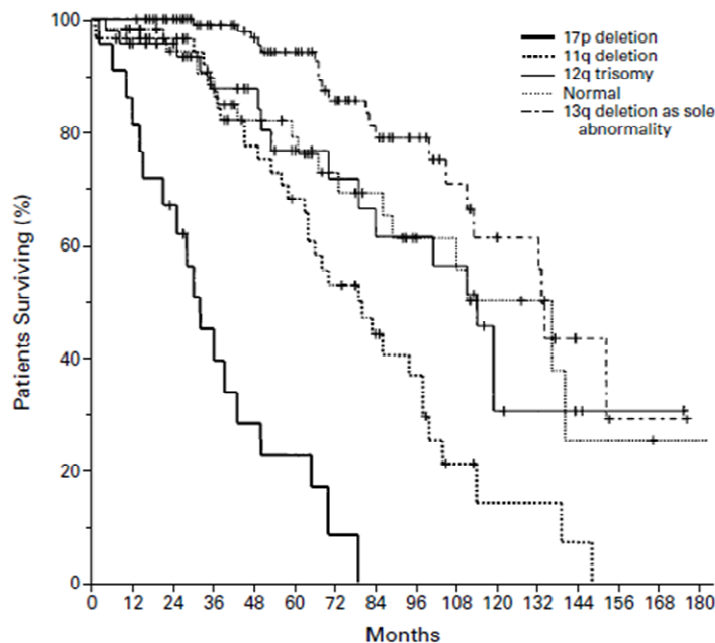


**Figure 5. Probability of survival among patients in the most common chromosomal alterations.** The median survival times for the groups with 17p deletion, 11q deletion, 12q trisomy, normal karyotype, and 13q deletion as single abnormality were 32, 79, 114, 111, and 133 months, respectively<sup>25</sup>.

**5) Telomerase expression and telomere length in B-CLL.** Activation of telomerase reverse transcriptase (hTERT) is essential for unlimited cell growth and plays a critical role in tumorigenesis<sup>26</sup>. Recently, the levels of telomerase activity (TA) and/or hTERT expression were related to clinical aggressiveness and prognosis in a variety of malignancies, including B-CLL.

During the last year, a study analyzed for the first time both hTERT levels and telomere length, and related them with IgV<sub>H</sub> mutational status and chromosomal aberrations in a large cohort of B-CLL patients. Although the main function of hTERT is to stabilize telomere length, an inverse relationship between hTERT levels and telomere lengths was found in B-CLL cases; B-CLL cases with high telomerase levels and short telomeres were frequently characterized by an unmutated IgV<sub>H</sub> status and high-risk chromosomal aberrations. Conversely, B-CLL cases with low telomerase levels and long telomeres were associated with a mutated IgV<sub>H</sub> status and low-risk abnormalities. Moreover, the unmutated IgV<sub>H</sub> B-CLL cases with short telomeres had higher levels of hTERT than the mutated IgV<sub>H</sub> cases with long telomeres. Unmutated IgV<sub>H</sub> status, 11q- or 17p- and +12 aberrations, high levels of hTERT, and low telomere length were all associated with a poor clinical outcome. Finding that the 13q-, characterized by low levels of hTERT, was associated with a prognosis even better than the normal group, supports the notion that hTERT may contribute to lymphomagenesis beyond just preservation of telomere length (figure 6). The evaluation of hTERT and telomere length might help the clinician in the management of B-CLL patients with mutated IgV<sub>H</sub> and/or no high-risk chromosomal aberrations since cases with high hTERT/short telomere B-CLL will progress more rapidly and might require therapy earlier than those with low hTERT/long telomeres<sup>27</sup>.

Recently, several microRNAs (miRNAs) have been proposed as prognostic markers for B-CLL and other human cancers. MicroRNAs are short (20-22 nucleotides in humans), endogenous non-coding single-strand RNA molecules that regulate gene expression via translational repression or transcript degradation and gene silencing. In particular, it was demonstrated that in B-CLL patients with an overexpression of the anti-apoptotic protein Bcl-2, miR-15a and miR-16-1 (localized in 13q14) are deleted or downregulated. Moreover, it was demonstrated that when B-CLL cells were transfected with miR-15a and miR-16-1, Bcl-2 is blocked and the normal apoptotic process is restored. Current studies aim to detect which miRNAs are involved in B-CLL in order to discover new prognostic factors as well as to develop new targeted gene therapy<sup>28</sup>.

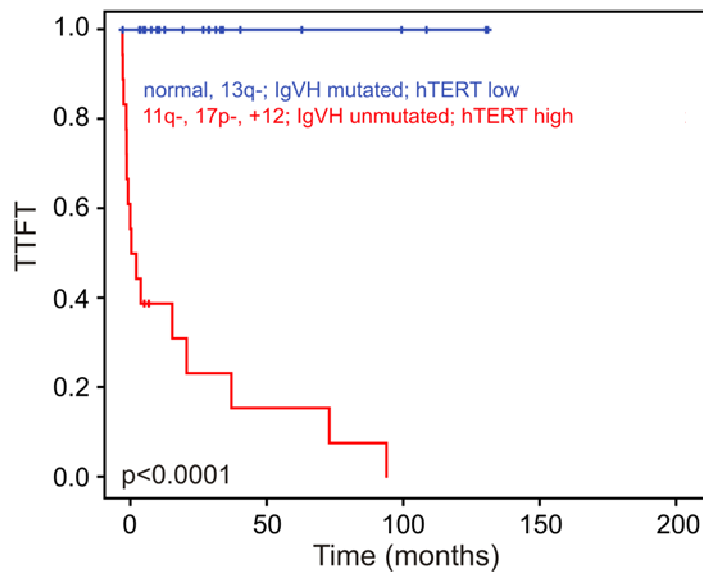


**Figure 6. Curves of treatment-free survival.** Time from diagnosis to first treatment (TTFT) according to IgV<sub>H</sub> mutational status, chromosomal categories, and hTERT level/telomere length profile<sup>27</sup>.

## 1.5 Treatment

Criteria for initiating treatment depend on clinic symptoms, stage and disease activity. In general practice, newly diagnosed patients with asymptomatic early-stage disease (Rai 0, Binet A) should be monitored without therapy unless they have evidence of progression. On the contrary, patients at intermediate (I and II) and high risk stages (III and IV), according to the modified Rai classification or at Binet stage B or C, usually benefit from the start of a treatment; some of these patients (in particular Rai intermediate risk or Binet stage B) can be monitored without therapy until they have evidence for progressive or symptomatic disease<sup>9</sup>.

Therapeutic possibilities comprehend drugs with different mechanisms of action, up to stem cells auto/allotransplantation. Since B-CLL is an incurable disease, current therapy is intended control the expansion of the neoplastic clone. The choice of the therapy is linked to patient age and general conditions. In older patients (>65) primary treatment consist of Chlorambucil (10mg/die for 1-4 weeks) associated with Prednisone (25mg/die for 1-4 weeks), while in other cases the therapy is based on Fludarabine, alone or in association with Cyclophosphamide. Chlorambucil treatment induces a response in 70% of cases, but only 10% shows a complete response (CR) and has no effect on survival;

these considerations make it suitable for palliative treatment. Steroids have not demonstrated a significant effect on survival, while their side effects, such as opportunistic infections, are well known. However, they are useful to contain autoimmune complications.

During the past years, basing on the experience on other lymphomas, therapeutic combinations such as CHOP (Cyclophosphamide, Vincristine, Prednisone, and Adriamycin) or COP (Cyclophosphamide, Vincristine, and Prednisone) were tested; although they display a high frequency of CR in respect of an increased toxicity, they did not improve survival<sup>29</sup>.

From the mid of '90 years, the first line treatment for B-CLL was the use of purine analogous. This class of drugs comprehends Pentostatin, an adenosine deaminase inhibitor, Clabridine, Fludarabine, and DNA-polimerase inhibitors. The more effective in B-CLL treatment is Fludarabine (25-30mg/die for 5 days, 3-6 month); 80% of cases show global response, and 30% a CR. Moreover, the time of remission is greater than the one obtained with Chlorambucil plus Prednisone<sup>30</sup> (figure 7).

Despite the positive overall response, Fludarabine and purine analogous are not so effective in improving the survival rate than Chlorambucil or alkylating agents<sup>31-33</sup>. The US Intergroup Trial has recently demonstrated that the combination of Cyclophosphamide and Fludarabine, compared to Fludarabine alone, gives higher overall responses (74.3% vs 59.5%), CR (23.4% vs 4.6%), and PFS (31.6 vs 19.2 months). Conversely, the combination of the two drugs resulted in a greater bone marrow toxicity, neutropenia, anemia, and thrombocytopenia with infectious complications<sup>34</sup>.

Monoclonal antibodies provided a significant advantage in the treatment of hematological malignancies. CD20, a surface membrane phosphoprotein, has become the preferred target of immunotherapy. The chimeric mouse anti-human monoclonal antibody Rituximab (IDEC-C2B8) is specific for the CD20 antigen and has been used in clinical trials to treat patients with Non-Hodgkin Lymphoma (NHL). Preclinical studies identified the ability of Rituximab to increase the effectiveness of cytotoxic drugs in resistant cell lines, blocking the anti-apoptotic signaling. The combination of Rituximab with other drugs results in a synergistic cytotoxicity and apoptosis<sup>35</sup>; Fludarabine, in fact, downmodulate the complement-

resistance proteins CD46, CD55, and CD59 on leukemia cells, thereby potentially making cells more vulnerable to Rituximab-induced complement-mediated lysis<sup>36</sup>. The combination of Rituximab with Fludarabine and Cyclophosphamide was evaluated both as initial therapy in those cases of recurrent or refractory to prior therapies. In previously untreated patients, PFS is greater than four years in about 2/3 of cases<sup>37</sup>. Rituximab side effects are essentially related to the intravenous infusion of cytokines (fever, chills, nausea, and hypotension). Alemtuzumab (Campath-1H) is a humanized anti-CD52 antibody; CD52 is expressed at high levels on most of normal and malignant mature lymphocytes but not on hematopoietic stem cells. It can be administered subcutaneously and it is very effective in inducing remission in relapsing B-CLL patients<sup>38</sup>. However, Campath-1H may cause a marked immunosuppression that require prophylactic therapy for *Pneumocystis carinii*, VZV, and CMV infections. The association with Fludarabine and Cyclophosphamide is burdened by significant toxicity to bone marrow, so precautions are necessary during Alemtuzumab administration.

The expression of the anti-apoptotic protein Bcl-2 is associated with the pathogenesis of B-CLL. As negative regulator of the intrinsic apoptotic pathway, overexpression of Bcl-2 confers chemoresistance in a number of hematologic cancers and solid tumors<sup>39</sup>. Although protein levels vary among cells and patients, Bcl-2 is expressed in virtually all patients with B-CLL and Bcl-2 upregulation plays a critical role in this disease. Deletion of miRNA regulators of Bcl-2 expression is frequently found in B-CLL cells also in association with Bcl-2 upregulation. Oblimersen, an antisense oligonucleotide that binds Bcl-2 mRNA, induces enzymatic cleavage of the mRNA preventing protein translation<sup>39</sup>.

Allogeneic and autologous stem cell transplantation (SCT) are increasingly considered for treatment of B-CLL patients. With appropriate supportive care, it is safe and can induce a long-lasting clinical and molecular remissions. Feasibility of autologous SCT appears to be best early during the course of the disease, but there is only limited hope that autotransplantation can cure the disease<sup>40</sup>.

Cytokines support from the malignant microenvironment prolong B-CLL cell survival, immune evasion, and resistance to therapy. Interrupting these prosurvival effects from the malignant microenvironment is a potential new approach in treating patients with B-CLL. Lenalidomide, a thalidomide analogue,

is an immunomodulating drug (IMiDs) with antitumor activity reported in various malignant disorders including multiple myeloma (MM) and myelodysplastic syndrome (MDS). Lenalidomide is also reported to modulate an immune response effector cells through the activation of T and NK cells, through directly inducing apoptosis in tumor cells. The immune properties activated by Lenalidomide make Lenalidomide itself an attractive therapeutic drug to add to Rituximab<sup>41</sup>. In addition to cytoreductive therapy, B-CLL treatment includes substitutive and support therapy, such as red cells and platelets transfusions, antibiotic therapy, and intravenous immunoglobulin administrations.

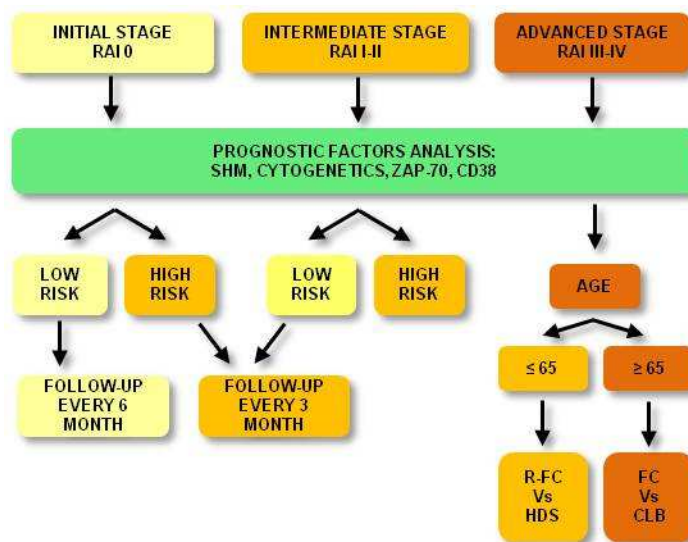


**Figure 7. Possible decisional pattern in B-CLL treatment.** R-FC: Rituximab, Fludarabine, Cyclophosphamide; HDS: High Doses Chemotherapy; CLB: Chlorambucil.

## 2. Neoplastic B lymphocytes

B-CLL is a disease characterized by an extremely heterogeneous clinical course, despite a substantial morphologic and immunophenotypic uniformity.

B cells are lymphocytes that participate in humoral immunity by producing antibodies (Abs) in response to antigen (Ag) stimulation. They can differentiate from "naive" lymphocytes to cells secreting antibodies against specific antigens (plasma cells), or to "memory" long-lived stimulated B lymphocytes that are ready for rapid response to a repeated exposure of the priming antigen.

The B-Cell Receptor (BCR) mediates antigen recognition. BCR is a multimeric complex composed by an sIg homodimer that is linked to plasmatic membrane<sup>24</sup> through its constant region (crystallizable fragment, Fc); the sIg antigen binding region (Fab) is outward and noncovalently linked to Ig $\alpha$ /Ig $\beta$  (CD79a/CD79b) heterodimer, deputy to intracellular signal transduction<sup>42</sup> (figure 8). The Fab region comprehends variable regions (V) of sIg light and heavy chains that give BCR specificity for a specific antigen. In turn, V regions are composed by three ipervariable regions, called "complementarity determining regions" (CDR) that allow high affinity binding with the antigen.

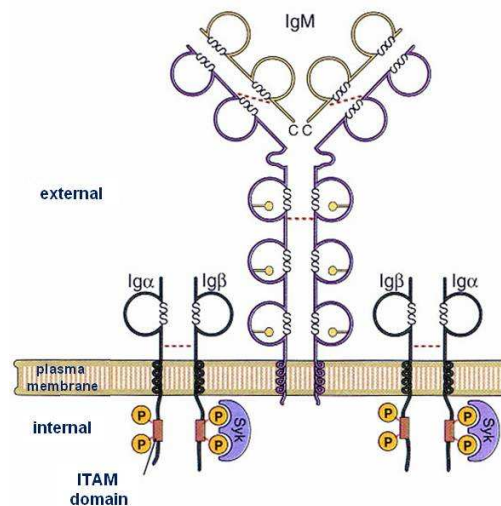


**Figura 8. Schematic representation of the BCR.** The complex is composed by a sIg, and Ig $\alpha$  and Ig $\beta$  that mediate signal transduction after antigen binding.

What differentiates a "naive" B lymphocyte from a "memory" B lymphocyte is the fact that the "naive" one presents an amino acid sequence identical to "germline" sequence, while the "memory" one is characterized by a different sequence. This is due to somatic hypermutation process that underlies the phenomenon of affinity maturation.

Once recognized a specific antigen, the "naive" B lymphocyte turns on and begins to proliferate inside lymphoid organs. Some of this progeny enters the lymphoid follicles and forms the germinal centre (GC) characterized by an intense proliferation. Here, Ig genes undergo point mutations that lead to the formation of clones with different affinities for the antigen. Clones are selected through contact

with follicular dendritic cells expressing antigen: lymphocytes that bind antigen with greater affinity survive, while others undergo apoptosis.

B-CLL lymphocytes are small "memory" B cells blocked in  $G_0/G_1$  and characterized by surface markers recognized by specific monoclonal antibodies; some of these markers, such as CD19 and CD21, are B-related, while others, like CD5, CD23, CD25, and HLA-DR (human Leukocyte Antigen D-related), are not specific for B lymphocytes (figure 9). In particular, B-CLL cells express markers typical of mature B cells localized in the mantle zone of secondary lymphoid follicles.

Recent studies have shown that 50-70% of B-CLL have undergone  $IgV_H$  hypermutation, a phenomenon that characterizes normal B cells subjected to a T cell-dependent GC reaction. This finding has led to the hypothesis that B-CLL cases displaying mutated  $IgV_H$  may derive from a cell that had transited through the GC, whereas those with germline  $IgV_H$  may derive from a GC-independent cells. This hypothesis has both biological and clinical relevance since the two subgroups have different prognosis, with  $IgV_H$ -mutated B-CLL (M-CLL) displaying a better clinical course<sup>43</sup>. The factors involved in B-CLL pathogenesis comprehend control of apoptosis, signal transduction BCR-mediated, proliferative activity and the microenvironment.

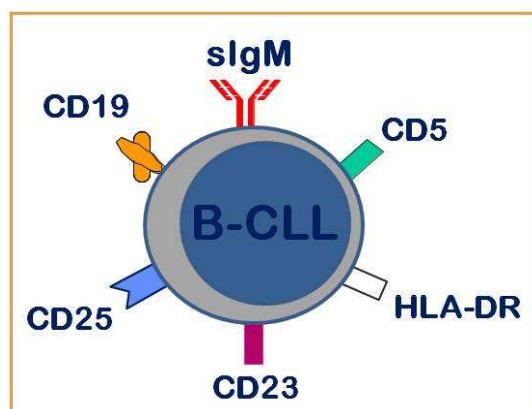


**Figure 9. Typical phenotype of a B-CLL lymphocyte.** CD19 is a B-related antigen, while CD23, CD25, CD5, HLA-DR and sIgM are not specific to the B lineage.

## 2.1 Control of apoptosis

The dysregulation of the process of programmed cell death (apoptosis) is now widely recognized as one of the main mechanism in the pathogenesis of

many tumors. The accumulation of B-CLL cells is related to the fact that they do not undergo apoptosis, thus failing the homeostatic mechanism that normally limits the number of circulating cells.

Paradoxically, when B-CLL cells derived from peripheral blood were cultured *in vitro*, a substantial proportion of them spontaneously died by apoptosis<sup>44</sup>. In this way, it is becoming increasingly clear that the B-CLL defective apoptosis has to be ascribed not only to intrinsic defects of the neoplastic cells, but also to extrinsic factors that influence their behavior. Malignant B cells retain the ability to respond to microenvironmental signals, but have devised a monothematic responsiveness. They have a specific sensitivity to anti-apoptotic signals that favour their survival and become insensitive to pro-apoptotic signals<sup>18</sup>. With respect to intrinsic factors, the balance between pro- and anti-apoptotic factors is very important. Among these, the principal apoptosis regulators are proteins of the Bcl-2 family (B-cell lymphoma-2 factors) that play a crucial role in this mechanism by inhibiting (Bcl-2, Bcl-x<sub>L</sub>, Bcl-w, Bfl-1, and Mcl-1) or promoting (Bax, Bak, Bcl-x<sub>S</sub>, Bid, Bik, and Hrk) apoptosis. Heterodimerization between pro- and anti-apoptotic members, and their relative levels, may determine the predisposition to respond to a given apoptotic stimulus (figure 10). Many investigators have reported altered expression of Bcl-2, Bax, and Mcl-1 in B-CLL<sup>45</sup>.

Other intrinsic factors, critical for apoptosis control, are 17p13 and 11q23 deletions containing 2 prominent tumor-suppressor genes mutated at varying proportions: TP53 (tumor protein 53) and ATM (Ataxia telangiectasia mutated), respectively. Mutations of TP53 and ATM, even in the absence of a chromosomal deletion, have been identified to have adverse effects on patient survival. p53 and ATM proteins are central regulators of the DNA-damage-response pathway and their activation leads to cell-cycle arrest and DNA repair, apoptosis, or senescence, depending on the cellular context. Impaired p53 function through mutations and/or deletions is the best-characterized factor associated with chemoresistance in B-CLL<sup>46</sup>.

Moreover, TOSO, also known as Fas-inhibitory molecule 3, was identified as a candidate gene overexpressed in B-CLL.

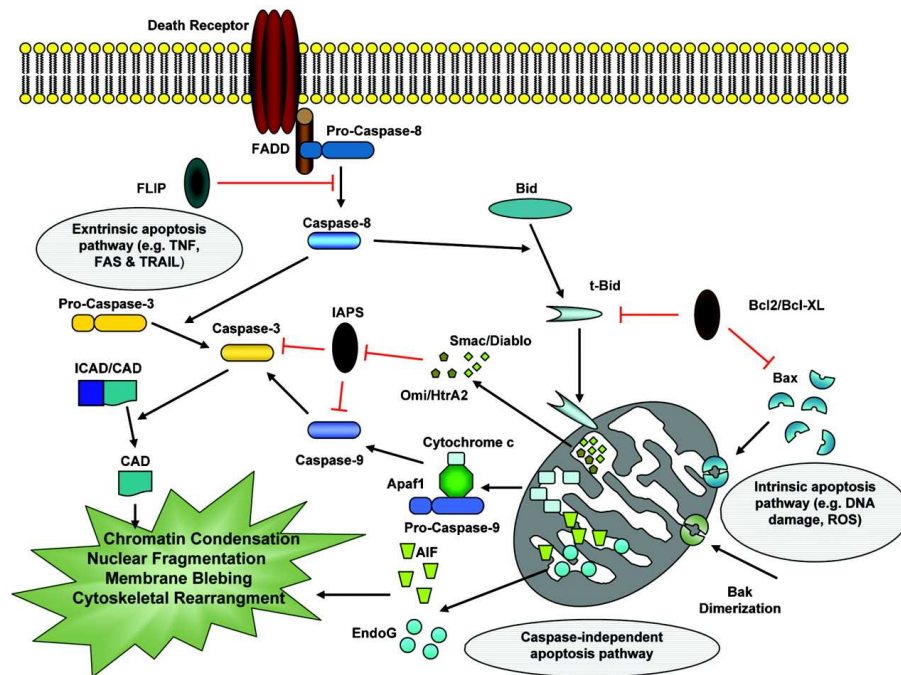


**Figure 10. The molecular mechanisms of apoptosis.** Apoptosis pathways can be initiated via different stimuli, that is, at the plasma membrane by death receptor ligation (extrinsic pathway) or at the mitochondria (intrinsic pathway). Stimulation of death receptors results in receptor aggregation and recruitment of the adaptor molecule Fas-associated protein with death domain (FADD) and caspase-8. Caspase-8 initiates apoptosis by direct cleavage of downstream effector caspases. Mitochondria are engaged via the intrinsic pathway, which can be initiated by a variety of stress stimuli, including ultraviolet (UV) radiation,  $\gamma$ -irradiation, heat, DNA damage, the actions of some oncoproteins and tumour suppressor genes (i.e. p53), viral virulence factors, and most chemotherapeutic agents. CAD, caspase activated DNase; FAS, fibroblast associated antigen. ICAD, inhibitor of CAD; ROS, reactive oxygen species; TNF, tumour necrosis factor; TRAIL, TNF related apoptosis inducing ligand<sup>47</sup>.

TOSO is a transmembrane protein that inhibits Fas-mediated apoptosis by binding Fas-associated death domain (FADD) via its C-terminal intracellular domain. In B-CLL, high levels of TOSO expression have been correlated with a more aggressive disease<sup>48</sup>.

## 2.2 BCR-mediated signal transduction

For effective humoral immunity, mature B cells must respond to foreign antigens and generate antigen-specific effector cells; so, it is not surprising that the BCR complex is required for the later stages of B-cell maturation. BCR has two main roles: the first is to transmit signals that regulate B-cell fate decision and the second is to mediate antigen processing leading to the presentation of antigen to T cells, which allows full activation of B cells in the effector phase. The BCR

complex consist of immunoglobulin heavy (IgH) and light (IgL) chains associated with Ig $\alpha$  and Ig $\beta$  containing ITAM (Immunoreceptor Tyrosine-based Activation Motif) domains. After BCR ligation by antigen, both the protein tyrosine kinases (PTKs) Syk and Lyn are activated. Then, Lyn phosphorylates ITAMs which, in turn, recruit and facilitate the activation of Syk and Tec-family PTKs. This phosphorylation results in the recruitment of other molecules involved in BCR-mediated signal transduction<sup>49</sup> (figure 11).

BCR signaling can be also regulated by the membrane organization of signaling components. Literature data proposed that in the absence of antigen binding, the BCR is already pre-assembled into oligomeric receptor complexes, which generate a basal level of signaling essential for B-cell maintenance<sup>50</sup>. The low levels of sIgs may explain the reduced ability of B-CLL cells to capture, present, and respond to antigen. Defects in the BCR of B-CLL have been attributed to functional deficiency in the CD79 heterodimer, especially CD79b, which is expressed at low levels on these tumor<sup>51</sup>. During B cells activation process, an important function is carried out by plasma membrane microdomains called lipid rafts. These domains are rich in glycosphingolipids and cholesterol which create a liquid-ordered phase within the plasma membrane. Lipid rafts are fluid at physiological temperatures, allowing lateral diffusion of proteins and lipids within the plane of the membrane. In addition, they are constitutively enriched in certain types of proteins such as glycosphingolipids-linked proteins and lipid chain-modified proteins, including heterotrimeric G proteins, the Src kinases Lyn and Fyn, and other molecules involved in signal transduction, such as Blk, Ras, c-Abl, and actin<sup>52</sup>.

Additional proteins, like CD45 and Syk, seem to be excluded from raft and recruited only after BCR translocation into them after the engagement by the Ag. In fact, according to the most recent model proposed to explain BCR functions in the activation of B cells, in resting B cells the BCR is initially excluded from lipid rafts; once having bound the antigen, BCR translocates into the rafts thus starting the signal transduction cascade.

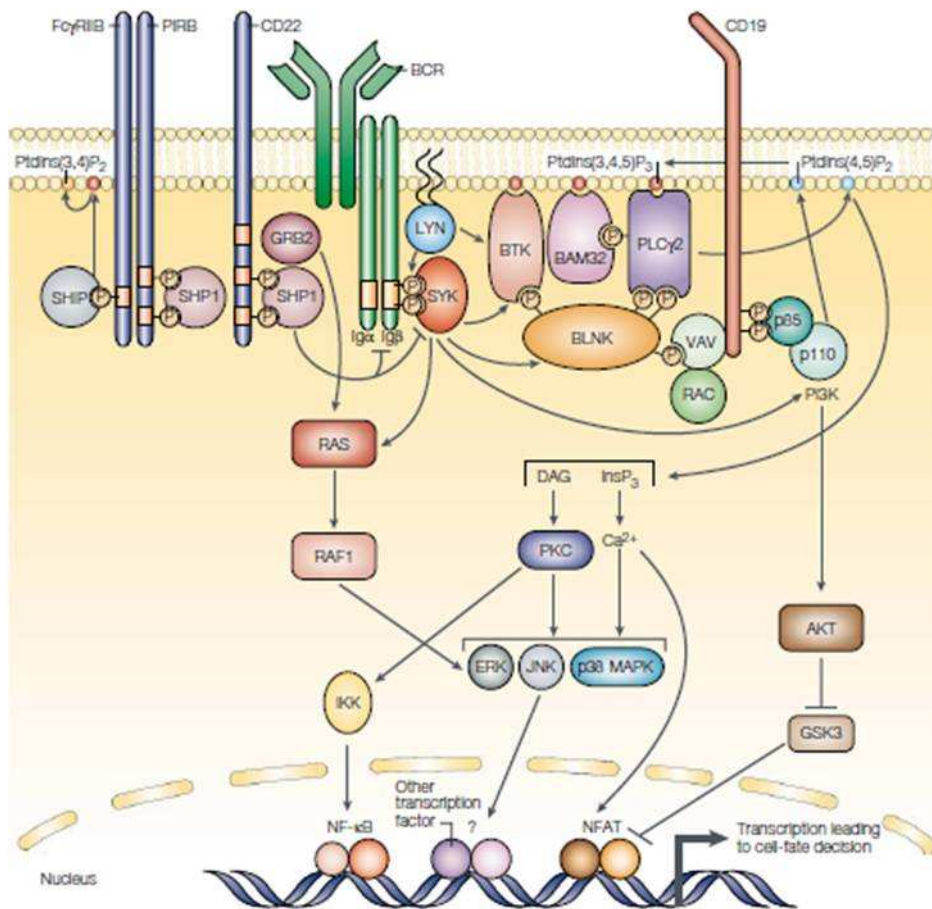


**Figure 11. BCR-induced signal transduction pathways.** After antigen ligation, tyrosine-kinase Lyn phosphorylates ITAMs of Ig $\alpha$  and Ig $\beta$ , creating binding sites to protein SH2 domain, such as Syk kinase. Follow different biochemical reactions that culminate in the B cell activation, differentiation and/or proliferation<sup>49</sup>

Lyn is a Src-family tyrosine kinase, which, with Blk and Fyn Src-like kinases, is necessary for BCR signaling considering its role in phosphorylation of the ITAM on Ig $\alpha$ /Ig $\beta$ . Tyrosine phosphorylated Ig $\alpha$ /Ig $\beta$  recruits Syk via the latter's tandem SH2 domains leading to downstream signaling events. Lyn also provide feedback inhibition of BCR signaling by phosphorylation of cell surface proteins containing immunoreceptor tyrosine-based inhibitory motifs (ITIMs). These ITIM-containing inhibitory receptors include the inhibitory Fc receptor for IgG, Fc $\gamma$ RIIb, and the sialic acid-binding protein expressed on B cells, CD22. The phosphorylation of these ITIMs generates binding sites for the membrane recruitment of phosphatases that inhibit BCR signaling, including the SH2-domain-containing inositol phosphatase (SHIP-1) and the SH2-domain-containing tyrosine phosphatase (SHP-1). The net result of Lyn-deficiency is an exaggerated

signaling by the BCR, a phenotype that is moderate in immature B cells and highly pronounced in mature follicular B cells. Lyn also acts inhibiting receptor signaling in myeloid cells and recent studies demonstrated that hyperactivity of myeloid cells contributes, in a relevant manner, to autoimmunity in *Lyn*<sup>-/-</sup> mice<sup>53</sup>. In B lymphocytes, Lyn may also be associated to the non-receptor tyrosin-kinase Fak (Focal Adhesion Kinase), involved in different signal transduction cascades. This complex may contribute to cytoskeletal reorganization after antigen binding<sup>54</sup>.

Our group demonstrated that in B-CLL, as compared to normal B cells, protein Lyn is upregulated and shows a different subcellular localization<sup>55</sup>. Moreover, Lyn displays a remarkable constitutive activity, which leads to an increased basal tyrosine protein phosphorylation and a low responsiveness to BCR ligation. Whereas Lyn was concentrated in membrane lipid rafts in normal B cells, the enzyme was present all over the cell surface membrane in B-CLL cells. Lyn was also detected in the cytosol of the malignant B cells. The release of Lyn into the cytosol following caspase-dependent cleavage of the tyrosine kinase at its N-terminus has been described as a general mechanism in hematopoietic cells during BCR-induced apoptosis<sup>56</sup>. The findings that B-CLL cells contain a cytosolic Lyn fraction and are defective in programmed cell death suggest that the tyrosine phosphorylation of specific cytosolic targets might account, at least in part, for cell resistance to apoptosis.

The activity of Lyn is critically regulated through its C-terminal Tyr507, which is phosphorylated by the tyrosine kinase Csk and dephosphorylated by the receptor tyrosine phosphatase CD45. In resting B lymphocytes, Lyn is present in its inactive conformation, as result of Csk phosphorylation of Tyr507, which gives rise to an intramolecular association of the phosphorylated residue with Lyn's own SH2 domain<sup>57</sup>. Since Csk, unlike Lyn, was similarly expressed in normal and B-CLL cells, the constitutive activity of Lyn could be due to the fact that the amount of Csk is insufficient to phosphorylate and downregulate its overexpressed substrate. However, it is likely that other factors are responsible for the presence of the active form of Lyn in B-CLL cells, first among which might be the dephosphorylation of Lyn at Tyr507 by the tyrosine phosphatase CD45, an abundant membrane protein that, in normal B cells, has access to Lyn only after

its migration to lipid rafts induced by BCR engagement<sup>52</sup>. Furthermore, the high concentration of Lyn in B-CLL cells could promote the kinase intermolecular autophosphorylation at Tyr396, which in turn induces Lyn activation<sup>58</sup>.

It is known that, after activation, SFK level is regulated by the balance of two opposing mechanisms: degradation by ubiquitinylation or rescue by association with Hsp90 (Heat shock protein of 90kDa), a chaperone interacting with the N-terminal lobe of the SFK catalytic domain<sup>59</sup>. Recently, we demonstrated that, in B-CLL cells, Lyn is an integral component of an aberrant cytosolic 600kDa complex, where Lyn is associated both with Hsp90 through its catalytic domain, HS1 (Hematopoietic lineage cell Specific protein 1), and SHP-1L through its SH3 domain. Moreover, Hsp90 stabilizes the complex by contributing to converting a network of transient interactions into permanent ones, thus maintaining Lyn in an active conformation and preventing its degradation<sup>60</sup>.

HS1, one of the most important Lyn substrate, is an F-actin binding protein involved in the apoptosis of several hematopoietic cell lines. HS1 phosphorylation occurs in a sequential model mediated by Syk and Lyn. It seems that tyrosin-phosphorylation of cortactin, an HS1 homologous protein involved in cell motility, occur by the same mechanism of recruitment of the SFKs.

PI3K and PLC $\gamma$ 2 are both crucial effector enzymes that generate key second messengers in BCR signaling. PI3K phosphorylates phosphatidylinositol-4,5-bisphosphate (PtdInsP<sub>2</sub>) to produce phosphatidylinositol-3,4,5-trisphosphate (PtdInsP<sub>3</sub>), which, in turn, recruits some BCR signaling molecules to the membrane through PH domains. PLC $\gamma$ 2 uses PtdInsP<sub>2</sub> to generate inositol-1,4,5-trisphosphate (InsP<sub>3</sub>) and diacylglycerol (DAG), which are required for the release of intracellular calcium (Ca<sup>2+</sup>) and activation of protein kinase C (PKC), respectively. Subsequently, Ca<sup>2+</sup> flux and PKC activation induce the activation of mitogen-activated protein kinase (MAPK)-family kinases, extracellular signal-regulated kinase (ERK), c-JUN NH<sub>2</sub>-terminal kinase (JNK), p38 MAPK, and transcription factors, including nuclear factor- $\kappa$ B (NF- $\kappa$ B) and nuclear factor of activated T cells (NFAT). It is probable that the profile of these activated transcription factors then determines B-cell fate.

Non-enzymatic adaptor proteins are also important in regulating BCR signaling. Among them, B-cell linker (BLNK) efficiently connects Syk and Btk

with PLC $\gamma$ 2. Disruption of the BLNK gene leads to impaired activation of PLC $\gamma$ 2 in B cells; BLNK also associates with Vav and Nck, both of which regulate cytoskeletal organization in B cells.

Another B-cell adaptor, B-lymphocyte adaptor molecule of 32kDa (BAM32), also binds PLC $\gamma$ 2 and regulates its activation. Since it is recruited to the membrane in a PI3K-dependent manner, BAM32 integrates the PI3K and PLC $\gamma$ 2 pathways. The B-cell-specific co-receptor CD19 can work as an adaptor for PI3K also in B cells<sup>49</sup>.

In mature B cells, BCR associates with lipid raft after Ag engagement and the signal transduction induces transcription of genes responsible for B cell activation. Then, the BCR is internalized and can be degraded or sent to an intracellular compartment called MIIC (MHC-class-II-peptide-loading-compartment) where Ag processing and the synthesis of peptide-MHC complexes to Ag presentation occur. These complexes are brought to cell surface, presented to T cells and then recognized by TCR of Th cells which activate B cells through cytokines release.

In immature B cells, BCR is excluded from lipid rafts even after Ag binding and, in this case, cell apoptosis is induced. A behavior similar to that of immature B cells is described also to cells rendered tolerant or anergic by chronic exposure to Ag: BCR is still excluded from rafts even after Ag binding and the result is the lack of a cellular response. Conversely, in B pre-lymphocytes a significant proportion of BCR and signaling molecules, such as PLC $\gamma$ 2 and PI3K, are constitutively associated with rafts and this seems to generate signals of survival and cell differentiation. In these cases, molecule such as PI3K, RAS, RAF, ERK and NF- $\kappa$ B are fundamental in signal transduction in association with BCR. PI3K activates and phosphorylates Akt/PKB which, in turn, phosphorylate cellular targets involved in cell survival including apoptotic factors and glycogen metabolism. One function of Akt is to inhibit the activation of the pro-apoptotic Bcl-2-family member BAD (Bcl-2 antagonist of cell death); moreover, Akt phosphorylates and inhibits glycogen synthase kinase 3 (GSK3) in B cells. In unstimulated cells GSK3 is constitutively active; it phosphorylates and destabilizes Myc and cyclin D, both of which are required for cell-cycle

progression. In this way, it seems that Akt functions to promote BCR-induced cell proliferation, as well as survival<sup>49</sup>.

### **2.3 Proliferative activity and centrosome aberrations**

The conceptual framework of the biology of B-CLL cells has changed in the course of the past decade. The traditional view consider B-CLL as a disease deriving from an apoptosis defect in which slowly proliferating B lymphocytes accumulate because of a diminished cell death. In this view these cells are relatively inert and divide minimally, rarely dying; they continue to accumulate passively until they reached an harmful level not more supportable by the patient. However, recent studies suggest that B-CLL is a dynamic condition, comprising leukemic cells that multiply and die at measurable rates. Furthermore, since B-CLL cells do not appear to be inherently immortal, the impairment of the patient does not occur from passive accumulation, but from active generation of subclones that, over time, develop dangerous genetic abnormalities which further change birth/death ratio<sup>61</sup>.

The centrosome is a cellular structure essential for a proper proliferative activity; it is a small non-membranous organelle (1-2 $\mu$ m in diameter) often denoted as a major microtubule organizing center (MTOC). During interphase, the centrosome organizes an astral array of microtubules (MTs) that participate in intracellular trafficking, cell motility, cell adhesion, and cell polarity. In proliferating cells, the centrosome starts duplicating just before, or at, the onset of S phase and the two newly formed centrosomes participate in the assembly and organization of the mitotic spindle, its orientation with respect to cortical cues, and the late events of cytokinesis. The animal centrosome consists of a pair of centrioles linked together through their proximal regions by a matrix consisting in part of large coiled-coil proteins of the pericentrin family (pericentrin,  $\gamma$ -tubulin, ninein, centriolin, katanin), which anchor other matrix components (figure 12). The architecture of the microtubule array in differentiated cell types results not only from the dynamic behavior of MTs but also from a balance between MTs nucleation and MTs-anchoring activities at the centrosome. Microtubules are nucleated by the  $\gamma$ -tubulin ring that is present throughout the cell cycle in the

matrix, close to the proximal walls of centrioles. Its levels increase significantly prior to mitosis, concurrently with the recruitment of MT-associated proteins required for mitotic spindle formation<sup>62</sup>.

Normally, the single centrosome of a G<sub>1</sub> cell duplicates precisely once prior to mitosis in a process that is intimately linked to the cell division cycle via cyclin-dependent kinase (cdk) 2 activity that couples centrosome duplication to the onset of DNA replication at the G<sub>1</sub>/S transition. Accurate control of centrosome duplication is critical for symmetric mitotic spindle formation and thereby contributes to the maintenance of genome integrity.

Numerical and structural centrosome abnormalities are hallmarks of almost all solid tumors and have been implicated in the generation of multipolar mitoses and chromosomal instability. In addition to solid neoplasias, centrosome aberrations have been described in several different hematological malignancies like acute myeloid leukemias, MDS, Hodgkin lymphoma as well as NHL, MM, and B-CLL. A correlation between centrosome abnormalities on the one hand and karyotype aberrations as well as clinical aggressiveness on the other hand seems to exist in myeloid malignancies, B-CLL and at least in some types of NHL<sup>63</sup>.

It was demonstrated that centrosome aberrations are already present in B lymphocytes from patients with monoclonal B-cell lymphocytosis (MBL), a lesion considered to represent a premalignant stage of B-CLL, suggesting that centrosome abnormalities do occur early during B-CLL evolution. In analogy to other NHLs, centrosomal abnormalities of circulating B-CLL cells might reflect cellular generation emanated from proliferation centers in lymph nodes and bone marrow of B-CLL patients.

The detailed mechanisms by which centrosome aberrations develop are still largely unknown. Several oncogenes and tumor suppressor genes, among the p53 and ATM, have been implicated in the formation of centrosomal defects in human malignancies. Both p53 and ATM abnormalities are associated with a poor prognosis in this disorder. Therefore, it is tempting to speculate that aberrations of the ATM/p53 pathway might be involved in the generation of centrosomal abnormalities in B-CLL<sup>64</sup>.

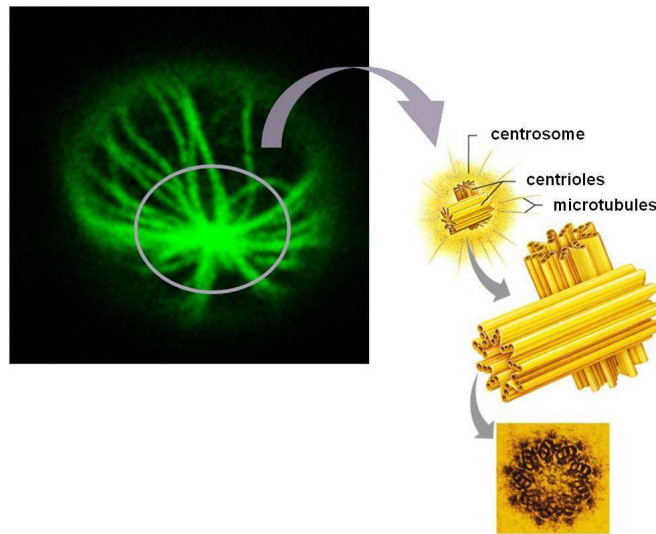


**Figure 12. Microtubules cytoskeleton structure.** Confocal microscopy analysis of microtubules in neoplastic B cells. Cells were stained with Ab anti- $\alpha$ -tubulin followed by secondary Ab Alexa-488. The point from which microtubules depart is the centrosome or MTOCs (circled). The image on the right shows in detail the structure of the centrosome.

## 2.4 Microenvironment

Bone marrow (BM) precursors derived from pluripotent stem cells are in intimate contact with stromal cells and generate B cells in an Ag-independent process. BM precursors differentiate to mature virgin B lymphocytes endowed with membrane Ag receptors that migrate to peripheral lymphoid tissues searching an Ag. The encounter with a foreign Ag triggers B cell activation, proliferation, and a second wave of differentiation. The microenvironment for the active social life of a mature B cell is provided by the germinal centers of secondary lymphoid organs. It is within GC that trafficking mature B cells are brought into close contact with specialized T cells and Ag-presenting cells. This dialogue, finely regulated by cytokines, adhesion structures, and surface molecules, leads to the generation of B memory cells and plasma cell precursors and to the apoptotic elimination of inefficient or potentially dangerous cells. As all normal B cells evolve and operate thanks to microenvironmental cross-talks, it becomes consequent to ask whether the microenvironment may also influence the natural history of B cell malignancies<sup>65</sup>.

Isolated B-CLL cells undergo relatively rapid apoptosis *in vitro*. This observation has led to the speculation that the microenvironment is necessary and/or plays a pivotal role in maintaining the enhanced survival of B-CLL cells *in*

*vivo*. Human bone marrow stromal cells (BMSCs) have been demonstrated to support the survival of B-CLL cells when both cell types were co-cultured *in vitro*. Further investigations have suggested that B-CLL cells need to have intimate contact with BMSC in bone marrow, with T cells in lymph nodes, and with nurse-like cells (NLCs) in lymphatic tissues to maintain survival<sup>66</sup>. Mesenchymal Stromal Cells (MSCs) from both normal healthy donors and B-CLL patients were able to protect leukemic cells from undergoing spontaneous and drug-induced apoptosis. Close contact between B-CLL cells and MSCs is capable to mediate the most effective drug-resistance and it is this latter interaction that could be the most important in providing a niche for residual B-CLL cells post treatment. Recent studies demonstrated the significance of CD49d ( $\alpha 4$  integrin) in the prognosis of B-CLL disease<sup>67,68</sup> as well as its biological role of regulating matrix metalloproteinase-9 (MMP-9)<sup>69</sup>. These observations imply that  $\alpha 4\beta 1$  integrin could be a critical mediator of tight interactions between MSCs and B-CLL cells and MSC-mediated B-CLL protection.

TNF-family cytokines can provide survival signals or alternatively induce apoptosis. T cells modulate survival of B-CLL cells through the CD40/CD40L system. The signals delivered for normal B-lymphocytes by activated T-cells through CD40L induce B-cell growth, differentiation, and rescue from apoptosis. In contrast to normal B cells, a subset of B-CLL cells expresses both CD40L and its receptor, enabling an autocrine loop by which B-CLL cells can promote survival signals on their own. CD40 stimulation of B-CLL cells had been shown to prevent apoptosis and induce proliferation *in vitro*. It has been observed a correlation between levels of the anti-apoptotic protein Bcl-2 and survival induced by stromal cell contact, suggesting a mechanism by which stromal cells induce protection of B-CLL cells against spontaneous apoptosis.

In contrast, it was found that normal CD5+ B lymphocytes were unable to survive in co-culture with stromal cells. Stromal cells can, in addition, induce survival of B-CLL cells by stromal cell-derived factor-1 (SDF-1/CXCL12), which is a homeostatic chemokine that signals through the CXCR4 chemokine receptor and plays an important role in lymphopoiesis. High-levels of SDF-1 are constitutively produced by stromal cells within the marrow, the primary site of early B cell differentiation. B-CLL cells express high levels of the CXCR4

surface receptor, and undergo chemotaxis in response to SDF-1. In addition, it has been demonstrated that marrow stromal cells attract B-CLL cells via the chemokine receptor CXCR4, providing a possible explanation accounting for the infiltration of marrow by B-CLL cells<sup>70</sup> (figure 13).

### **3. Microtubule inhibitors**

#### **3.1 Microtubules**

The ability of eukaryotic cells to adopt different forms and perform coordinated movements depends on a complex network of protein filaments called cytoskeleton, which extends throughout the cytoplasm. The cell cytoskeleton consists of actin microfilaments, intermediate filaments and microtubules.

Microtubules are long, filamentous, tube-shaped protein polymers that are crucial in the development and maintenance of cell shape, in the transport of vesicles, mitochondria and other components throughout cells, in cell signaling, as well as in cell division and mitosis. Microtubules are composed of  $\alpha$ - and  $\beta$ -tubulin heterodimers (4nm  $\times$  5nm  $\times$  8nm) arranged in the form of slender filamentous tubes that can be several micrometres long (figure 14). They are highly dynamic polymers and their polymerization dynamics are tightly regulated both spatially and temporally.

The functional diversity of microtubules is achieved in several ways: i) through the binding of various regulatory proteins, including microtubule-associated proteins (MAPs), to soluble tubulin and to the microtubule surfaces and ends; ii) by expression of different tubulin isotypes, which have different functions; iii) through several post-translational modifications of tubulin. The polymerization dynamics of microtubules are created by the gain and loss of a short region of tubulin-GTP or tubulin-GDP-inorganic phosphate (Pi) at the two microtubule ends, called the GTP cap (figure 15a). Tubulin-GTP is hydrolysed to tubulin-GDP and Pi at the time that tubulin-GTP adds to the microtubule ends, or shortly after. Finally, the cap dissociates from the microtubule, leaving a microtubule core consisting of tubulin with stoichiometrically bound GDP in  $\beta$ -

tubulin. The tubulin-GDP remains non-dissociable and non-exchangeable until the tubulin subunit dissociates from the microtubule<sup>71</sup>.

Polymerization of microtubules occurs through two important steps: nucleation and elongation. Initially, an oligomer consisting of 6-12  $\alpha\beta$ -tubulin dimers is formed in the nucleation step. Further, the GTP bound to  $\alpha\beta$ -tubulin dimers add up to the nucleus of  $\gamma$ -tubulin and lead to its elongation and formation of the protofilament. After a rapid elongation phase, the assembly of microtubules reaches the steady state, where the addition and the dissociation of tubulin subunits at the ends of the microtubules are balanced and there is not a net increase in the polymer level. Hydrolysis of GTP introduces unusual equilibrium behaviors in microtubules. Microtubules are labile polymers that display two types of dynamic behaviors: "treadmilling" and "dynamic instability".

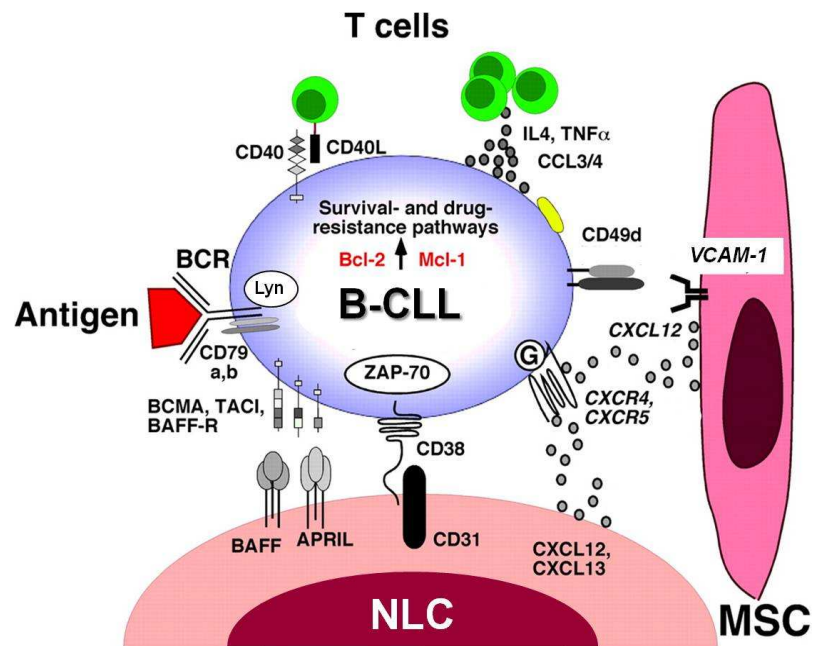


**Figure 13. Molecular crosstalk between B-CLL cells and microenvironment.** Contact between B-CLL cells and NLCs or MSCs is established and maintained by chemokine receptors and adhesion molecules. NLCs express the chemokines CXCL12 and CXCL13, whereas MSCs predominantly express CXCL12. NLCs and MSCs attract B-CLL cells via the chemokine receptors CXCR4 and CXCR5, which are expressed at high levels on B-CLL cells. Integrins, particularly CD49d, expressed on the surface of B-CLL cells, cooperate with chemokine receptors in establishing cell-cell adhesion through respective ligands on the stromal cells (VCAM-1). NLCs also express the TNF family members BAFF and a proliferation-inducing ligand, providing survival signals to B-CLL cells via corresponding receptors (BCMA, TACI, BAFF-R). CD38 expression allows B-CLL cells to interact with CD31 on stromal and NLCs. Ligand of CD38 activates ZAP-70 and downstream survival pathways. Stimulation of the BCR complex (BCR and CD79a,b) induces downstream signaling by recruitment and activation of Lyn, Syk and ZAP-70. BCR stimulation and co-culture with NLCs also induce B-CLL cells to secrete high levels of CCL3 and CCL4 chemokines, which are potent T cell-attracting chemokines. Through this mechanism, B-CLL cells can actively recruit T cells for cognate T-cell interactions with B-CLL cells. CD40L<sup>+</sup> T cells are preferentially found in B-CLL proliferation centers and can interact with B-CLL cells via CD40. Collectively, this crosstalk between B-CLL cells and accessory cells results in activation of survival and drug resistance pathways, such as those provided by Bcl-2 and Mcl-1. (Modified from Bruger J A *et al.*<sup>72</sup>).

Treadmilling refers to a net addition of tubulin dimers at the plus end coupled with a net dissociation at the minus end producing a flow of subunits from one end of the microtubule to the other end without significantly changing the average length of microtubules. Microtubule ends also alternate between growing and shortening phases, which is called as dynamic instability. A transition from a growing phase to a shortening phase is termed as a "catastrophe" while a transition from a shortening phase to a growing phase is termed as a "rescue"<sup>73</sup> (figure 15b).

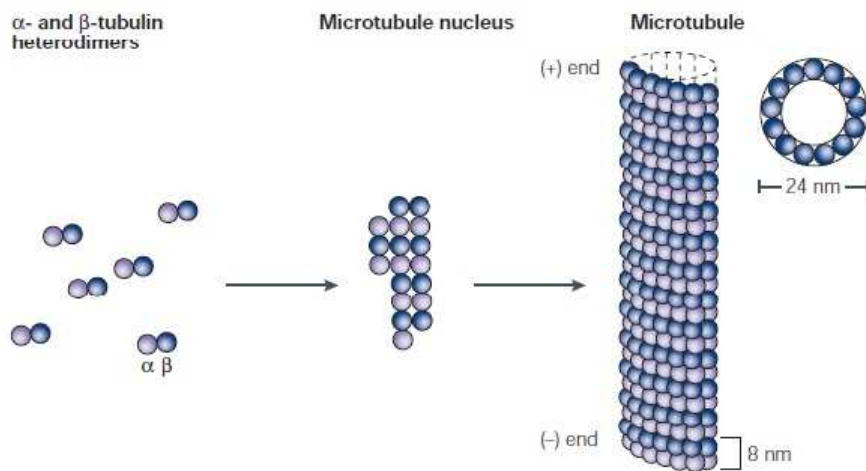


**Figure 14. Polymerization of microtubules.** Heterdimers of  $\alpha$ - and  $\beta$ -tubulin assemble to form a short microtubule nucleus. Nucleation is followed by elongation of the microtubule at both ends to form a cylinder that is composed of tubulin heterodimers arranged head-to-tail in 13 protofilaments. Each microtubule has a so-called plus (+) end, with  $\beta$ -tubulin facing the cytoplasm, and a minus end (-), with  $\alpha$ -tubulin facing the cytoplasm<sup>71</sup>.

B-CLL malignant cells are characterized by abnormalities that suggest defects of cytoskeletal functions. B-CLL cells have low mobility, show decreased capping by different ligands, and are unusually susceptible to microtubule disrupting drugs<sup>74</sup>. In particular, in B-CLL cells, microtubules are tightly connected with abnormalities of the BCR: in fact, molecules associated with BCR-mediated signal transduction, such as Syk, Vav, and Cbl bind tubulin and BCR members, like CD79a and CD79b, co-immunoprecipitate with tubulin<sup>75</sup>. Moreover, in rat basophilic leukemia Lyn kinase is complexed with  $\gamma$ -tubulin of cell centrosome<sup>76</sup>.

Microtubules are involved in a large number of cellular functions including chemotaxis, membrane and cellular scaffolding, intracellular transport, secretory processes, and transmission of receptor signaling<sup>77</sup>. For this reason

microtubules are already considered as potential drug targets for several diseases including cancer, neuronal diseases, fungal, and parasitic diseases<sup>73</sup>. In this context, microtubule inhibitors may have an important role in B-CLL treatment as they already have in other diseases.

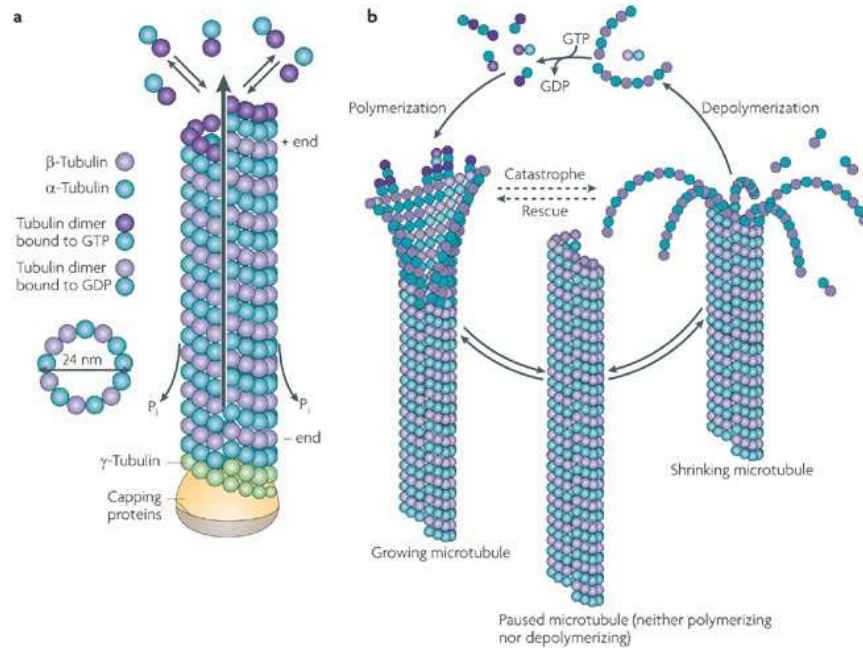


**Figure 15. Polymerization dynamics and the GTP cap.** **a)** The head-to-tail association of the  $\alpha\beta$  heterodimers makes microtubules polar structures and they have different polymerization rates at the two ends. In each protofilament, the  $\alpha\beta$  heterodimers are oriented with their  $\beta$ -tubulin monomer pointing towards the faster-growing end (plus end) and their  $\alpha$ -tubulin monomer exposed at the slower-growing end (minus end). A third tubulin isoform,  $\gamma$ -tubulin, functions as a template for the correct assembly of microtubules. On addition of a new dimer at the plus end, the catalytic domain of  $\alpha$ -tubulin contacts the nucleotide exchangeable site (E site) of the previous  $\beta$ -subunit and becomes ready for hydrolysis; the plus end generally has a minimum GTP cap of one tubulin layer that stabilizes the microtubule structure. **b)** When this GTP cap is stochastically lost, the protofilaments splay apart and the microtubule rapidly depolymerizes. During, or soon after the polymerization, the tubulin subunits hydrolyse their bound GTP and become non-exchangeable. Thus, the microtubule lattice is predominantly composed of GDP-tubulin, with depolymerization being characterized by the rapid loss of GDP-tubulin subunits and oligomers from the microtubule plus end. At the minus end, contact is made between the E site of the new dimer and the catalytic region of the last subunit at the end; therefore, no GTP cap should be present. Tubulin-bound GTP is hydrolysed to tubulin-GDP and inorganic phosphate ( $P_i$ ) at the time that tubulin adds to the microtubule ends, or shortly thereafter.  $P_i$  dissociates from the microtubule, leaving a microtubule core consisting of tubulin with stoichiometrically bound GDP. A microtubule end containing tubulin-bound GTP or GDP- $P_i$  is stable, or "capped", against depolymerization. Hydrolysis of tubulin-bound GTP, and the subsequent release of  $P_i$ , induces conformational changes in the tubulin molecules that destabilize the microtubule polymer, resulting in catastrophe and shortening of the microtubule<sup>78</sup>.

### 3.2 Microtubule-interfering agents

A large number of chemically different compounds, many of which are derived from natural products, are able to bind tubulin or microtubules and inhibit

proliferation by acting on the mitotic spindle. Some of these compounds inhibit microtubule polymerization, whereas others stabilize them. Although these compounds exert opposite effects on microtubules, both types of microtubule-interfering agents (MIAs) share the common property of suppressing microtubule dynamics and thereby microtubule function, leading to the disruption of the mitotic spindle function and blocking cell cycle progression.

Microtubule-interfering agents are divided in:

### 1) Depolymerizing agents:

a) The *Vinca* alkaloids. The *Vinca* alkaloids have been responsible for many stories of successful chemotherapy since their introduction into the clinic 40 years ago. The naturally occurring members of the family, vinblastine and vincristine, were isolated from the leaves of the periwinkle plant *Catharanthus roseus*. They came into widespread use for the single-agent treatment of childhood haematological and solid malignancies and, shortly after, also for adult haematological malignancies. Their principle side effects are peripheral neuropathy and reversible myelosuppression. The *Vinca* alkaloids bind to  $\beta$ -tubulin near the GTP-binding site<sup>71</sup> (figure 16a).

b) Colchicine. Colchicine was originally extracted from plants of the genus *Colchicum*. The interaction of colchicine with tubulin and microtubules presents one more variation in the mechanisms by which microtubule-active drugs inhibit microtubule functions. Colchicine inhibits microtubule polymerization substoichiometrically, indicating that it inhibits microtubule polymerization by binding to microtubule ends rather than to the soluble-tubulin pool (figure 16b).

Tubulin-colchicine complexes might have a conformation that disrupts the microtubule lattice in a way that slows, but does not prevent, new tubulin addition. The incorporated tubulin-colchicine complex must bind more tightly to its tubulin neighbours than tubulin itself does, so that the normal rate of tubulin dissociation is reduced<sup>71</sup>.

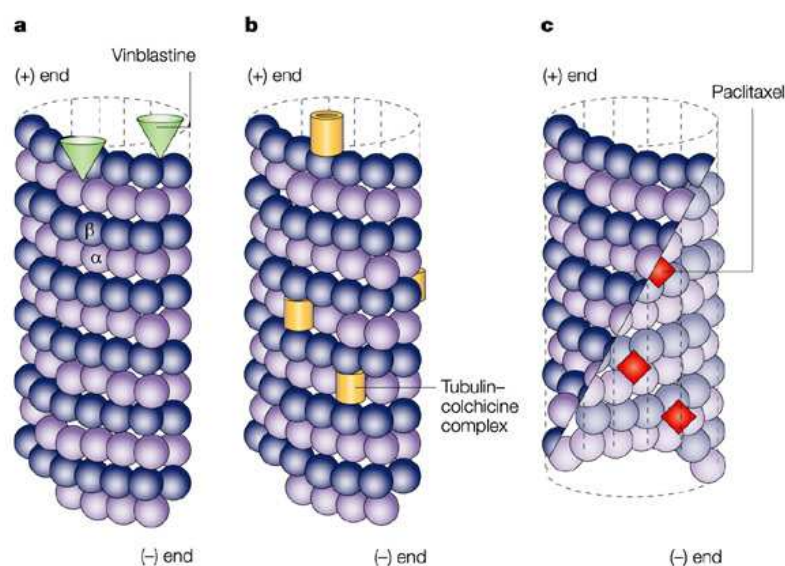


**Figure 16. Antimitotic drugs bind to microtubules at diverse sites. a)** A few molecules of vinblastine bound to high-affinity sites at the microtubule plus end are sufficient to suppress microtubule dynamics. **b)** Colchicine forms complexes with tubulin dimers and copolymerizes into the microtubule lattice, suppressing microtubule dynamics. **c)** A microtubule section to display the interior surface is shown. Paclitaxel binds along the interior surface of the microtubule, suppressing its dynamics<sup>71</sup>.

At doses required for antitumor effect, colchicine present important toxicity and the clinician has excluded its use. Relatively recently (2007) colchicine has been use in the treatment of pericarditis and in preventing the recurrence of the inflammatory process; in fact, by its destabilizing effect on microtubules, colchicine prevents leukocyte motility, thus blocking the inflammatory phenomenon<sup>79</sup>.

c) Estramustine. Estramustine is an estradiol molecule linked to a nitrogen mustard through a carbamate ester group and was rationally synthesized as an alkylating agent for the treatment of prostate carcinoma. However, estramustine has been shown to bind to tubulin and MAPs, which results in their dissociation from microtubules and subsequently in microtubule disassembly and metaphase arrest, leading to apoptosis. Thus, estramustine is considered as a microtubule-active drug currently in use for the treatment of advanced prostatic carcinoma and for hormone resistant prostate cancer patients. In addition, experimental data concerning the antitumor effect of estramustine in other malignancies are accumulating and clinical studies are ongoing. Estramustine has potent

antiproliferative effects against malignant glioma both *in vitro* and *in vivo*, whereas non-neoplastic astrocytes are spared<sup>77</sup>. The estramustine-binding site on tubulin has been suggested to be distinct from the colchicine and vinblastine sites and may partially overlap with the Taxol-binding site in tubulin<sup>80</sup>.

## 2) Microtubules stabilizer:

a) Taxanes. The taxanes are diterpenes produced by the plants of the genus *Taxus*. As their name suggests, they were first derived from natural sources, but some have been then synthesized artificially. Taxanes include paclitaxel (Taxol) and docetaxel (Taxotere). Taxanes bind directly, with high affinity, to tubulin along the length of the microtubule (figure 16c). Paclitaxel binding site is located in the  $\beta$ -subunit, which is on the inner surface of the microtubule. It is thought that, to gain access to its binding sites, paclitaxel diffuses through small openings in the microtubule or fluctuations of the microtubule lattice. Binding of paclitaxel to microtubule inner site stabilizes microtubules and increases their polymerization, presumably by inducing a conformational change in the tubulin that, by an unknown mechanism, increases its affinity for neighbouring tubulin molecules. Paclitaxel can induce cell death by the activation of apparently different signal transduction pathways, depending on drug concentration. Incubation of cells with high concentrations ( $\geq 200\text{nM}$ ) of paclitaxel stabilizes extensively the microtubule polymerization, causing the formation of stable bundles of microtubules that disrupt the normal polymerization/ depolymerization cycle of microtubules and thereby suppressing microtubule dynamics, resulting in the arrest of cells in mitosis<sup>77</sup>. The clinical success of the taxanes has led to a search for other drugs that enhance microtubule polymerization, yielding several promising compounds, including discodermolide, eleutherobin, laulimalide, the sarcodictyins, and the epothilones. Some of these compounds compete with paclitaxel for binding to microtubules and are said to bind at or near the taxane site (epothilones, discodermolide, eleutherobins and sarcodictyins); others, such as laulimalide, seem to bind to unique sites on microtubules<sup>71</sup>.

b) Epothilones. Epothilones are secondary metabolites that are produced by myxobacteria and that were first discovered in a screening program for secondary metabolites by virtue of their selective antifungal activity against *Mucor hiemalis*. In contrast to paclitaxel, epothilones were also shown to inhibit the growth of cells overexpressing the P-glycoprotein efflux pump, thus indicating that these compounds (or related analogs) might eventually be useful for the treatment of multidrug-resistant tumors. Epothilones have also been quoted as being significantly more water-soluble than paclitaxel. This should allow the use of formulation vehicles less problematic than cremaphor, which in the case of Taxol is believed to contribute to the drug's clinical side-effects<sup>81</sup>.

Different studies initiated in the past are till now valuating the possible anti-neoplastic efficacy of microtubules inhibitors in B-CLL. In particular, it was analyzed vincristine efficacy in chemotherapeutic combinations, such as CHOP and COP. Results were so positive to introduce its use in B-CLL treatment in the last decade<sup>82</sup>.

More recently it was evaluated the efficacy of Bryostatin 1, a macrocyclic lactone isolated from the marine invertebrate *Bugula neritina*. Short-term exposure activates protein kinase C, a family kinase involved in cell proliferation and apoptosis. Despite its limited single agent activity, Bryostatin 1 has demonstrated the ability to potentiate the cytotoxicity of several chemotherapeutic agents. Preclinical data suggest the superiority of Bryostatin 1 in combination with CHOP when compared with CHOP alone. In combination with fludarabine, for indolent NHL and B-CLL, Bryostatin 1 did not appear to add significant toxicity to full-dose fludarabine<sup>83</sup>.

### **3.3 Nocodazole**

The synthetic drug nocodazole (methyl N-[6-(thiophene-2-carbonyl)-1H-benzimidazol-2-yl] carbamate) is a depolymerizing agent and is reported to have antimetabolic and antitumoral activity. Its molecular structure is C<sub>14</sub>H<sub>11</sub>N<sub>3</sub>O<sub>3</sub>S (figure 17). The potential usefulness of this drug is due to its action being readily

reversible, rapid, and specific toward malignant cells<sup>84</sup>. The target site of this drug is tubulin; in earlier studies it was shown that nocodazole inhibits the polymerization of brain tubulin *in vitro*<sup>85</sup> and the presence of microtubule-associated proteins does not amplify the inhibitory effect of the drug. Furthermore, results from structural studies show that the sulfhydryl residues become more accessible to chemical modifications, indicating that binding of nocodazole induces significant structural changes in tubulin. It was reported that nocodazole binds to purified tubulin dimer with a stoichiometry of one and the drug competitively inhibits colchicine binding to microtubule proteins even though there is no structural similarity between these two drugs<sup>85,86</sup>.

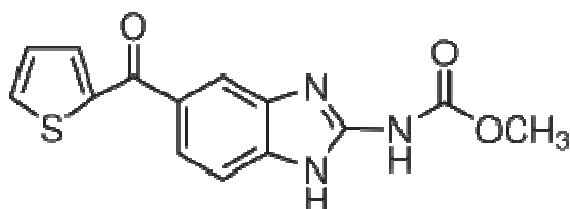


**Figura 17. Nocodazole molecular structure.** IUPAC name: methyl N-[6-(thiophene-2-carbonyl)-1H-benzimidazol-2-yl] carbamate.

Previous studies have demonstrated that nocodazole increases the GTPase activity of tubulin and that, unlike colchicine, no preincubation with tubulin is required to elicit this increase in activity. Currently, it is not known whether nocodazole remains bound to tubulin subunits after stimulating hydrolysis or whether it is released, allowing it to force hydrolysis on additional subunits<sup>87</sup>. As shown by Vandecandelaere *et al.*<sup>88</sup>, small increases in the soluble pool of tubulin-GDP subunits can significantly modulate MT dynamics. The results of Vandecandelaere include pauses in assembly, reduced rates of elongation and shortening, and an increase in catastrophe frequency. This increased concentration of tubulin-GDP subunits increases the likelihood of tubulin-GDP incorporation at the MT ends.

Nocodazole-mediated cell-cycle arrest was accompanied by higher rate of apoptosis and upregulation of p53<sup>89</sup>. Activation of this protein occurs in an indirect way by damage caused on the mitotic spindle, which cause changes in the chromosomes. p53, in turn, induces the transcription of p21<sup>waf/cip1</sup>, an inhibitor of cyclin-dependent kinase 2 essential for the transition from G<sub>1</sub> to S. In this way, apoptotic cells are then blocked in G<sub>1</sub> phase. Moreover, nocodazole induces Lats2

translocation from centrosomes to the nucleus and p53 accumulation. Lats2 (Large Tumor Suppressor 2) interacts physically with Mdm2 inhibiting p53 ubiquitination and promoting its activation. This interaction is enhanced in cells treated with nocodazole, which causes microtubule and mitotic spindle damage<sup>90</sup>.

Beswick *et al.*<sup>91</sup> have analyzed nocodazole effects in B-CLL cells finding that it causes selective death of neoplastic cells. They show that the mechanism of nocodazole-induced apoptosis involves mitochondrial membrane depolarisation, caspase activation and PARP cleavage; in particular, caspase-9 activation is the important route of nocodazole-induced death in B-CLL. In order to analyze the mechanism of apoptosis induction by nocodazole it was considered the known link between microtubule network and apoptosis: microtubule damage induces Bcl-2 phosphorylation on specific residues including serine-70. A recent suggestion is that phosphorylated Bcl-2 may exist for lengthy periods after microtubule damage representing a pre-apoptotic phase. In this scheme subsequent dephosphorylation initiates apoptosis. In cycling cells nocodazole causes mitotic arrest, which in turn leads to apoptosis. An effect on non-cycling B-CLL cells is, therefore, unexpected. Beswick *et al.* proposed two major explanations for nocodazole-induced apoptosis in B-CLL. Firstly, primary disturbances in the apoptotic machinery, which may include alterations in the relative amounts of pro- and anti-apoptotic proteins, could be sufficient to lead to apoptosis in B-CLL cells at lower nocodazole concentrations than in normal cells. Alternatively primary abnormalities of microtubule quantity or quality could increase sensitivity to the effects of depolymerising agents. It is interesting, in this regard, that there is considerable variation in tubulin content in B-CLL<sup>91</sup>.



## AIM OF THE STUDY

B-CLL cells are characterized by abnormalities that depend also on cytoskeletal defects; neoplastic B cells, in fact, have low mobility<sup>5</sup>, show decreased capping by different ligands<sup>92,93</sup> and are susceptible to microtubule disrupting drugs<sup>7</sup>. In particular, in B-CLL cells microtubules are tightly connected with functional anomalies of the B Cell Receptor (BCR): molecules associated with BCR-mediated signal transduction bind tubulin, and BCR members, like CD79a and CD79b, co-immunoprecipitate with  $\beta$ -tubulin<sup>8</sup>.

Microtubules are important targets in the anti-tumor therapy for the crucial role they play in cancer cell functions, including mitosis, motility and cell-cell contacts<sup>73,77</sup>. Microtubule inhibitors are already employed in pathologies such as Hodgkin lymphoma or acute lymphocytic leukemia. In spite of their potent anti-cancer action, many anti-microtubule drugs show limited clinical use because of their strong toxic effects. Hence the importance of identifying new microtubule inhibitors highly selective for leukemic cells and not damaging for the other cell types.

Nocodazole is an anti-neoplastic agent which exerts its cellular effects by favouring microtubule depolymerization<sup>94</sup>. It is highly effective in altering microtubule dynamics and arresting cell-cycle progression at mitosis phase<sup>95</sup>. It induces significant structural changes in tubulin and the usefulness of this drug is due to its action, that is readily reversible, rapid and specific towards malignant cells<sup>84,86</sup>.

During this PhD program we planned to further investigate nocodazole acting and to analyze how nocodazole exerts its effect specifically on B-CLL. In particular, we studied:

- nocodazole action on several cell types (normal B cells, B and T cells from B-CLL patients, MSCs from both B-CLL patients and donors, Jurkat, Raji, and K562 cell lines;
- nocodazole apoptotic effect on B-CLL cells and residual T lymphocytes obtained from the same patients;
- nocodazole effects on B-CLL cells co-cultured with MSC and/or in presence of CD40L or plasma;
- the molecular mechanisms of nocodazole activity.



# MATERIALS AND METHODS

## 1. Patients

We analyzed 52 B-CLL patients (37 males and 15 females), aged between 44 and 80 years, enrolled by the Hematology and Clinical Immunology branch (chief Prof. G. Semenzato), Padova University School of Medicine.

Clinical characteristics of patients are listed in Table I. In particular, for each patient we reported: the number of white blood cells (WBCs), the percentage of lymphocytes, mutational status of IgV<sub>H</sub> genes and the expression of ZAP-70. All neoplastic B cells of the 52 patients examined were positive for CD5, CD19 and CD23 markers, typically co-expressed in B-CLL and those of 12 subjects were also CD38 positive.

B lymphocytes obtained from peripheral blood of 10 healthy subjects were used as normal controls.

## 2. Immunophenotypic analysis

The immunophenotypic analysis on lymphocytes obtained from peripheral blood of B-CLL patients was performed through flow cytometry. This technique allows a multiparametric evaluation of antigenic characteristic of the single cells by the analysis of visible and fluorescent light they emit when flow through a liquid medium.

The immunophenotyping is based on the identification of surface and intracellular Ag using mAb conjugated with fluorochromes. The presence of a certain Ag is revealed and used as an indicator of belonging to a cell line as well as its level of maturation. The fluorochromes used in this thesis were fluorescein isothiocyanate (FITC), which emits a fluorescence signal at 530nm (green), phycoerythrin (PE) emitting at 585nm, tri-color (TC) that emits at 667nm when hit by a monochromatic laser beam with  $\lambda$  equal to 488nm, and finally, the

**Table I. Clinical characteristics of analyzed B-CLL patients**

Patient n°	Age (years)	Sex	RAI Stage	WBC (/mm <sup>3</sup> )	Lymphocytes %	CD19/5 %	Mutational Status (1)	ZAP70 Expression (2)	CD38 (3)
1	68	F	nd	4700	36	22	ne	POS	NEG
2	59	M	3	5700	23.8	7	unmutated	NEG	POS
3	74	F	1	6400	60.5	46	unmutated	POS	NEG
4	75	M	nd	9600	56.6	55	mutated	nd	NEG
5	66	M	0	9900	55.3	47	mutated	NEG	NEG
6	68	F	0	10500	67	86	unmutated	POS	POS
7	75	M	0	11900	67.3	75	mutated	NEG	NEG
8	70	M	4	12700	87	81	mutated	POS	POS
8	70	M	4	19000	87.8	82	mutated	POS	POS
9	66	M	nd	14000	55	52	ne	nd	NEG
10	80	F	0	14600	58.1	58	unmutated	POS	NEG
11	79	F	0	19000	74	78	mutated	NEG	NEG
12	44	F	0	21200	81.6	50	unmutated	NEG	POS
13	55	F	3	29400	84	53	mutated	POS	NEG
14	62	F	4	30400	87	79	mutated	NEG	NEG
15	76	M	1	41700	80	97	ne	NEG	NEG
15	76	M	1	17980	79.6	79	ne	NEG	NEG
16	80	M	1	42800	84.7	80	mutated	NEG	NEG
17	78	F	4	58400	91	84	unmutated	NEG	POS
18	79	M	4	86200	85	91	mutated	NEG	NEG
18	79	M	4	15550	67	73	mutated	NEG	NEG
19	74	M	1	99200	89	89	unmutated	NEG	NEG
20	73	F	nd	100200	86	95	mutated	NEG	NEG
21	84	F	2	105000	84.3	95	unmutated	nd	NEG
22	66	M	2	110500	83	80	unmutated	NEG	NEG
22	66	M	2	21000	75	83	unmutated	NEG	NEG
23	65	F	nd	116000	90	70	unmutated	nd	NEG
24	67	M	2	216000	90	84	unmutated	NEG	NEG
24	67	M	2	6570	48.6	51	unmutated	NEG	NEG
25	71	M	2	300000	95	92	mutated	NEG	NEG
26	59	M	1	36000	72	76	unmutated	POS	NEG
27	78	M	1	10100	60.9	39	mutated	POS	POS
28	68	M	0	131000	92.7	98	mutated	NEG	NEG
28	68	M	0	88500	93.2	99	mutated	NEG	NEG
29	64	M	2	37360	57	50	mutated	NEG	NEG
30	67	M	2	26680	87	82	unmutated	POS	NEG
31	72	M	2	79770	91.2	90	mutated	POS	NEG
32	78	M	4	112200	97.3	81	mutated	POS	NEG
33	61	M	0	60000	70	90	unmutated	POS	NEG
34	75	M	1	18620	78.8	86	mutated	NEG	NEG
35	53	F	2	90900	82	90	mutated	NEG	NEG
36	75	F	1	102600	90	89	ne	POS	POS
37	71	M	nd	23560	82	62	ne	nd	NEG
38	74	M	nd	24360	80	87	unmutated	POS	NEG
39	69	M	nd	30300	86	95	unmutated	NEG	POS
40	62	M	nd	113800	95	94	ne	nd	POS
41	64	F	nd	91920	85	60	unmutated	POS	nd
42	65	M	nd	20620	80	80	ne	nd	POS
43	79	F	nd	9880	95.3	71	unmutated	NEG	POS
44	61	F	nd	30500	62	73	mutated	NEG	NEG
45	63	M	nd	63670	84.6	94	unmutated	NEG	NEG
46	75	F	nd	42800	84.8	94	unmutated	POS	NEG
47	74	M	nd	57700	81	93	nd	nd	nd
48	69	F	nd	31000	82	96	unmutated	NEG	NEG
49	78	F	nd	15710	78.8	89	nd	nd	nd
60	74	F	nd	50300	90.4	91	nd	nd	nd
51	64	M	nd	22000	73	83	nd	nd	nd
52	63	M	nd	33510	67	99	ne	NEG	NEG

(1) Immunoglobulin heavy chain variable region (IgV<sub>H</sub>) mutational status: patients with <2% differences from the most similar germline gene in both the expressed V<sub>H</sub> and V<sub>L</sub> genes were define unmutated; mutated cases were defined as those in which the B-CLL cells displayed ≥2% differences in either the expressed V<sub>H</sub> or V<sub>L</sub> gene;

nd: not detected;

ne: not evaluable;

(2) Parameter assessed by flow cytometric analysis (ratiometric method, cut-off> 0.5);

(3) Parameter assessed by flow cytometric analysis (cutoff> 30%);

NEG: negative;

POS: positive.

allophycocyanin (APC) that emits a fluorescence signal at 690nm when excited by a laser beam with  $\lambda$  of 635nm. The cell samples were analyzed by the flow cytometer FACScan (Becton Dickinson; Franklin Lakes, NJ) and data obtained were processed using the program Cell Quest. For each analysis 15.000 events were acquired.

### 3. Isolation of B lymphocytes from peripheral blood

B lymphocytes were isolated from peripheral blood of B-CLL patients. From a sample of heparinized venous blood, mononuclear cells were obtained proceeding with a layering on Ficoll/Hypaque (F/H) (Amersham Biosciences; San Francisco, CA). This method exploits the difference of density of mononuclear cells (lymphocytes and monocytes) with respect to the other elements of the blood. Mononuclear cells, which have lower density, focus on the layer of F/H while the red blood cells and granulocytes are collected on the bottom of the tube. Considered the high WBC count in B-CLL patients, peripheral blood was first diluted in 1:6 ratio with 0.9% sodium chloride (saline) at room temperature, gently agitated, and later layered slowly over F/H solution. We proceeded with a centrifugation at 900g for 20 min at 20°C, without brake. The ring of mononuclear cells formed at F/H interface was aspirated and subjected to two successive washes with saline by centrifugation at 400g for 10 minutes at 20°C (figure 18). The pellet was resuspended in a adequate amount of saline and the cells were counted in a Burker chamber.

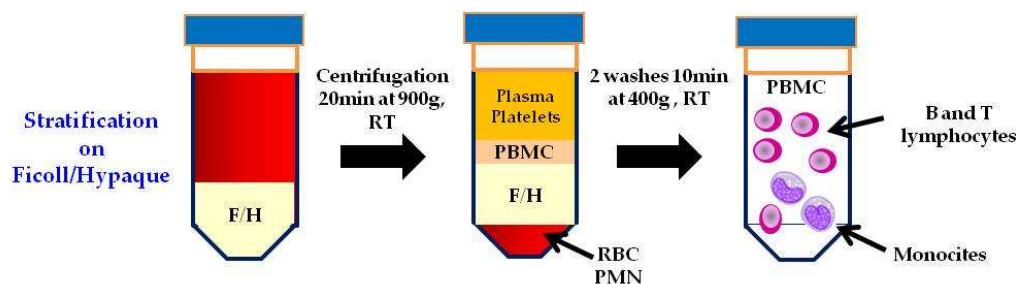


**Figure 18. Isolation of mononuclear cells from peripheral blood by stratification on Ficoll/Hypaque.** By centrifugation on F/H, mononuclear cells were isolated from peripheral blood. Mononuclear cells and platelets were concentrated above the layer of F/H because they have lower density; on the contrary, the red blood cells (RBC) and granulocytes (PMN) have a higher density than the F/H and collect on the bottom of the tube. RT: room temperature.

### 3.1 Purification of B lymphocytes with sheep red blood cells (SRBCs)

In most of B-CLL cases, the percentage of leukemic B cells was greater than 90% of PBMCs (peripheral blood mononuclear cells) isolated.

When the cell population had more than 10% of T lymphocytes, we further performed the purification of B lymphocytes by SRBC method. This purification allows the removal of T cells from the other mononuclear cells, taking advantage from their ability to bind and form complexes, called "rosettes", with SRBCs. The latter, in fact, express on their surface a specific receptor for the T lymphocyte marker CD2; SRBCs treatment with neuraminidase make more accessible the receptor to CD2 binding.

$25 \times 10^6$  aliquots of PBMCs were transferred into a 10ml centrifuge tube and 1ml of SRBC treated with neuraminidase was added. PBMCs and SRBCs were then incubated at 37°C for 25 min, centrifuged at 4°C for 10 min at 200g without brake, and finally subjected to a new incubation at 4°C for 30 min. The supernatant was then aspirated and culture medium RPMI 1640 (Invitrogen; Paisley, UK) was added. The mixture was gently resuspended, layered over F/H solution, and centrifuged at 4°C for 20 min at 900g without brake. T cells, surrounded by SRBCs, accumulated to the bottom of the tube, having a density greater than F/H, while the non-T mononuclear cells (monocytes and B cells) were concentrated above the F/H layer. The interface layer, which contains B cells, was transferred into a 10ml tube. Two washes with saline were performed at 400g at 20°C for 10 min and, in the end, cells were resuspended in an adequate amount of saline and counted in a Burker chamber (figure 19).

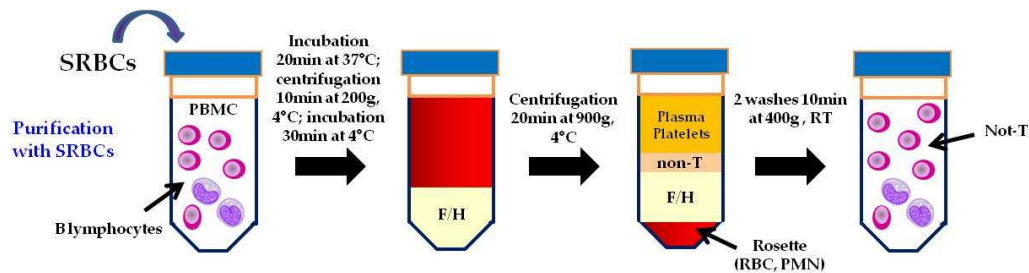


**Figure 19. Purification with SRBCs.** When the mononuclear cells obtained by separation over F/H contained a percentage of lymphocytes  $T \geq 10\%$ , we used SRBCs to remove them. This method exploits the ability of T cells to bind, through their marker CD2, to SRBCs treated with neuraminidase and forming rosettes that are removed by further stratification on F/H.

### 3.2 Purification of B lymphocytes using RosetteSep kit

We used the RosetteSep kit (StemCell Technologies; Vancouver, CN) to obtain B cells from whole blood of normal healthy donors. The kit consists of a cocktail of antibodies directed against surface antigens expressed by hematopoietic cells (CD2, CD3, CD16, CD36, CD56, CD66b) and glycophorin A expressed by red blood cells. This mixture of antibodies binds "not-B" cells and red blood cells creating immunorosette. In this way, CD19<sup>+</sup> B lymphocytes were isolated from whole blood by negative selection.

Each ml of blood was incubated with 50 $\mu$ l of RosetteSep at room temperature for 20 minutes. The samples were then diluted 1:2 with PBS (Phosphate Buffered Saline)1X + 2% FBS (Fetal Bovine Serum), gently agitated, and then layered over F/H. We proceeded with a centrifugation at 900g for 30 minutes at room temperature, followed by the aspiration of the ring formed at the F/H interface containing B cells. It was resuspended in PBS1X + 2% FBS and centrifuged at 400g for 10 minutes. Finally, the cells were resuspended in PBS1X and counted in a Burker chamber (figure 20).

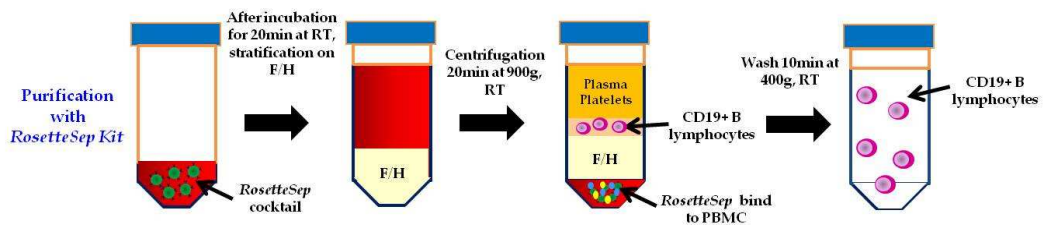


**Figure 20. Purification with RosetteSep kit.** CD19<sup>+</sup> B lymphocytes were isolated from whole blood of healthy donors by negative selection. 10ml of venous whole blood were incubated for 20 min at RT with 500 $\mu$ l of RosetteSep. Afterwards, through stratification on F/H, we get the CD19<sup>+</sup> B cells, which are concentrated just above the layer of F/H, while the rest of the cells related to the rosettes were collected on the bottom of the tube.

### 4. Cell cultures

Aliquots of B (CD19<sup>+</sup>/CD5<sup>+</sup>) and T lymphocytes (CD5<sup>+</sup>) obtained from patients with B-CLL, normal B lymphocytes (CD19<sup>+</sup>) and cell lines (Raji, Jurkat, and K562) were cultured in RPMI 1640 medium with 10% FBS and antibiotics at a concentration of 1x10<sup>6</sup>/ml in 24 or 48-well plates. Cells were incubated at 37°C in a humidified atmosphere containing 5% CO<sub>2</sub> with or without 16 $\mu$ M nocodazole

for 24, 48 and 72 hours. The same experiments were also performed on MSC from healthy subjects or from B-CLL patients. MSCs were previously obtained and characterized in our laboratory (CD19+/CD105+/CD73+; CD34-/CD14-/CD45-/CD31-; differentiation into adipocytes and osteocytes).

Nocodazole concentration of 16 $\mu$ M was chosen according to the article by Beswick *et al*<sup>91</sup>.

## 5. Co-cultures

For co-culture experiments, 2x10<sup>5</sup>/well MSCs from B-CLL were seeded into 12 well plates and incubated a few days before the experiment at 37°C in 5% CO<sub>2</sub> up to confluence. Then B-CLL cells were added to MSCs layer at a ratio of 2,5:1. Cells were then treated with 16 $\mu$ M nocodazole for 24, 48, 72 hours and 5 days to evaluate a possible resistance to this agent due to the co-culture with MSCs.

In other experiments we added CD40L 1 $\mu$ g/ml and its enhancer 1 $\mu$ g/ml (Enzo Life Sciences; Inc. Farmingdale, NY), according to the instructions provided by the kit, or 10% plasma coming from the same patients.

In order to compare the results, the B-CLL cells were also plated under the same conditions but not in co-culture.

## 6. Preparation of cell lysates

For each sample aliquots of 250.000 and 500.000 B lymphocytes were lysed in 50 $\mu$ l of the following buffer:

- 50mM Tris (hydroxymethyl) aminomethane hydrochloride (Tris-HCl) pH 6.8;
- 5mM Ethylenediaminetetraacetic acid (EDTA);
- 10% glycerol;
- 2% SDS (sodium dodecyl sulphate);
- 1%  $\beta$ -mercaptoethanol;
- Dye (Bromophenol blue or pyronin) (Sigma-Aldrich; Milan, IT).

Subsequently, the lysates were vortex, boiled at of 100°C for 5 minutes and then subjected to SDS-PAGE (polyacrylamide gel electrophoresis).

## **7. Polyacrylamide gel electrophoresis in SDS (SDS-PAGE)**

The polyacrylamide gel electrophoresis in SDS is one of the methods used to separate a mixture of proteins on the basis of their molecular weight. SDS is a ionic detergent that binds tightly to proteins causing their denaturation. In the presence of an excess of SDS, approximately 1.4g of detergent will bind to each gram of protein, providing a constant amount of negative charge per unit mass. Therefore, during electrophoresis, all protein-SDS complexes move toward the anode, and thanks to the molecular sieve properties of the gel, their mobility is inversely proportional to their molecular weight. By the migration of standard proteins of known molecular weight simultaneously to samples, it is possible to determine the protein sample weights.

SDS polyacrylamide gel is prepared following Laemmli method<sup>96</sup>. The electrophoretic plate consists of two types of gel:

- *Stacking gel* at pH 6.8, which concentrates the protein samples so that they are all aligned at the start of electrophoresis;
  - *Running gel* at pH 8.8, in which the real separation of proteins occurs.
- The plate size of 10×8cm is fixed in the Hoefer Mighty Small-If 250 Scientific Instruments machine (Amersham Biosciences). The electrophoresis was run for about 2 hours at 25mA.

## **8. Western blotting**

The western blotting (WB) or immunoblotting is an immunoassay able to detect traces of a specific protein in a heterogeneous mixture, combining the high resolving power of gel electrophoresis with the specificity of the antibodies. The WB is a technique with high sensitivity, able to detect quantities of protein in the order of nanogram.

After SDS-PAGE, proteins are transferred onto a nitrocellulose membrane by the action of an electric field, obtained by applying the appropriate current of 350mA for 2 hours and 30 minutes. The buffer used for the transfer consists of: 25mM Tris, 192mM glycine, 20% methanol and 0.1% SDS with a final pH of 8.0 (buffer A). After the transfer, the membrane is left overnight in the saturation buffer consisting of 50mM Tris-HCl, pH 7.5, 150mM NaCl and 5% bovine serum albumin (BSA) (buffer B), for nonspecific sites saturation. Follows the incubation for 2 hours and 30 min at RT of the primary Abs, diluted in: 50mM Tris-HCl, pH 7.5, 150mM NaCl, 1% BSA (buffer C).

For our study we used the following antibodies: anti-P-Tyr, which recognizes proteins phosphorylated on tyrosine residues; polyclonal anti-Lyn (Cell Signaling Technology Inc.; Danvers, MA); anti-Lyn-Tyr396, which recognizes the protein only when phosphorylated in Lyn active site (Epitomics Onc.; Burlingame, CA); and anti- $\beta$ -actin (Sigma-Aldrich). In addition, for apoptosis study, we used an anti-PARP Ab (Cell Signaling Technology Inc.).

Three washes of 10 min, each at RT were subsequently performed, using buffer C supplemented with 0.1% Tween. Membranes were then incubated for 30 minutes with a secondary anti-IgG Ab, obtained against the animal species immunized for the primary Ab. The secondary Ab is conjugated with horseradish peroxidase (Amersham International Biotechnology; Buckinghamshire, UK) and diluted in buffer C. After three additional washes, the membrane was subjected to the detection antibody with the enhanced ChemiLuminescence system (ECL) (Pierce; Rockford, Illinois): the membrane is incubate for 1 min with 1ml of luminol and 1 ml of H<sub>2</sub>O<sub>2</sub>, which in contact with the peroxidase and, as a result, with the Ag-Ab complex, giving rise to an oxidation reaction with light emission. The membrane is placed over a autoradiographic plate, which is impressed by the light emitted.

The densitometric analysis of bands obtained in the plate was performed using the Image J program.

## 9. Apoptosis analysis by flow cytometry

Apoptosis of different cell samples (pathological and normal B lymphocytes, T lymphocytes from B-CLL, MSCs, and cell lines) was assessed using the Annexin V Apoptosis Detection Kit (Becton Dickinson).

During the early stages of apoptosis the plasma membrane undergoes profound changes that indicate the status of apoptotic cells to macrophages, which ensure its elimination. Phosphatidylserine (PS), a negatively charged aminofosfolipide normally expressed only on the inner side of the plasma membrane, is exposed on the outer surface. The Annexin V is a protein that, in the presence of high concentrations of  $\text{Ca}^{2+}$ , recognizes and binds selectively the PS, making it useful for the identification of apoptotic cells that expose the phospholipid on their surface. After 24 hours of incubation with  $16\mu\text{M}$  nocodazole (or 24, 48, 72 hours and 5 days according to the experiment) aliquots of  $5 \times 10^5$  cells were harvested, washed, and incubated for 10 min in the dark and at RT with:  $100\mu\text{l}$  of binding buffer, a  $\text{Ca}^{2+}$ -rich solution that optimizes the binding of Annexin V to the PS,  $5\mu\text{l}$  of Annexin V-FITC, and  $10\mu\text{l}$  of Propidium iodide (PI), provided by the kit ( $1\mu\text{l}/\text{ml}$  final concentration). After the incubation,  $100\mu\text{l}$  of binding buffer were added and cells were analyzed by flow cytometer FACScan. For each sample 20.000 events were acquired and the number of apoptotic cells was expressed as percentage of Annexin V positive cells in the total cells analyzed.

For the assessment of apoptosis of MSC, cells were detached from the bonding surface by trypsinization (incubation for a few minutes in 25% trypsin/EDTA).

To differentiate the percentage of apoptosis in B and T cells from the same patient with B-CLL, the following antibodies were used: Annexin V FITC (Bender Medsystem; Vienna, A), anti-CD5 PE-Cy5 (Becton Dickinson) and anti-CD19 APC (Invitrogen). The number of apoptotic cells was expressed as percentage of  $\text{CD19}^+/\text{CD5}^+/\text{Annexin V}^+$  cells for B lymphocytes, and  $\text{CD5}^+/\text{Annexin V}^+$  for T lymphocytes, respectively (figure 21).

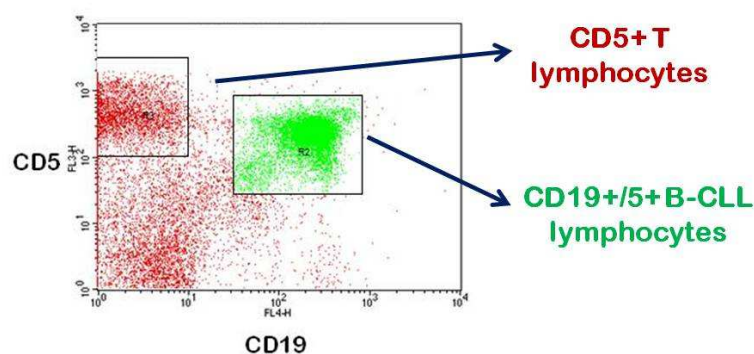


**Figure 21.** Cytogram relating to B-CLL samples with a T residual population of 15-20%. T cells are exclusively positive for CD5, while the population of leukemic B cells showed double positivity: CD19+/CD5+.

## 10. Confocal microscopy analysis

Aliquotes of the different cell samples (pathological and normal B lymphocytes, T lymphocytes from B-CLL, cell lines and MSCs), after 24 hours of incubation in medium alone or with 16 $\mu$ M nocodazole were collected, washed and plated on polylysine coated slides. MSCs were let adhere on chambers slide (Nalge Nunc International; Rochester, NY). Cells were then fixed in 4% paraformaldehyde for 10min, washed twice with PBS1X and permeabilized with 0.1% Triton X-100 (Sigma-Aldrich) for 4 min. Prior to staining, non-specific binding sites were saturated by incubating the slides for at least 30min in 2% BSA. Then cells were stained with a FITC-conjugated anti-tubulin Ab (Sigma-Aldrich) diluted 1:1000 for at least 1 hour at room temperature or overnight at 4°C in the dark. Cells were then washed 3 times in PBS1X and the slides were finally sealed with coverslips and observed under the confocal microscope Ultra View LCI (Perkin Elmer; Waltham, MA).

## 11. RNA extraction

Total RNA was extracted from 4x10<sup>6</sup> lymphocytes obtained from peripheral blood of patients using the Protocol RNeasy Mini Kit (Qiagen; Hilden, Germany), as indicated by the supplier. Cells were lysed using a solution containing  $\beta$ -mercaptoethanol and subsequently processed by repeated aspirations

with a 20G needle. After addition of 350µl of 70% ethanol, samples were transferred to a purification column (supplied by the kit) and then centrifuged at 10.000rpm for 15 seconds, followed by eluate removal. After the addition of 350µl of RW1 buffer (supplied by the kit), samples were again centrifuged at 10.000 rpm for 15 seconds and the eluates were discarded. Then we proceeded with 20 minutes of incubation with 80µl of a DNase I solution. After having washed with 350µl of RW1buffer, followed by centrifugation at 10.000rpm for 15 seconds, the collector tube was replaced. 500µl of RPE buffer (supplied by the kit) were added, the samples were centrifuged at 10.000rpm for 15 seconds, and the eluates were discarded. After adding 500µl of RPE buffer, a centrifugation at 15.000g for 2 minutes was carried out. Columns were then transferred to 1.5ml tubes, 30µl of H<sub>2</sub>O were added on the membrane-free RNase, and purification was performed by centrifugation at 10.000 rpm for 1 minute, so as to dissociate the RNA from the membranes and bring it into solution.

To check the quality of RNA obtained, 2µl of sample were sown in a 1% agarose gel in tris-acetate (TAE) 1X with ethidium bromide (10mg/ml) 5% V/V; electrophoresis was performed at 60V for 20 minutes. The RNA extracted was then quantified by reading in a spectrophotometer Ultrospec 1100 pro (Amersham Biosciences). It was prepared 1:200 dilution of RNA samples, and the absorbance (A), at wavelengths of 260nm ( $\lambda$  nucleotides) and 280nm ( $\lambda$  proteins), were determined. It has been estimated, therefore, the A<sub>260</sub>/A<sub>280</sub> ratio: if a value less than 2, the RNA preparation is contaminated with protein and is not usable. It was finally calculated the concentration of RNA sample, using the following formula:

$$A_{260} \times \text{dilution factor} \times 40 = \text{RNA concentration in } \mu\text{g/ml}.$$

The value of 40 corresponds to the concentration of RNA expressed in µg/ml, which A<sub>260</sub> obtained is 1.

## **12. cDNA synthesis**

The reverse transcription from mRNA to cDNA (complementary DNA) uses a DNA-dependent RNA polymerase, which generates a cDNA strand from a template of mRNA. In this thesis it has been used as template total RNA and the

reaction was performed in the presence of an oligo-dT primer, able of pairing to the tail of poly-3' mRNA reverse transcriptase. The RT used is the Myeloblastoma Avian Virus (AMV) polymerase; this enzyme has 5'→3' activity (with RNA or DNA as a template) and an 3'→5' RNase H, which degrades the RNA filament of the double helix DNA-RNA produced during cDNA synthesis. For cDNA synthesis the Reverse Trascription System kit (Promega Corporation; Madison, Wis.) was used.

The reaction mixture is composed of:

- 4µl of 25mM MgCl<sub>2</sub>;
- 2µl of 10X RT buffer;
- 2µl of the mixture of the 4 deoxynucleosides triphosphates (dNTP mix) 10mM;
- 0.5µl of an enzyme inhibitor of RNase 40µg/µl;
- 0.75µl of AMV RT 25µg/µl;
- 1µl of primer Oligo (dT) 0.5mg/ml;
- 2µg of RNA;
- RNase-free H<sub>2</sub>O to final volume of 20µl.

This mixture was incubated at 42°C for 15 minutes, then placed at 95°C for 5 minutes (to stop the reaction) and, finally, put on ice for a few minutes. Thus, the cDNA obtained was stored at -80°C or used immediately to set up the amplification reaction by means of polymerase chain reaction (PCR) of the strand of DNA complementary to mRNA target (Reverse Transcriptase-PCR, RT-PCR).

### **13. Evaluation of Lyn gene expression through real-time RT-PCR**

After having extracted and reverse-transcribed RNA from B cells of B-CLL patients, we proceeded with the quantification of mRNA encoding for Lyn by real-time RT-PCR. The amplification of the genes of interest were obtained using ABI PRISM 7000 sequence detection system (Applied Biosystems; Foster City, CA) in a volume of 15µl. The master mix used, SYBR Green PCR, was provided by the company Applied Biosystems, containing AmpliTaq Gold DNA

polymerase; the primers (5µM) and 1.5µl of cDNA for a final reaction volume of 15µl were added.

The primers used for amplification of Lyn and GAPDH were:

- Lyn:

*forward 5'-GCT CAG ATT GCA GAG GGA ATG G-3'*

*reverse 5'-GAG CCG TCC ACT TAA TAG GGA AC-3'*

- GAPDH:

*forward 5'-AAT GGA AAT CCC ATC ACC ATC T - 3'*

*reverse 5'-CGC CCC ACT TGA TTT TGG - 3'*

These primers were obtained using Primer Express software (Applied Biosystems).

The reaction conditions were:

- Denaturation at 95°C for 10 minutes;
  - Annealing at 60°C for 15 seconds;
  - Extension at 72°C for 1 second.
- } for 45 cycles

Each sample was amplified in duplicate. For each Master Mix was performed a negative control; both for Lyn and GAPDH were generated two standard curves using the cDNA of Raji cell line to the following dilutions: 1, 1:5, 1:25, and 1:125. The relative amount of mRNA was determined by comparison with standard curves. The result of each sample was normalized to GAPDH expression. A dissociation curve to distinguish specific from nonspecific amplification was also generated.

## 14. Statistical analysis

Statistical analysis of apoptosis in patients analyzed was performed using Student's *t* test, paired Student's *t* test, and ANOVA. Data were expressed as mean ± standard deviation (SD) and were considered statistically significant when *p* values were <0.05.



# RESULTS

## 1. Nocodazole effect on cytoskeletal tubulin

Nocodazole induces significant structural changes in tubulin and the usefulness of this drug is due to its action, that is readily reversible, rapid, and specific towards malignant cells<sup>86</sup>.

In this project we performed confocal microscopy experiments to verify nocodazole function on tubulin polymerization on different cell types. Normal B cells, B and T cells from B-CLL patients, MSCs from both B-CLL patients and healthy donors, and 3 different cell lines (Jurkat, Raji, and K562) were cultured alone or in presence of nocodazole, collected and harvested after 24 hours. As shown in figure 22, cells cultured in medium alone have a regular cytoskeleton with a single centrosome (MTOC) and tubulin filaments easily recognizable. The centrosome is localized near the nucleus with microtubules radiating from it in different directions through the intracellular space. The treatment with nocodazole causes the disruption of cytoskeleton architecture and the disappearance of the centrosome, index of tubulin depolymerization and drug effectiveness, in all analyzed cells.

## 2. Nocodazole kills specifically B-CLL cells

CD19+/CD5+ neoplastic B cells from 52 B-CLL patients and CD19+ normal B cells obtained from 10 healthy donors were cultured alone or in presence of nocodazole. To assess cell viability, the flow-cytometric test Annexin V/PI was performed after 24 hours of incubation. Our results confirmed that only cells from B-CLL patients underwent apoptosis after nocodazole treatment, while normal B cells were not affected<sup>91</sup>. The difference in viability percentage between normal and leukemic cells after the treatment was statistically significant ( $98\pm 6\%$  vs  $57\pm 25\%$ , respectively;  $p < 0.0001$ ; data are expressed as mean $\pm$ SD of alive cells) (figure 23A, box-plots I and II).

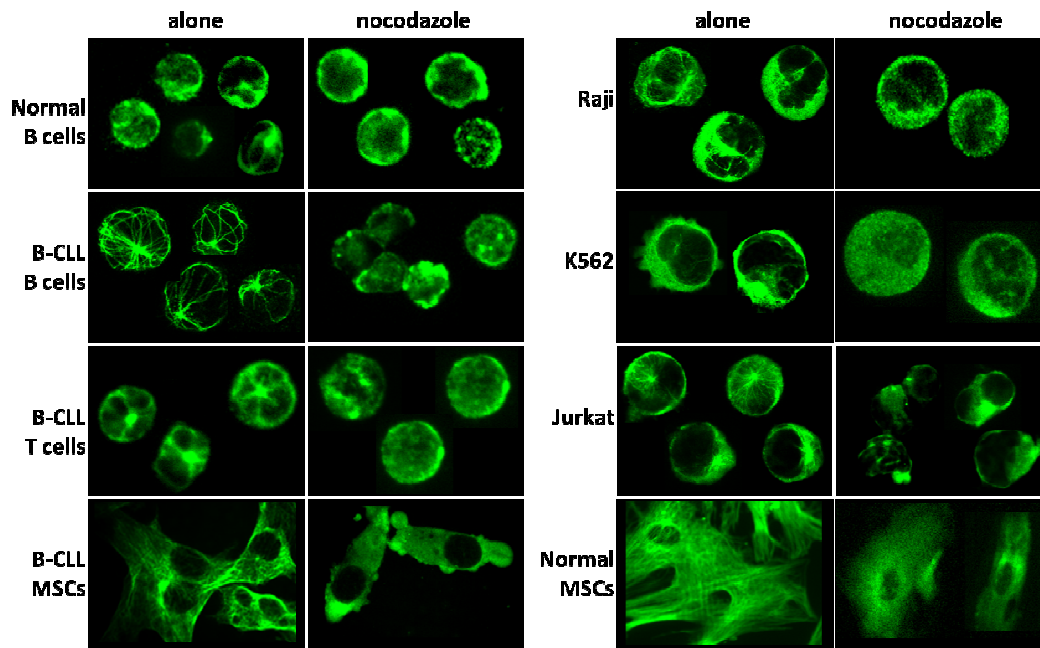


**Figure 22. Confocal microscopy analysis of different cell types before and after 24 hours treatment with 16 $\mu$ M nocodazole.** Cells were stained with an anti- $\alpha$ -tubulin Ab, followed by the appropriate FITC-conjugated secondary Ab (green). We analyzed normal B cells, B and T cells from B-CLL patients, MSCs both from B-CLL patients and healthy donors, and Jurkat, Raji, and K562 cell lines. The figure is representative of experiments performed in triplicate for each cell type.

Furthermore, we did not find any reduction of survival in examined cell lines (Jurkat, 105 $\pm$ 11%; Raji, 107 $\pm$ 8%; K562, 98 $\pm$ 11%, figure 23A, box-plots III, IV and V). In addition MSCs obtained from healthy donors and B-CLL patients did not undergo apoptosis when treated with nocodazole (normal MSCs, 102 $\pm$ 3%; B-CLL MSCs, 99 $\pm$ 20 %, figure 23A, box-plots VI and VII). To verify that nocodazole treatment was significantly effective only on B-CLL cells, we performed a Paired Student's *t*-Test comparing each pair of data (cell viability before and after treatment) for each set of experiments. The p values were the following: B-CLL p=0.000; normal B cells p=0.289; Jurkat cell line p=0.633; Raji cell line p=0.267; K562 cell line p=0.723; B-CLL MSCs p=0.840; normal MSC p=0.581 (figure 23B). By ANOVA test the p value was highly significant (p<0.0001). All the statistic tests performed confirmed the selectivity of nocodazole in killing B-CLL cells with respect to normal and other cell types.

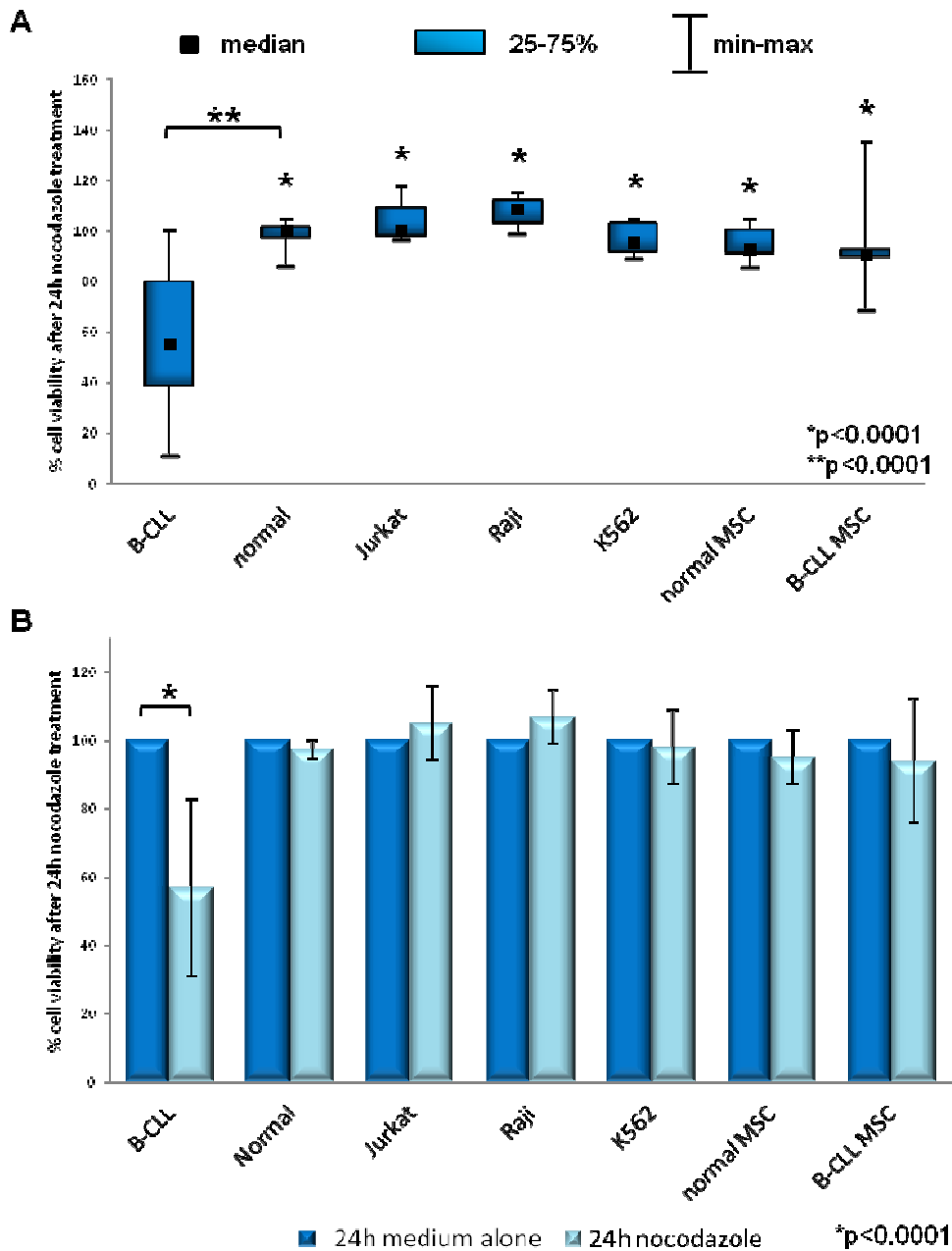


**Figure 23. A. Percentage of cell viability after 24 hours of culture with 16µM nocodazole.** Cell apoptosis was assessed by Annexin V/PI test. The graph shows the percentage of cell viability after 24h of nocodazole treatment. Data are expressed as median, upper and lower quartiles, minimum and maximum. \*p<0.0001 ANOVA test between all the cell types analyzed; \*\*p<0.0001 Paired Student's *t*-Test between leukemic and normal B cells. **B. Percentage of cell viability after 24 hours of culture with or without nocodazole.** Histograms show the mean±SD of cell viability percentage after 24h of cell analyzed in point A with and without the addition of 16µM nocodazole (B-CLL, n=52; normal B, n=10; Jurkat, n=3; Raji, n=3; K562, n=3; normal MSC, n=3; B-CLL MSC, n=8), \*p<0.0001, compared with cells cultured in medium alone, Paired Student's *t*-Test.

Considering the high variability of nocodazole effect on B-CLL cells (the range varies from 11% to 100% of viable cells after 24 hours of treatment), we compared the viability of normal and leukemic B cells after 24, 48 and 72 hours

of treatment. B cells obtained from healthy donors (figure 24A, right panel) were not damaged even after 72 hours of nocodazole treatment; conversely, approximately only 1/3 of leukemic B cells was still alive after 72 hours of treatment ( $15\pm 10\%$ ; figure 24A, left panel).

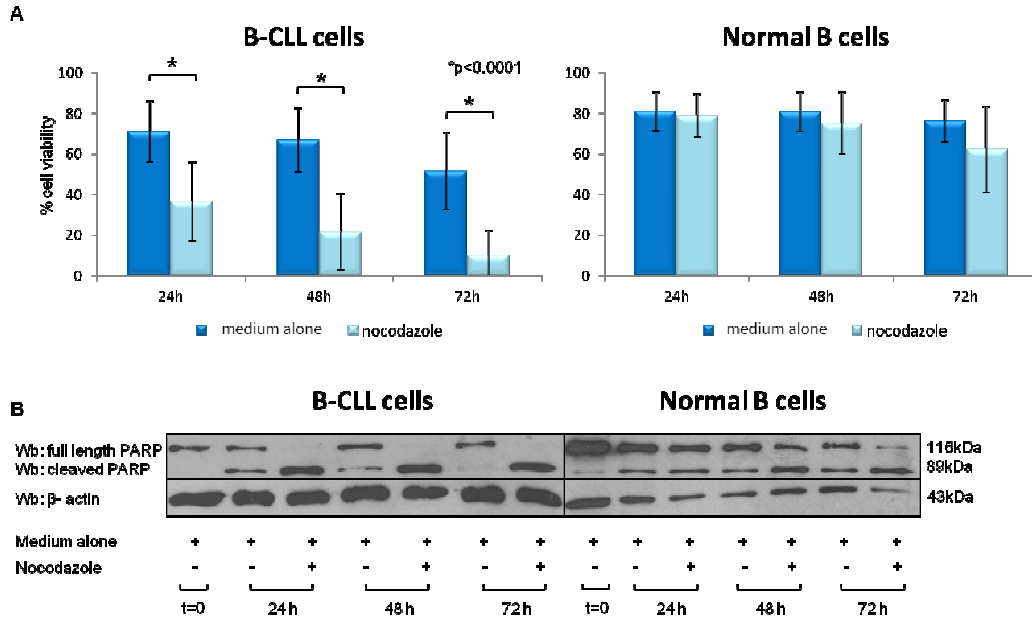


**Figure 24. A. Percentage of cell viability after incubation with or without nocodazole in normal and leukemic B cells.** Histograms show the mean $\pm$ SD of percentage viability of normal B cells and B-CLL cells (left) with or without  $16\mu\text{M}$  nocodazole after 24, 48 and 72 hours of all cases analyzed.  $*p < 0.0001$ , Paired Student's *t*-Test between treated and untreated cells. **B. PARP protein expression.** B-CLL and normal B cells were cultured alone or in the presence of  $16\mu\text{M}$  nocodazole for 24, 48 and 72 hours. The total cell lysates were subjected to SDS-PAGE, transferred to nitrocellulose membrane and detected sequentially with anti-PARP Ab, to highlight the apoptosis, and anti- $\beta$ -actin Ab. As control we used a lysate freshly isolated from B-CLL or normal B cells ( $t=0$ ). The figure shows a representative case of B-CLL cells and one of normal B cells.

To confirm the effect of nocodazole on neoplastic B cell viability, we assessed the PARP protein expression in normal and leukemic B cells after 24, 48 and 72 hours of treatment by immunoblotting. The results obtained show the maintenance of the whole form of PARP (116kDa electrophoretic band) even after 72 hours of treatment in normal B cells (figure 24B, right panel). In B-CLL cells, starting from 24 hours, nocodazole treatment causes the 89kDa band of the cleaved form of PARP, index of apoptosis induction (figure 24B, left panel), and the disappearance of the full length of PARP.

### 3. Nocodazole kills specifically B-CLL cells with preference for unmutated B cell clones

B-CLL cases have mutated as well as unmutated IgV<sub>H</sub> genes which largely correlate with a favorable and unfavorable clinical prognosis, respectively<sup>16</sup>.

Therefore, we correlated the ability of nocodazole to induce apoptosis in B-CLL cells with the presence or absence of somatic hypermutations in IgV<sub>H</sub> genes<sup>90</sup>. Taken into account the cell viability of B-CLLs after nocodazole treatment, obtained in previous experiments. After 24 hours of nocodazole treatment, mutated B-CLL cells showed a viability average of 67%±24, whereas those unmutated showed a viability average of 50%±24 (figure 25), demonstrating that nocodazole is more effective on unmutated vs mutated patients (p<0.05, Student's *t* test).

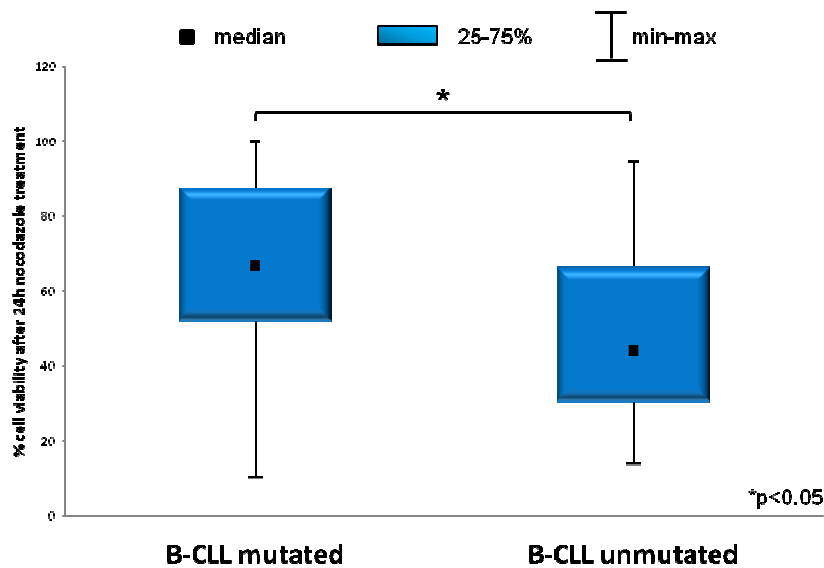


Figure 25. Correlation of leukemic B cell mutational status and cell viability after 24 hours of nocodazole treatment. Cell apoptosis was assessed by Annexin V/PI test. The graph shows the percentage of cell viability after 24h of nocodazole treatment. Data are expressed as median, upper and lower quartiles, minimum and maximum. \*p<0.05, Student's *t*-Test.

#### **4. Nocodazole kills leukemic B cells whereas it does not affect T cells from the same patients**

Nocodazole is unable to induce Jurkat cell (a T cell line) apoptosis (figure 23A, box-plots III). This evidence prompted us to analyze residual normal T cells from B-CLL patients. In B-CLL samples with a discrete T cell subset (at least 25-30% of lymphocytes), we evaluated nocodazole action on T lymphocytes performing a specific Annexin V/PI staining for different cell populations (CD19+/5+ neoplastic B cells and CD5+ T cells).

Figure 26A shows a representative case. The overall data obtained from all patients analyzed are summarized in the histograms in figure 26B. Interestingly, nocodazole killed B cells but it did not affect T cells obtained from the same B-CLL PBMCs pool ( $70\pm 23\%$  vs  $30\pm 12\%$ ; data are expressed as percentage of viable cells after 24 hours treatment with or without nocodazole), showing a very low toxicity for T cells (figure 26B). Data were confirmed by western blotting analysis of cleaved form of PARP on separated B and T cell subsets. Only B, but not T, cells showed an high amount of the PARP cleaved form, index of apoptosis induction (figure 26C). The observation that nocodazole is not effective on T cells is intriguingly; in fact, B-CLL patients which still have a certain percentage of T cells show a stable disease with a relatively less aggressive clinical course. In this view, nocodazole could be used, after proper studies, to treat these B-CLL patients, preserving the T cell population.

#### **5. Nocodazole effect on B-CLL cells is not counteracted by mesenchymal stromal cells**

Mesenchymal stromal cells (MSCs) regulate normal hematopoiesis by providing attachment sites and secreted or surface-bound growth factors that constitute the bone marrow microenvironment.

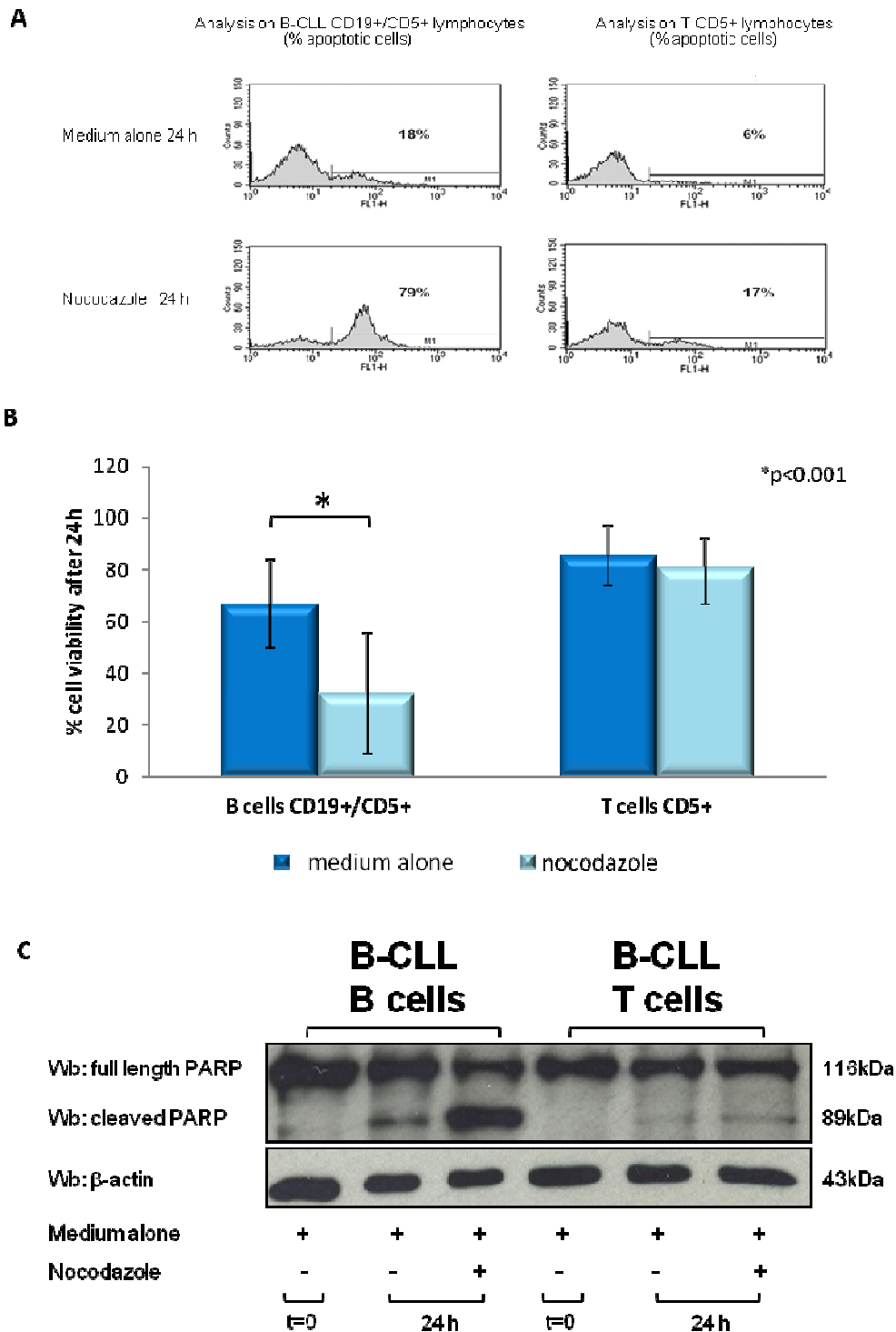


**Figure 26. A. Percentage of annexin-positive B and T cells from the same B-CLL patients after 24 hours of nocodazole treatment.** Cytograms are relative to a representative case in which the apoptosis of B and T cells from a B-CLL patient was evaluated by Annexin V/PI test after 24 hours of incubation with or without 16μM nocodazole. **B. Histograms of cell viability percentage of B and T cells from B-CLL patients after 24 hours of nocodazole treatment.** Histograms show the mean±SD of the percentage of viable CD19+/CD5+ B cells (left) and CD5+ T cells after 24 hours with and without 16μM nocodazole of all patients analyzed (n=19). \*p<0.001, Paired Student's *t*-Test. **C. PARP protein expression.** B and T cells from the same B-CLL patients were cultured in medium alone or in presence of 16μM nocodazole for 24 hours. The total cell lysates were subjected to SDS-PAGE, transferred to nitrocellulose membrane and detected sequentially with the anti-PARP Ab, to highlight the apoptosis, and the anti-β-actin Ab. As control we used freshly isolated B and T lymphocytes lysates from B-CLL patients (t=0). The figure shows a representative case.

Growing evidence suggests that MSCs protect B-CLL cells from conventional drugs (fludarabine, dexamethasone and cyclophosphamide)<sup>97</sup>.

In this context, we investigated the reciprocal effects between nocodazole and MSCs, obtained from B-CLL patients and healthy donors. We previously demonstrated that MSCs from donors ( $102\pm 3\%$ ,  $p=0.840$ ) and from B-CLL patients ( $99\pm 20\%$ ,  $p=0.581$ ) did not undergo apoptosis when cultured with nocodazole (figure 23A, box-plots VI and VII).

Subsequently, we performed co-cultures of leukemic B and MSC cells obtained from B-CLL patients to verify the role of bone marrow environment influence on nocodazole activity. Surprisingly, MSCs were not able to protect B neoplastic cells from nocodazole-mediated apoptosis. Figure 27A shows the percentage of B-CLL viability of leukemic B cells cultured with or without a MSC layer and incubated in presence or in absence of nocodazole for 24, 48, 72, and 120 hours (5 days). Moreover, to increase the effectiveness of the "*in vitro* environment", we performed the same experiments adding CD40L to MSCs layer, mimicking the effect of T lymphocytes on CD40 receptor present on leukemic B cell surface, that improves B-CLL cell survival.

Viability of leukemic B cells co-cultured with MSC without nocodazole (B-CLL+MSC, blue line, figure 27A) remains high and essentially unchanged for the duration of the experiment. Data on the culture of cells with nocodazole and without the MSC layer (positive control; B-CLL+nocodazole, green line, figure 27A) confirm the apoptotic effect of the drug; there is, in fact, an important decrease of viable cells after 24 hours of incubation, and a further gradual reduction in subsequent detections. Data obtained from the two experimental conditions, cultures with nocodazole (B-CLL+MSC+nocodazole, red line, figure 27A) and co-cultures in the presence of nocodazole and CD40L (B-CLL+MSC+nocodazole+CD40L, light blue line, figure 27A), are substantially overlapping; in fact, the percentage of viable cells is reduced at all time points analyzed. These observations indicate that the apoptotic effect of nocodazole overcomes the protective action given by bone marrow microenvironment.

To confirm these evidences, we evaluated the PARP protein expression by western blotting analysis (figure 27B). The results obtained show the preservation

of the electrophoretic band of 116kDa relative to PARP full length only when B cells were co-cultured with MSC at 24, 48, 72 hours and 5 days. On the contrary, the incubation of B-CLL cells co-cultured with MSC and nocodazole, or with MSC, nocodazole and CD40L, revealed an absolute prevalence of the electrophoretic band of 89kDa relative to the cleaved form of PARP, index of apoptosis.

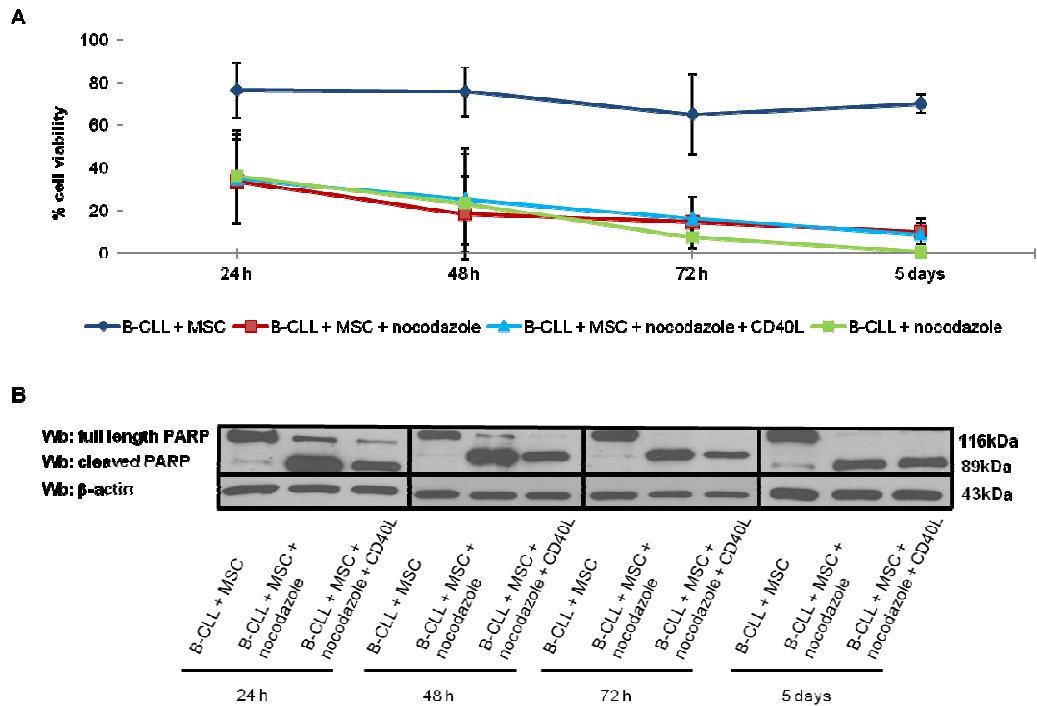


**Figure 27. A. Percentage viability of B-CLL cells co-cultured with MSCs at different conditions.** B-CLL cells were co-cultured for 24, 48, 72 hours and 5 days with MSCs obtained from B-CLL patients at the following conditions: medium alone (B-CLL+MSC, blue line), with the addition of 16µM nocodazole (B-CLL+MSC+nocodazole, red line) and with the addition of nocodazole and CD40L (B-CLL+MSC+nocodazole+CD40L, light blue line); the positive control (B-CLL+nocodazole, green line) is represented by cells treated with nocodazole but not in co-culture. The graph shows the mean±SD of results obtained in all cases analyzed (n=31). **B. PARP protein expression.** B-CLL cells were co-cultured with MSCs in medium alone, with 16µM nocodazole, and with nocodazole and CD40L for 24, 48, 72 hours and 5 days. The total cell lysates were subjected to SDS-PAGE, transferred to nitrocellulose membrane and detected sequentially with the anti-PARP Ab, to highlight the apoptosis, and the anti-β-actin Ab. The figure shows a representative case.

Finally, we performed experiments adding patient's plasma to the culture of B-CLL with MSCs and evaluating viability percentages after 24, 48 and 72 hours of nocodazole treatment (figure 28). Once more, nocodazole activity was not blocked.

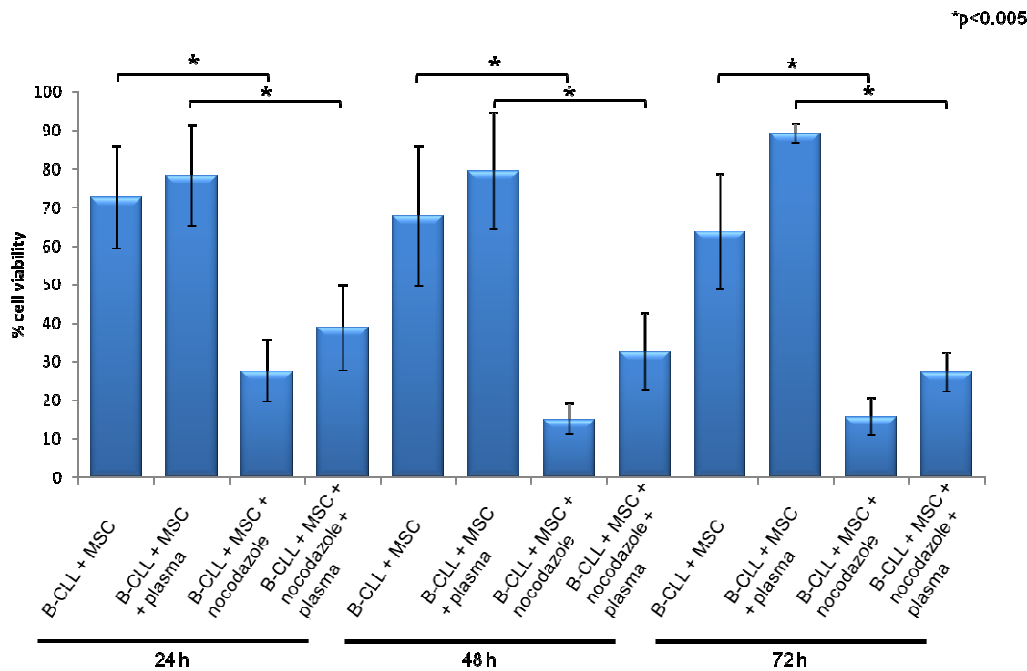


**Figure 28. Percentage of B-CLL cells viability after incubation with nocodazole and plasma.** B-CLL cells were incubated with MSCs for 24, 48, 72 hours with 16 $\mu$ M nocodazole and with the addition of plasma coming from the same patients. The graph shows the mean $\pm$ SD of results obtained in all cases analyzed (n=5). \*p<0.005 between B-CLL+MSC and B-CLL+MSC+nocodazole and between B-CLL+MSC+plasma and B-CLL+MSC+nocodazole+plasma treatment, Paired Student's *t*-Test.

## 6. Nocodazole targets Lyn kinase activity

Tyrosine kinase Lyn is the protein that, through its phosphorylation activity, initiates the signal transduction cascade induced by BCR stimulation. In B-CLL this protein is overexpressed, constitutively activated, and part of an abnormal cytosolic complex of 600kDa.

Moreover, Lyn is responsible for the increased tyrosine phosphorylation of B-CLL cells and sustains the survival of the neoplastic clone<sup>55,60</sup>. The constitutive Lyn activation correlates with extended cell survival and defective apoptosis. In fact, the inhibition of Lyn activity, obtained by treating leukemic cells with Lyn specific inhibitors, is sufficient to restore cell apoptosis, providing a correlation between high basal Lyn activity and defects in the induction of the programmed cell death in B-CLL cells<sup>55</sup>.

The treatment of neoplastic cells with nocodazole revealed a decrease of total tyrosine phosphorylation in cell lysate, which was directly correlated with the apoptosis of neoplastic clone (see PARP protein detection, figure 29).

According to these results, we analyzed nocodazole effect on Lyn kinase activity. The activity is controlled by tyrosine phosphorylation in two opposite ways: the tyrosine phosphorylation of Lyn C-terminal Tyr507 inhibits Lyn activity, while the phosphorylation, or autophosphorylation, at Tyr396 induces Lyn activation. After nocodazole treatment, the expression level of Lyn protein did not change while the phosphorylation level of Lyn active site Tyr396 was significantly reduced (figure 29), suggesting that nocodazole may inhibit Lyn kinase activity thus preventing B-CLL survival.

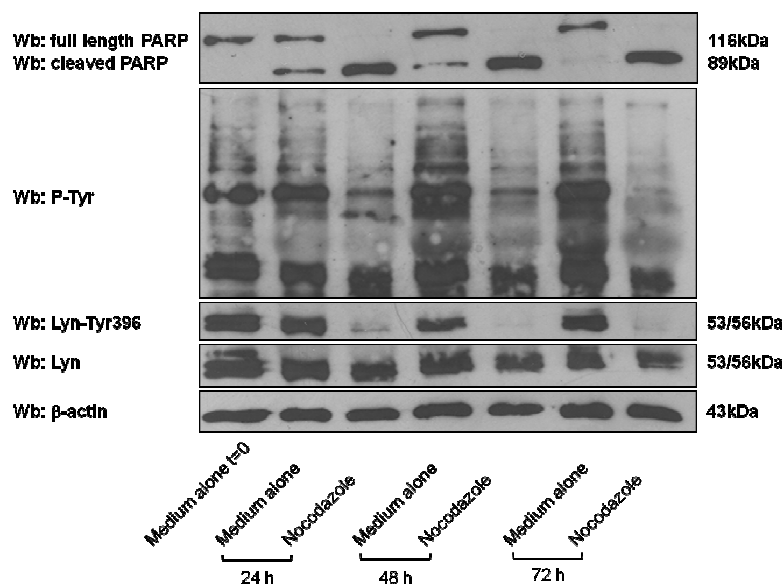


**Figure 29. B-CLL proteic profile after nocodazole treatment.** B-CLL cells were cultured in medium alone or in presence of 16 $\mu$ M nocodazole for 24, 48 and 72 hours. The total cell lysates were subjected to SDS-PAGE, transferred to nitrocellulose membrane and detected sequentially with: anti-PARP Ab to highlight the apoptosis, anti-P-Tyr which recognizes phosphorylated tyrosines, anti-Lyn-Tyr396 Ab which recognizes Lyn active conformation, anti-Lyn Ab which recognizes the entire form of Lyn, and anti- $\beta$ -actin Ab. As control we used a lysate from freshly isolated B-CLL cells (t=0). The figure shows a representative case.

In addition, by real time RT-PCR, we analyzed the expression of mRNA encoding for Lyn in B-CLL cells co-cultured with MSCs and in presence of nocodazole and CD40L (see paragraph 4, figure 27). The results obtained show that the treatment with nocodazole reduce mRNA level of Lyn, and this effect is not counteracted by the presence of CD40L (figure 30A). However, these are preliminary data, and ulterior analysis have to be performed to understand Lyn mRNA behavior after nocodazole treatment.

Furthermore, we assessed Lyn-Tyr396 expression of the same samples by immunoblotting (figure 30B). Also in this case, the phosphorylation level of Lyn

active site Tyr396 is significantly reduced, while the total Lyn expression level is not affected, further supporting our hypothesis that nocodazole could be used Lyn inhibitor.

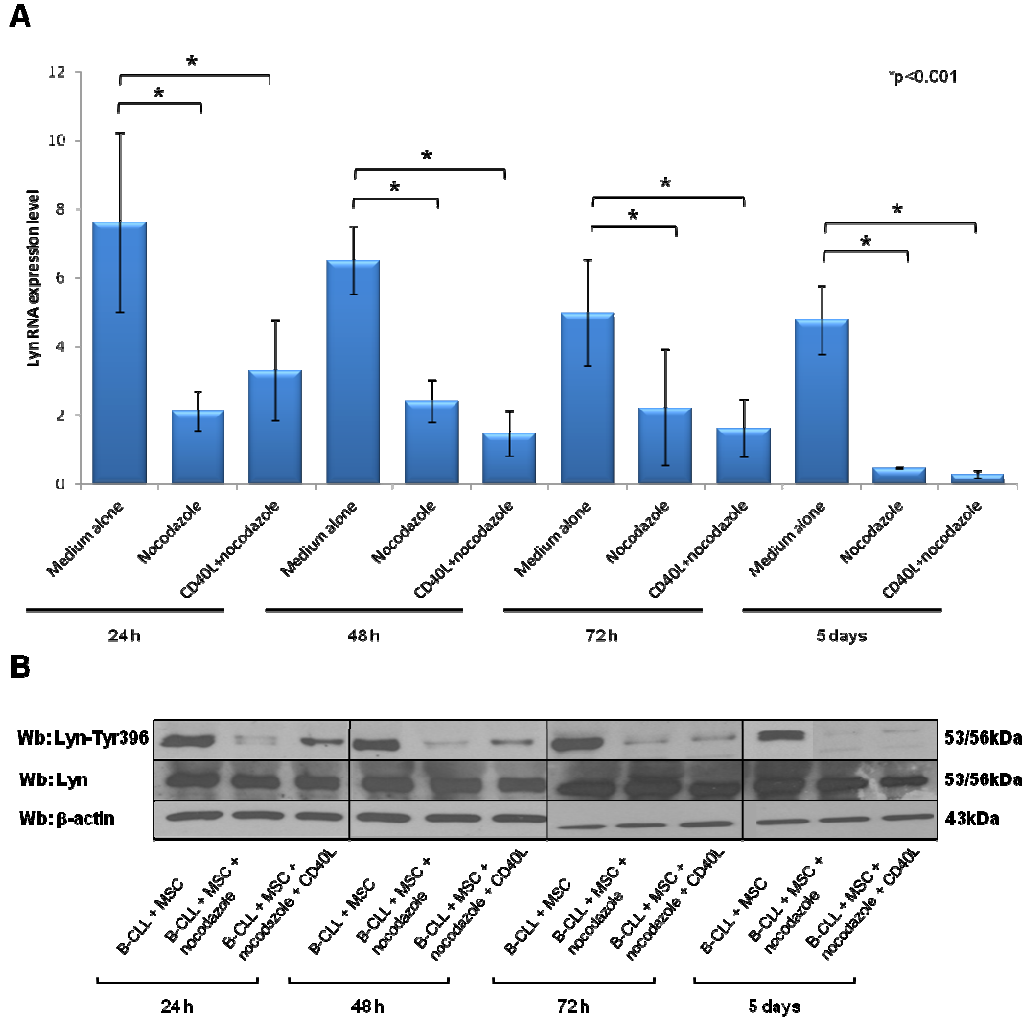


**Figure 30. A. Quantification of mRNA of Lyn by real time RT-PCR of B-CLL cells co-cultured with MSC.** B-CLL cells were co-cultured for 24, 48, 72 hours and 5 days with MSCs obtained from B-CLL patients with the addition of 16 $\mu$ M nocodazole and with CD40L+nocodazole. From all the conditions the RNA was extracted and retro-transcribed to analyze the Lyn gene expression by real time RT-PCR. The graph shows the mean $\pm$ SD of results obtained in all cases analyzed (n=6). \*p<0.001 between medium alone and nocodazole treatment and between medium alone and CD40L+nocodazole, Paired Student's *t*-Test. **B. Lyn-Tyr396 and Lyn protein expression.** B-CLL cells were co-cultured with MSCs in medium alone, with 16 $\mu$ M nocodazole, and with nocodazole and CD40L for 24, 48, 72 hours and 5 days. The total cell lysates were subjected to SDS-PAGE, transferred to nitrocellulose membrane and detected sequentially with anti-Lyn-Tyr396 Ab which recognizes Lyn active conformation, anti-Lyn Ab which recognizes the entire form, and anti- $\beta$ -actin Ab. The figure shows a representative case.

## DISCUSSION

B-cell Chronic Lymphocytic Leukemia (B-CLL) is a monoclonal lymphoproliferative disorder characterized by the accumulation of B cells due to increased proliferation and defects in apoptotic mechanisms<sup>1</sup>. In addition, the behavior of leukemic cells suggests the presence of alterations involving cytoskeleton functions: in fact, these cells have a reduced ability to bind several ligands and are susceptible to microtubule disrupting drugs<sup>75</sup>. In B-CLL cells microtubules, composed of  $\alpha\beta$  tubulin dimers, are tightly connected with functional anomalies of the BCR: molecules associated with BCR-mediated signal transduction, such as Syk, Vav, and Cbl, bind tubulin. On the other side BCR members, like CD79a and CD79b, co-immunoprecipitate with  $\beta$ -tubulin<sup>75,76</sup>.

Microtubules are important chemotherapeutic targets for the crucial role they play in cancer cell functions. Agents that disrupt microtubule dynamics are important in both curative and palliative cytotoxic chemotherapeutic regimen. Microtubule inhibitors are already employed in hematologic malignances such as Hodgkin lymphoma (HL) or acute lymphocytic leukemia (ALL), and they will probably become useful drugs in B-CLL therapy. However, microtubule inhibitor usefulness has been limited by the high toxicities they show on microtubules of normal cells. In fact, microtubule-interfering compounds may affect both neoplastic and non-malignant cells in interphase, in addition to the mitotic phase of the cell cycle. This essential lack of selectivity for tumor cells leads to a variety of toxic side effects and to a rather low therapeutic index, enhancing the importance of identifying new highly selective microtubule inhibitors for malignant cells.

Previous data demonstrated that nocodazole, a synthetic agent that depolymerizes microtubules, seems able to selectively kill leukemic cells from B-CLL inducing changes associated to Bcl-2 expression and phosphorylation<sup>91</sup>. Basing on this reports, during this PhD program a series of experiments were performed to further investigate this aspect.

We verified the depolymerizing effect of nocodazole on tubulin, and investigated the apoptosis induced by this drug in B-CLL cells, and in a large spectrum of different cells, such as normal B cells from healthy donors, Mesenchymal Stromal Cells (MSCs) both from B-CLL patients and donors, T lymphocytes from B-CLL patients, Jurkat, Raji, and K562 cell lines. The obtained results confirmed that only B-CLL cells undergo apoptosis after nocodazole treatment while the other cell types are not affected by this inhibitor. It is actually unclear the molecular mechanism underlying the specific anti-cancer activity of nocodazole vs B-CLL cells. To further deepen the analysis regarding nocodazole activity on B-CLL cells, we related nocodazole effects to the mutational status of B-CLL clones, in order to investigate whether nocodazole action changes between B-CLL subgroups (mutated or unmutated). Interestingly, our results demonstrated that nocodazole effect was significantly higher in the subset of B-CLL cells with unmutated IgV<sub>H</sub> genes, which is related to unfavorable prognosis, suggesting a possible role of nocodazole in the treatment of unmutated B-CLLs, in association with conventional chemotherapy.

On the other side, nocodazole was unable to induce apoptosis in Jurkat cell line (a T cell line). This evidence prompted us to analyse residual T cells from B-CLL patients. Our results demonstrated that nocodazole kills B cells but does not affect T cells obtained from the same B-CLL PBMC pool, showing a very low toxicity for T lymphocyte viability. The observation that nocodazole is not effective on T cells is intriguing: in fact, patients who still have a discrete percentage of T cells, show a stable disease with a relatively less aggressive clinical course, suggesting a possible role of nocodazole also in the treatment of these B-CLL patients, thus preserving the T cell population. Recent data indicate that also T lymphocytes from B-CLL patients present functional deficiencies and a compromised ability during the immune response<sup>98</sup>. This situation can be resolved with the administration of lenalidomide, an immunomodulatory drug, which is able to restore the T-dependent anti-tumor immune response<sup>98,99</sup>. These data, together with our results, open the possibility of a combined use of nocodazole and lenalidomide in B-CLL treatment and maintenance, in order to achieve a selective pro-apoptotic action against leukemic B cells and a recovery of T cell functions.

In conclusion, in this first part of the research program, we can state that nocodazole has an extreme selectivity in inducing B-CLL cell apoptosis, demonstrating at the same time the absence of any toxicity vs other cell types, with a fine ability to discriminate malignant from normal cells.

A key role for B-CLL cell survival is exerted by MSCs; they regulate normal hematopoiesis by providing attachment sites and secreted or surface-bound growth factors that strongly contribute to the marrow microenvironment<sup>100</sup>. Growing evidence suggests that MSCs protect B-CLL cells from conventional drugs, such as fludarabine, dexamethasone and cyclophosphamide<sup>97</sup>. When we tested nocodazole effects on leukemic B cells co-cultured with MSCs (from patients and normal donors) we demonstrate that nocodazole acts also in presence of MSCs, avoiding the protective effect they have on neoplastic clone survival. Moreover, to increase the strength of the "*in vitro* environment", we added patient's plasma or CD40L to MSCs layer, mimicking the effect of CD40L (T cells)/CD40 (B cells) interaction, that improves B-CLL cell survival. The contemporary presence of CD40L and MSCs or the presence of plasma are, once more, unable to counteract nocodazole apoptotic effect. In addition, we verified that nocodazole neutralized survival and protection stimuli provided by MSCs on leukemic B cells, without affecting MSC viability and likely their role in hematopoiesis process. The blocking of such a protective interaction could restore B-CLL cells apoptosis induced by cytotoxic therapies.

It is unknown how nocodazole exerts these effects. We can speculate that nocodazole, depolymerizing and then blocking tubulin cytoskeleton, does not allow the intracellular transport of molecules such as cytokines and chemokines, which support the neoplastic clone survival. Nocodazole may act also on cell-cell contact mediated by surface integrins. Contact between B-CLL cells and Nurse-Like Cells (NLCs) or MSCs is established and maintained by chemokine receptors and adhesion molecules. NLCs and MSCs attract B-CLL cells via the chemokine axes CXCR4/CXCL12 and CXCR5/CCL5. Integrins expressed on the surface of B-CLL cells cooperate with chemokine receptors in establishing cell-cell adhesion through respective ligands on the stromal cells (VCAM-1)<sup>72</sup>. The damage caused by nocodazole might disrupt the tubulin-actin interactions and the

cytoskeleton, altering the correct docking site for the integrins on the inner surface of the plasma membrane.

The attempt to understand nocodazole remarkable selectivity for leukemic B cells prompted us to evaluate its actions in relation to cellular kinase activity. In fact, it was recently demonstrated that nocodazole cell treatment induces significant phosphoproteomic changes in a variety of tumor cell lines, such as HeLa (cervical cancer), HCT-116 (colorectal carcinoma), and NCI-H460 (lung cancer), suggesting that nocodazole may modulate kinase activity. In addition, docking simulations indicate that the aminobenzimidazole moiety of nocodazole can fit into the ATP binding sites of kinases, displaying high affinity toward a set of cancer-related kinases, including ABL, c-KIT, BRAF, and MEK<sup>101</sup>. We demonstrated that in B-CLL Lyn, a Src-kinase, is overexpressed and crucially involved in the neoplastic B cell survival. Our experiments showed that nocodazole modifies the anomalous Lyn-mediated phosphorylation restoring apoptosis sensibility. In fact, nocodazole is able to down-modulate the phosphorylation of Lyn at Tyr396, its active site. Moreover, nocodazole treatment decreases mRNA encoding for Lyn, strongly suggesting that kinase Lyn may be one of nocodazole targets.

Recently, we showed that, in B-CLL cells, Lyn is an integral component of an aberrant cytosolic 600kDa complex, where Lyn is associated both with Hsp90, HS1 (Hematopoietic lineage cell Specific protein 1), and SHP-1L. Hsp90 stabilizes the complex by contributing to converting a network of transient interactions into permanent ones, thus maintaining Lyn in an active conformation and preventing its degradation<sup>60</sup>. In this context, after proper studies, nocodazole may be used to disrupt the aberrant complex, restoring the normal apoptosis process. In fact, although several Src-family inhibitors are available and already used in clinical management for other lymphomas, i.e. Imatinib and Dasatinib, it is crucial to find specific inhibitors of Lyn, considering its fundamental role in B-CLL. There are several encouraging pre-clinical reports on the use of Dasatinib in B-CLL treatment, but they have shown few significant clinical responses. Considering that B-CLL cells also harness a number of additional stimuli for survival, it is possible that, *in vivo*, B-CLL cells may be rescued from apoptosis by additional microenvironment factors. The pro-apoptotic effect of Dasatinib on

B-CLL *in vitro* is significantly reduced in the presence of stromal cells<sup>102</sup>, while our results demonstrate that nocodazole is able to overcome their protective effect.

The generation of phosphotyrosine residues by Lyn and Syk results in the activation of multiple pathways. Constitutively activated protein tyrosine kinases (PTKs) may contribute to activate multiple signal transducers and pathways including the PI3K/Akt/mTOR pathway, the RAS/RAF/MAPK and ERK kinase cascade, phospholipase C $\gamma$ 2 and PKC, with subsequent activation of downstream transcription factors promoting cell survival<sup>103,104</sup>. Considering the fact that nocodazole influences Lyn kinase activity, we can speculate that, despite it is a known microtubule inhibitor which use is actually limited to laboratory practice, a new role as therapeutic compound for B-CLL treatment could be taken into account.



## BIBLIOGRAPHY

1. Caligaris-Cappio F, Hamblin TJ. B-cell chronic lymphocytic leukemia: a bird of a different feather. *J Clin Oncol*. 1999;17:399-408.
2. Siegel R, Ward E, Brawley O, Jemal A. Cancer statistics, 2011: the impact of eliminating socioeconomic and racial disparities on premature cancer deaths. *CA Cancer J Clin*;61:212-236.
3. Landgren O, Gridley G, Check D, Caporaso NE, Morris Brown L. Acquired immune-related and inflammatory conditions and subsequent chronic lymphocytic leukaemia. *Br J Haematol*. 2007;139:791-798.
4. Landgren O, Rapkin JS, Mellemkjaer L, Gridley G, Goldin LR, Engels EA. Respiratory tract infections in the pathway to multiple myeloma: a population-based study in Scandinavia. *Haematologica*. 2006;91:1697-1700.
5. Wiernik PH, Ashwin M, Hu XP, Paietta E, Brown K. Anticipation in familial chronic lymphocytic leukaemia. *Br J Haematol*. 2001;113:407-414.
6. Barcellini W, Capalbo S, Agostinelli RM, et al. Relationship between autoimmune phenomena and disease stage and therapy in B-cell chronic lymphocytic leukemia. *Haematologica*. 2006;91:1689-1692.
7. Binet JL, Caligaris-Cappio F, Catovsky D, et al. Perspectives on the use of new diagnostic tools in the treatment of chronic lymphocytic leukemia. *Blood*. 2006;107:859-861.
8. Landgren O, Pfeiffer RM, Stewart L, et al. Risk of second malignant neoplasms among lymphoma patients with a family history of cancer. *Int J Cancer*. 2007;120:1099-1102.
9. Hallek M, Cheson BD, Catovsky D, et al. Guidelines for the diagnosis and treatment of chronic lymphocytic leukemia: a report from the International Workshop on Chronic Lymphocytic Leukemia updating the National Cancer Institute-Working Group 1996 guidelines. *Blood*. 2008;111:5446-5456.
10. Cheson BD, Bennett JM, Grever M, et al. National Cancer Institute-sponsored Working Group guidelines for chronic lymphocytic leukemia: revised guidelines for diagnosis and treatment. *Blood*. 1996;87:4990-4997.
11. Rassenti LZ, Huynh L, Toy TL, et al. ZAP-70 compared with immunoglobulin heavy-chain gene mutation status as a predictor of disease progression in chronic lymphocytic leukemia. *N Engl J Med*. 2004;351:893-901.

12. Mauro FR, De Rossi G, Burgio VL, et al. Prognostic value of bone marrow histology in chronic lymphocytic leukemia. A study of 335 untreated cases from a single institution. *Haematologica*. 1994;79:334-341.
13. Melo JV, Catovsky D, Galton DA. Chronic lymphocytic leukemia and prolymphocytic leukemia: a clinicopathological reappraisal. *Blood Cells*. 1987;12:339-353.
14. Hallek M, Langenmayer I, Nerl C, et al. Elevated serum thymidine kinase levels identify a subgroup at high risk of disease progression in early, nonsmoldering chronic lymphocytic leukemia. *Blood*. 1999;93:1732-1737.
15. Sarfati M, Chevret S, Chastang C, et al. Prognostic importance of serum soluble CD23 level in chronic lymphocytic leukemia. *Blood*. 1996;88:4259-4264.
16. Damle RN, Wasil T, Fais F, et al. Ig V gene mutation status and CD38 expression as novel prognostic indicators in chronic lymphocytic leukemia. *Blood*. 1999;94:1840-1847.
17. Ibrahim S, Keating M, Do KA, et al. CD38 expression as an important prognostic factor in B-cell chronic lymphocytic leukemia. *Blood*. 2001;98:181-186.
18. Ghia P, Caligaris-Cappio F. The indispensable role of microenvironment in the natural history of low-grade B-cell neoplasms. *Adv Cancer Res*. 2000;79:157-173.
19. Stevenson FK, Caligaris-Cappio F. Chronic lymphocytic leukemia: revelations from the B-cell receptor. *Blood*. 2004;103:4389-4395.
20. Poulain S, Benard C, Daudignon A, Le Baron F, Morel P, Duthilleul P. Is ZAP-70 expression stable over time in B chronic lymphocytic leukaemia? *Leuk Lymphoma*. 2007;48:1219-1221.
21. Degheidy HA, Venzon DJ, Farooqui MZ, et al. Methodological comparison of two anti-ZAP-70 antibodies. *Cytometry B Clin Cytom*. 2011. Epub ahead of print.
22. Grever MR, Lucas DM, Dewald GW, et al. Comprehensive assessment of genetic and molecular features predicting outcome in patients with chronic lymphocytic leukemia: results from the US Intergroup Phase III Trial E2997. *J Clin Oncol*. 2007;25:799-804.
23. Krober A, Seiler T, Benner A, et al. V(H) mutation status, CD38 expression level, genomic aberrations, and survival in chronic lymphocytic leukemia. *Blood*. 2002;100:1410-1416.
24. Oscier DG, Gardiner AC, Mould SJ, et al. Multivariate analysis of prognostic factors in CLL: clinical stage, IGVH gene mutational status, and loss or mutation of the p53 gene are independent prognostic factors. *Blood*. 2002;100:1177-1184.

25. Dohner H, Stilgenbauer S, Benner A, et al. Genomic aberrations and survival in chronic lymphocytic leukemia. *N Engl J Med.* 2000;343:1910-1916.
26. Terrin L, Trentin L, Degan M, et al. Telomerase expression in B-cell chronic lymphocytic leukemia predicts survival and delineates subgroups of patients with the same igVH mutation status and different outcome. *Leukemia.* 2007;21:965-972.
27. Rampazzo E, Bonaldi L, Trentin L, et al. Telomere length and telomerase levels delineate subgroups of B-cell chronic lymphocytic leukemia with different biological characteristics and clinical outcomes. *Haematologica.* 2012. Epub ahead of print.
28. Ward BP, Tsongalis GJ, Kaur P. MicroRNAs in chronic lymphocytic leukemia. *Exp Mol Pathol;*90:173-178.
29. Chemotherapeutic options in chronic lymphocytic leukemia: a meta-analysis of the randomized trials. CLL Trialists' Collaborative Group. *J Natl Cancer Inst.* 1999;91:861-868.
30. Rai KR, Peterson BL, Appelbaum FR, et al. Fludarabine compared with chlorambucil as primary therapy for chronic lymphocytic leukemia. *N Engl J Med.* 2000;343:1750-1757.
31. Dillman RO, Mick R, McIntyre OR. Pentostatin in chronic lymphocytic leukemia: a phase II trial of Cancer and Leukemia group B. *J Clin Oncol.* 1989;7:433-438.
32. Robak T, Blonski JZ, Kasznicki M, et al. Cladribine with prednisone versus chlorambucil with prednisone as first-line therapy in chronic lymphocytic leukemia: report of a prospective, randomized, multicenter trial. *Blood.* 2000;96:2723-2729.
33. Yamauchi T, Nowak BJ, Keating MJ, Plunkett W. DNA repair initiated in chronic lymphocytic leukemia lymphocytes by 4-hydroperoxycyclophosphamide is inhibited by fludarabine and clofarabine. *Clin Cancer Res.* 2001;7:3580-3589.
34. Flinn IW, Neuberg DS, Grever MR, et al. Phase III trial of fludarabine plus cyclophosphamide compared with fludarabine for patients with previously untreated chronic lymphocytic leukemia: US Intergroup Trial E2997. *J Clin Oncol.* 2007;25:793-798.
35. Alas S, Emmanouilides C, Bonavida B. Inhibition of interleukin 10 by rituximab results in down-regulation of bcl-2 and sensitization of B-cell non-Hodgkin's lymphoma to apoptosis. *Clin Cancer Res.* 2001;7:709-723.
36. Wierda W, O'Brien S, Wen S, et al. Chemoimmunotherapy with fludarabine, cyclophosphamide, and rituximab for relapsed and refractory chronic lymphocytic leukemia. *J Clin Oncol.* 2005;23:4070-4078.

37. Montillo M, Cafro AM, Tedeschi A, et al. Safety and efficacy of subcutaneous Campath-1H for treating residual disease in patients with chronic lymphocytic leukemia responding to fludarabine. *Haematologica*. 2002;87:695-700.
38. Stilgenbauer S, Dohner H. Campath-1H-induced complete remission of chronic lymphocytic leukemia despite p53 gene mutation and resistance to chemotherapy. *N Engl J Med*. 2002;347:452-453.
39. O'Brien S, Moore JO, Boyd TE, et al. Randomized phase III trial of fludarabine plus cyclophosphamide with or without oblimersen sodium (Bcl-2 antisense) in patients with relapsed or refractory chronic lymphocytic leukemia. *J Clin Oncol*. 2007;25:1114-1120.
40. Dreger P, Montserrat E. Autologous and allogeneic stem cell transplantation for chronic lymphocytic leukemia. *Leukemia*. 2002;16:985-992.
41. Chanan-Khan A, Miller KC, Musial L, et al. Clinical efficacy of lenalidomide in patients with relapsed or refractory chronic lymphocytic leukemia: results of a phase II study. *J Clin Oncol*. 2006;24:5343-5349.
42. Dighiero G. CLL biology and prognosis. *Hematology Am Soc Hematol Educ Program*. 2005:278-284.
43. Klein U, Tu Y, Stolovitzky GA, et al. Gene expression profiling of B cell chronic lymphocytic leukemia reveals a homogeneous phenotype related to memory B cells. *J Exp Med*. 2001;194:1625-1638.
44. Collins RJ, Verschuer LA, Harmon BV, Prentice RL, Pope JH, Kerr JF. Spontaneous programmed death (apoptosis) of B-chronic lymphocytic leukaemia cells following their culture in vitro. *Br J Haematol*. 1989;71:343-350.
45. Saxena A, Viswanathan S, Moshynska O, Tandon P, Sankaran K, Sheridan DP. Mcl-1 and Bcl-2/Bax ratio are associated with treatment response but not with Rai stage in B-cell chronic lymphocytic leukemia. *Am J Hematol*. 2004;75:22-33.
46. Mohr J, Helfrich H, Fuge M, et al. DNA damage-induced transcriptional program in CLL: biological and diagnostic implications for functional p53 testing. *Blood*. 2011;117:1622-1632.
47. Ghavami S, Hashemi M, Ande SR, et al. Apoptosis and cancer: mutations within caspase genes. *J Med Genet*. 2009;46:497-510.
48. Pallasch CP, Wendtner CM. Overexpression of the Fas-inhibitory molecule TOSO: a novel antiapoptotic factor in chronic lymphocytic leukemia. *Leuk Lymphoma*. 2009;50:498-501.
49. Niiri H, Clark EA. Regulation of B-cell fate by antigen-receptor signals. *Nat Rev Immunol*. 2002;2:945-956.

50. Schamel WW, Reth M. Monomeric and oligomeric complexes of the B cell antigen receptor. *Immunity*. 2000;13:5-14.
51. Cragg MS, Chan HT, Fox MD, et al. The alternative transcript of CD79b is overexpressed in B-CLL and inhibits signaling for apoptosis. *Blood*. 2002;100:3068-3076.
52. Gupta N, DeFranco AL. Visualizing lipid raft dynamics and early signaling events during antigen receptor-mediated B-lymphocyte activation. *Mol Biol Cell*. 2003;14:432-444.
53. Gross AJ, Proekt I, DeFranco AL. Elevated BCR signaling and decreased survival of Lyn-deficient transitional and follicular B cells. *Eur J Immunol*. 2011. Epub ahead of print.
54. Mlinaric-Rascan I, Yamamoto T. B cell receptor signaling involves physical and functional association of FAK with Lyn and IgM. *FEBS Lett*. 2001;498:26-31.
55. Contri A, Brunati AM, Trentin L, et al. Chronic lymphocytic leukemia B cells contain anomalous Lyn tyrosine kinase, a putative contribution to defective apoptosis. *J Clin Invest*. 2005;115:369-378.
56. Luciano F, Ricci JE, Auberger P. Cleavage of Fyn and Lyn in their N-terminal unique regions during induction of apoptosis: a new mechanism for Src kinase regulation. *Oncogene*. 2001;20:4935-4941.
57. Thomas ML, Brown EJ. Positive and negative regulation of Src-family membrane kinases by CD45. *Immunol Today*. 1999;20:406-411.
58. Donella-Deana A, Cesaro L, Ruzzene M, Brunati AM, Marin O, Pinna LA. Spontaneous autophosphorylation of Lyn tyrosine kinase at both its activation segment and C-terminal tail confers altered substrate specificity. *Biochemistry*. 1998;37:1438-1446.
59. Caplan AJ, Mandal AK, Theodoraki MA. Molecular chaperones and protein kinase quality control. *Trends Cell Biol*. 2007;17:87-92.
60. Trentin L, Frasson M, Donella-Deana A, et al. Geldanamycin-induced Lyn dissociation from aberrant Hsp90-stabilized cytosolic complex is an early event in apoptotic mechanisms in B-chronic lymphocytic leukemia. *Blood*. 2008;112:4665-4674.
61. Chiorazzi N. Cell proliferation and death: forgotten features of chronic lymphocytic leukemia B cells. *Best Pract Res Clin Haematol*. 2007;20:399-413.
62. Azimzadeh J, Bornens M. Structure and duplication of the centrosome. *J Cell Sci*. 2007;120:2139-2142.
63. Kramer A, Neben K, Ho AD. Centrosome aberrations in hematological malignancies. *Cell Biol Int*. 2005;29:375-383.

64. Hensel M, Zoz M, Giesecke C, et al. High rate of centrosome aberrations and correlation with proliferative activity in patients with untreated B-cell chronic lymphocytic leukemia. *Int J Cancer*. 2007;121:978-983.
65. Ghia P, Granziero L, Chilosi M, Caligaris-Cappio F. Chronic B cell malignancies and bone marrow microenvironment. *Semin Cancer Biol*. 2002;12:149-155.
66. Ding W, Nowakowski GS, Knox TR, et al. Bi-directional activation between mesenchymal stem cells and CLL B-cells: implication for CLL disease progression. *Br J Haematol*. 2009;147:471-483.
67. Gattei V, Bulian P, Del Principe MI, et al. Relevance of CD49d protein expression as overall survival and progressive disease prognosticator in chronic lymphocytic leukemia. *Blood*. 2008;111:865-873.
68. Shanafelt TD, Geyer SM, Bone ND, et al. CD49d expression is an independent predictor of overall survival in patients with chronic lymphocytic leukaemia: a prognostic parameter with therapeutic potential. *Br J Haematol*. 2008;140:537-546.
69. Redondo-Munoz J, Jose Terol M, Garcia-Marco JA, Garcia-Pardo A. Matrix metalloproteinase-9 is up-regulated by CCL21/CCR7 interaction via extracellular signal-regulated kinase-1/2 signaling and is involved in CCL21-driven B-cell chronic lymphocytic leukemia cell invasion and migration. *Blood*. 2008;111:383-386.
70. Munk Pedersen I, Reed J. Microenvironmental interactions and survival of CLL B-cells. *Leuk Lymphoma*. 2004;45:2365-2372.
71. Jordan MA, Wilson L. Microtubules as a target for anticancer drugs. *Nat Rev Cancer*. 2004;4:253-265.
72. Burger JA, Ghia P, Rosenwald A, Caligaris-Cappio F. The microenvironment in mature B-cell malignancies: a target for new treatment strategies. *Blood*. 2009;114:3367-3375.
73. Singh P, Rathinasamy K, Mohan R, Panda D. Microtubule assembly dynamics: an attractive target for anticancer drugs. *IUBMB Life*. 2008;60:368-375.
74. Caligaris-Cappio F, Bergui L, Tesio L, Corbascio G, Tousco F, Marchisio PC. Cytoskeleton organization is aberrantly rearranged in the cells of B chronic lymphocytic leukemia and hairy cell leukemia. *Blood*. 1986;67:233-239.
75. Fernandez JA, Keshvara LM, Peters JD, Furlong MT, Harrison ML, Geahlen RL. Phosphorylation- and activation-independent association of the tyrosine kinase Syk and the tyrosine kinase substrates Cbl and Vav with tubulin in B-cells. *J Biol Chem*. 1999;274:1401-1406.

76. Draberova L, Draberova E, Surviladze Z, Draber P, Draber P. Protein tyrosine kinase p53/p56(lyn) forms complexes with gamma-tubulin in rat basophilic leukemia cells. *Int Immunol*. 1999;11:1829-1839.
77. Mollinedo F, Gajate C. Microtubules, microtubule-interfering agents and apoptosis. *Apoptosis*. 2003;8:413-450.
78. Conde C, Caceres A. Microtubule assembly, organization and dynamics in axons and dendrites. *Nat Rev Neurosci*. 2009;10:319-332.
79. Imazio M, Bobbio M, Cecchi E, et al. Colchicine in addition to conventional therapy for acute pericarditis: results of the COLchicine for acute PERicarditis (COPE) trial. *Circulation*. 2005;112:2012-2016.
80. Mohan R, Panda D. Kinetic stabilization of microtubule dynamics by estramustine is associated with tubulin acetylation, spindle abnormalities, and mitotic arrest. *Cancer Res*. 2008;68:6181-6189.
81. Altmann KH, Wartmann M, O'Reilly T. Epothilones and related structures--a new class of microtubule inhibitors with potent in vivo antitumor activity. *Biochim Biophys Acta*. 2000;1470:M79-91.
82. Jaksic B, Brugiattelli M, Krc I, et al. High dose chlorambucil versus Binet's modified cyclophosphamide, doxorubicin, vincristine, and prednisone regimen in the treatment of patients with advanced B-cell chronic lymphocytic leukemia. Results of an international multicenter randomized trial. *International Society for Chemo-Immunotherapy, Vienna. Cancer*. 1997;79:2107-2114.
83. Barr PM, Lazarus HM, Cooper BW, et al. Phase II study of bryostatin 1 and vincristine for aggressive non-Hodgkin lymphoma relapsing after an autologous stem cell transplant. *Am J Hematol*. 2009;84:484-487.
84. De Brabander MJ, Van de Veire RM, Aerts FE, Borgers M, Janssen PA. The effects of methyl (5-(2-thienylcarbonyl)-1H-benzimidazol-2-yl) carbamate, (R 17934; NSC 238159), a new synthetic antitumoral drug interfering with microtubules, on mammalian cells cultured in vitro. *Cancer Res*. 1976;36:905-916.
85. Hoebeke J, Van Nijen G, De Brabander M. Interaction of oncodazole (R 17934), a new antitumoral drug, with rat brain tubulin. *Biochem Biophys Res Commun*. 1976;69:319-324.
86. Head J, Lee LL, Field DJ, Lee JC. Equilibrium and rapid kinetic studies on nocodazole-tubulin interaction. *J Biol Chem*. 1985;260:11060-11066.
87. Vasquez RJ, Howell B, Yvon AM, Wadsworth P, Cassimeris L. Nanomolar concentrations of nocodazole alter microtubule dynamic instability in vivo and in vitro. *Mol Biol Cell*. 1997;8:973-985.
88. Vandecandelaere A, Martin SR, Bayley PM. Regulation of microtubule dynamic instability by tubulin-GDP. *Biochemistry*. 1995;34:1332-1343.

89. Kallas A, Pook M, Maimets M, Zimmermann K, Maimets T. Nocodazole treatment decreases expression of pluripotency markers Nanog and Oct4 in human embryonic stem cells. *PLoS One*. 2011;6:e19114.
90. Aylon Y, Michael D, Shmueli A, Yabuta N, Nojima H, Oren M. A positive feedback loop between the p53 and Lats2 tumor suppressors prevents tetraploidization. *Genes Dev*. 2006;20:2687-2700.
91. Beswick RW, Ambrose HE, Wagner SD. Nocodazole, a microtubule depolymerising agent, induces apoptosis of chronic lymphocytic leukaemia cells associated with changes in Bcl-2 phosphorylation and expression. *Leuk Res*. 2006;30:427-436.
92. Braun J, Unanue ER. The lymphocyte cytoskeleton and its control of surface receptor functions. *Semin Hematol*. 1983;20:322-333.
93. Cohen HJ. Human lymphocyte surface immunoglobulin capping. Normal characteristics and anomalous behavior of chronic lymphocytic leukemic lymphocytes. *J Clin Invest*. 1975;55:84-93.
94. Modriansky M, Dvorak Z. Microtubule disruptors and their interaction with biotransformation enzymes. *Biomed Pap Med Fac Univ Palacky Olomouc Czech Repub*. 2005;149:213-215.
95. Polioudaki H, Kastrinaki MC, Papadaki HA, Theodoropoulos PA. Microtubule-interacting drugs induce moderate and reversible damage to human bone marrow mesenchymal stem cells. *Cell Prolif*. 2009;42:434-447.
96. Wu X, Koiwa H. One-step casting of Laemmli discontinued sodium dodecyl sulfate-polyacrylamide gel electrophoresis gel. *Anal Biochem*;421:347-349.
97. Kurtova AV, Balakrishnan K, Chen R, et al. Diverse marrow stromal cells protect CLL cells from spontaneous and drug-induced apoptosis: development of a reliable and reproducible system to assess stromal cell adhesion-mediated drug resistance. *Blood*. 2009;114:4441-4450.
98. Ramsay AG, Johnson AJ, Lee AM, et al. Chronic lymphocytic leukemia T cells show impaired immunological synapse formation that can be reversed with an immunomodulating drug. *J Clin Invest*. 2008;118:2427-2437.
99. Gorgun G, Ramsay AG, Holderried TA, et al. E(mu)-TCL1 mice represent a model for immunotherapeutic reversal of chronic lymphocytic leukemia-induced T-cell dysfunction. *Proc Natl Acad Sci U S A*. 2009;106:6250-6255.
100. Roberts R, Gallagher J, Spooncer E, Allen TD, Bloomfield F, Dexter TM. Heparan sulphate bound growth factors: a mechanism for stromal cell mediated haemopoiesis. *Nature*. 1988;332:376-378.

101. Park H, Hong S, Hong S. Nocodazole is a High-Affinity Ligand for the Cancer-Related Kinases ABL, c-KIT, BRAF, and MEK. *ChemMedChem*. 2012;7:53-56.
102. McCaig AM, Cosimo E, Leach MT, Michie AM. Dasatinib inhibits B cell receptor signalling in chronic lymphocytic leukaemia but novel combination approaches are required to overcome additional pro-survival microenvironmental signals. *Br J Haematol*. 2011. Epub ahead of print.
103. Wickremasinghe RG, Prentice AG, Steele AJ. Aberrantly activated anti-apoptotic signalling mechanisms in chronic lymphocytic leukaemia cells: clues to the identification of novel therapeutic targets. *Br J Haematol*;153:545-556.
104. Ma S, Rosen ST. Signal transduction inhibitors in chronic lymphocytic leukemia. *Curr Opin Oncol*. 2011;23:601-608.